EXAMINING THE ROLE OF *Gbx1* IN SPINAL CORD DEVELOPMENT AND ITS CONTRIBUTION TO MAMMALIAN LOCOMOTION

A Dissertation

Presented to

The Faculty of the Graduate

At the University of Missouri

In Partial Fulfillment

Of the Requirements for the Degree

Doctor of Philosophy

By

Desirè M. Buckley

Samuel T. Waters, Dissertation Advisor

Doctor of Philosophy of Biological Sciences

May 2015

The undersigned, appointed by the dean of the Graduate School,

have examined the dissertation entitled

Examining the Role of *Gbx1* in Spinal Cord Development and its Contribution to Mammalian Locomotion

Presented by Desirè M. Buckley

A candidate for the degree of

Doctor of Philosophy of Biological Sciences

And hereby certify that, in their opinion, it is worthy of acceptance.

_____

Dr. Samuel T. Waters, Dissertation Advisor

_____

Dr. Elizabeth Bryda

_____

Dr. David Schulz

_____

Dr. Anand Chandrasekhar

ACKNOWLEDGEMENTS

First, I would like to thank my research advisor, Dr. Samuel T. Waters. He has greatly assisted in my development as a scientist. Training in his lab allowed me to learn invaluable technical skills, and refine my scientific expertise through his mentorship. The most memorable statement he made to me during my training was "a good scientist is one who is continuously eager to learn, because there is no one who knows everything". Dr. Waters thoroughly enjoyed scientific conversations with his students, he was always available to answer questions, he was willing to offer words of wisdom as he saw fit for any situation and he even put on gloves to instruct bench work alongside his students! Dr. Waters, I am forever grateful for the experiences you provided.

I would like to thank my graduate committee members Dr. Elizabeth Bryda, Dr. David Schulz and Dr. Anand Chandrasekhar for their support and guidance. Dr. Elizabeth Bryda is a great role model of a successful female scientist and challenged me to better understand mouse genetics to design valuable experiments with genetically-modified mouse models. As my neuroscience professor, Dr. David Schulz was instrumental to my understanding of key neurobiology concepts. He also assisted in translating the importance of my research to captivate the scientific community, for purposes such as grant writing. Dr. Anand Chandrasekhar was a great source for new scientific perspectives of my research and pivotal in improving my overall scientific writing.

I would next like to thank my entire family for their endless support and love. The greatest appreciation of all is for my Mother who passed away during my graduate career. She was the biggest supporter of my passion for science. She would show off my conference program books because my name was listed as a presenter and would boast about my fellowship awards as if they were hers. She was proud of every accomplishment I made, which gave me the motivation to continue even after her passing. This one's for you. To my Father, thank you for always believing in me. Your love and guidance helped me through many situations and I could have not reached this point without you. To my daughter, Kinley, I thank you for giving me a brand new outlook on the meaning of life. To my siblings: Jordan, Miranda, Aubrey, Kierra, Aaliyah and Noah, because of you all I strive to be the best role model, academically and otherwise. Thank you all for giving me a reason to keep on going.

I give thanks to my former lab mates, Dr. David Roeseler and Dr. Jessica Burroughs-Garcia. The both of you were essential to my survival in the lab and graduate school. The technical skills I learned from each of you are invaluable. The social interactions we shared science or non-science related made my graduate career enjoyable and a memorable experience. I wish you luck in all future endeavors.

I would like thank all collaborators, colleagues, friends, faculty and staff that have assisted and supported me during my scientific endeavors.

Lastly I owe thanks to the sources that made my graduate school career possible: The University of Missouri, Department of Biological Sciences, The Bond Life Sciences Center, the Molecular Life Sciences Fellowship, the Gus T. Ridgel Fellowship and the National Science Foundation Graduate Research Fellowship Program.

TABLE OF CONTENTS

LIST OF FIGURES

ABSTRACT

Animals explore their environment through locomotion. Motion is generated by the activity of sensorimotor circuits formed in the spinal cord during embryogenesis, which are further refined postnatally. These circuits are composed of spinal sensory interneurons and motor neurons, which integrate proprioceptive somatosensation mediated by peripheral sensory neurons. Together, peripheral proprioceptive sensory neurons and spinal motor neurons constitute the simplest sensorimotor circuit controlling locomotion, the monosynaptic stretch reflex circuit.

Transcription factors expressed during embryogenesis play a critical role in the assembly of sensorimotor circuits that facilitate locomotive behaviors. *Gbx1* is a member of the murine Gbx family of homeodomain-containing transcription factors. It is dynamically expressed in neuronal populations in the dorsal and ventral spinal cord throughout embryonic development. In the dorsal spinal cord, *Gbx1* is required to maintain a subset of inhibitory $PAX2^{+}$ interneurons. It is also required for normal locomotor output of the hindlimbs. The other Gbx family member, *Gbx2*, is also expressed in spinal neuron populations during embryonic development. However, its function has been best characterized in establishment and development of the mid-hindbrain boundary and anterior hindbrain. The studies presented in this dissertation provide the first functional analysis for *Gbx1* in the spinal cord and were designed to examine the role of *Gbx1* in locomotion.

To examine the role of *Gbx1* in the developing spinal cord, we generated mice carrying a loss-of-function allele for *Gbx1* (*Gbx1*$^{-/-}$). By postnatal day 15, *Gbx1*$^{-/-}$ mice begin to display a gross locomotive defect that specifically affects hindlimb gait. Molecular analysis of mutant embryos revealed premature termination of 1a afferents, axons of proprioceptive sensory neurons, in the dorsal spinal cord. In addition, a subset of motor neurons in the ventral spinal cord is lost, at mid-embryonic stages. Both observations persisted at postnatal stages. The loss of motor neurons prompted us to investigate the underlying mechanism, which we identified as apoptosis-mediated cell death. Notably, the cell types affected by loss of *Gbx1* are highly involved in controlling locomotor output.

We also briefly assessed possible interaction of *Gbx1* with its family member *Gbx2* in spinal neuron development using *Gbx1*$^{-/-}$; *Gbx2*$^{-/-}$ double knockout mutant embryos. Genetic inactivation of *Gbx* family members independently, result in significant reduction of PAX2^{+} cells in the superficial layers (laminae I-II) of the dorsal spinal cord. However, this phenotype was not exacerbated in double knockout embryos. Together these data suggest that Gbx family members are required to maintain PAX2 cell fate in the dorsal spinal cord, but not functionally redundant for this shared function.

Data herein demonstrate a requirement for *Gbx1* in normal locomotor output. Additionally, identification of the mechanism resulting in death of motor neurons has revealed a novel requirement for *Gbx1* in spinal motor neuron survival. Collectively, data presented herein support a model for involvement of *Gbx1* in development of monosynaptic stretch reflex circuit components.

CHAPTER 1

INTRODUCTION AND BACKGROUND

OVERVIEW

The brain and spinal cord (SC), organs of the central nervous system (CNS), are largely responsible for perception and interpretation of the external environment (Neff and Goldberg, 1960). Through our senses, we perceive the environment and our respective relationship to it. This important process allows us to respond efficiently and precisely to variation in our surroundings, whether it be running from a bear; steering a bike left and right along a trail; answering a question asked by another person; or any other activity we might encounter in our daily lives. In all cases, the relationship between sensory input and motor output must be highly organized to ensure the appropriate reflex is elicited.

In response to sensory stimuli, the SC generates vital spinal reflexes that control movement and locomotion (Goulding, 2009). Spinal locomotor circuits assembled during embryonic development have a critical role in defining the control of motor output. They are composed of sensory interneurons (INs) and motor neurons (MNs) in the SC that interact with sensory neurons from the periphery. Each neuronal cell type requires molecular mechanisms that establish progenitor pool sizes and subsequently regulates differentiation of precursors into unique subpopulations of post-mitotic

neurons. Additionally, these mechanisms regulate the formation of synapses between appropriate synaptic partners for the establishment of functional neural connections (Dasen, 2009). Elucidation of mechanisms that help to establish locomotor circuitry in the developing SC will expand our understanding of this developmental process molecularly, which is currently most-defined anatomically.

Numerous transcription factors (TFs) underlie regulatory networks that contribute to the specification, organization and functional connectivity of spinal neurons, which contribute to motor control systems (Ericson et al., 1992; Ericson et al., 1997; Tanabe et al., 1998; Arber et al., 1999; Briscoe et al., 1999; Jungbluth et al., 1999; Sander et al., 2000). While many of these TFs have been characterized through gene inactivation studies, much work is still needed to definitively elucidate the transcriptional regulation exerted by each factor during the formation of neural networks. Furthermore, elucidating key intrinsic mechanisms that contribute to sensorimotor circuit development will help to shed light on motor dysfunction after injury and aid in rehabilitation (Dietz, 2002). Thus, understanding how sensorimotor circuits develop and maximally operate in the SC is an important research area of interest for developmental biologist.

FORMATION OF THE CENTRAL NERVOUS SYSTEM

The developmental events discussed in this dissertation are in context of the murine (*Mus musculus*) species.

1.1 GASTRULATION

Morphogenesis of the early embryo is a complex event that occurs during embryonic development and is well described by many classic studies (Tam et al.,

1993; Tam and Behringer, 1997). Prior to development of the CNS, cells are organized into distinct layers that establish a primitive organism body plan. The process responsible for this critical developmental event, termed gastrulation, assists with the massive reorganization of the inner cell mass (ICM) into a tri-layered cell framework (Tam and Behringer, 1997). Gastrulation initially results in three "inside-out" germ layers: ectoderm (inner layer), mesoderm (middle layer), and endoderm (outer layer). This composes a blueprint for subsequent development of the embryo.

Gastrulation begins at embryonic (E) day 6.5, post-implantation of the blastocyst into the uterine wall (Tam and Behringer, 1997). It is preceded by epithelial-to-mesenchymal transition (EMT), a process during which cells lose their epithelial characteristics, downregulate E-cadherin, and become migratory (Gheldof and Berx, 2013). This segregates cells within the ICM into two layers: 1) primitive endoderm which gives rise to extraembryonic tissues that do not directly contribute cells to the actual embryo, and 2) a cup-shaped epiblast which gives rise to germ layers of the embryo proper (Tam et al., 1993). It is then followed by development of organ systems, or organogenesis. Gastrulation begins at the posterior end of the epiblast with formation of an organizing center called "the node". The node is a specialized group of cells that secrete molecular signals, namely fibroblast growth factors (FGFs). These assist in the specification and migration of adjacent cells through the newly formed primitive streak, a groove on the ventral side of the epiblast (Ciruna and Rossant, 2001). Also, formation of this signaling center establishes the left-right axis and provides the first indication of polarity within the gastrulating embryo to distinguish the head (anterior end) from the tail (posterior end). Cells from the epiblast which are internal to the embryo proper, ingress

through the primitive streak to become mesendoderm in a manner in which the cup-shaped layer expands and turns inside out, placing these cells on the outside of the gastrula (Tam and Loebel, 2007).

The ectodermal layer is engulfed by the mesendoderm, which forms the CNS and skin. Upon folding of the ectoderm into the mesendoderm, this layer differentiates into anteriorly positioned mesoderm forming the bony skeleton, muscles and internal organs, or posteriorly positioned ectoderm forming gut and respiratory systems (Tam and Behringer, 1997). Another key consequence of gastrulation is defining the embryonic midline along the anterior-posterior (AP) axis by a structure called the notochord. This forms when a portion of cells from the node coalesce and bud off towards the ventral half embryo (Tam and Loebel, 2007). The notochord is responsible for sending inductive signals to the neuroectoderm positioned directly above, which subsequently becomes the neural plate and gives rise to the entire CNS (Narasimha and Leptin, 2000).

1.2 NEURULATION

The ectoderm, the outermost germ layer covering the developing embryo, segregates into three domains during development. The domains become divergent through a process called neurulation, which involves the induction and differentiation of a homogenous population of ectodermal cells into three molecularly and functionally unique derivatives (Colas and Schoenwolf, 2001). The three domains include: 1) surface ectoderm which becomes epidermal cells of the skin, hair, nails and lens; 2) central ectoderm which becomes the neural crest, a multipotent migratory cell type that

forms the peripheral nervous system (PNS), pigment and cartilage; and lastly, 3) neural plate ectoderm which later becomes the neural tube that gives rise to the major organs of the CNS, the brain and SC (Copp et al., 2003).

The neural plate results from induced thickening and differentiation of ectoderm overlying the notochord at E8.5 (Copp et al., 2003). Immediately following, in a process called primary neurulation, cells adjacent to the neural plate begin proliferating and direct invagination of the plate to form a cylindrical hollow tube. Primary neurulation is accomplished through a simultaneous, multi-step event (Ybot-Gonzalez et al., 2007; Ybot-Gonzalez et al., 2007; Greene and Copp, 2009). First, massive proliferation of the neural plate surface area elongates and extends the AP axis. Next, invagination of the plate resulting from thickening of the lateral domains that are in contact with surrounding tissue occurs (Ybot-Gonzalez and Copp, 1999). This creates neural folds that act as hinges to direct closure of the neural tube. Dorsal lateral hinge points are anchored on either side of the neural tube by the surface ectoderm, whereas a medial hinge point is ventrally anchored by the notochord. Together, these hinges cause the plate to bend creating a midline furrow and mergence of the lateral edges, ultimately forming a hollow tube (Colas and Schoenwolf, 2001). The last step in formation of the neural tube is closure. This occurs when the neural folds meet and fully adhere, due to convergence of the dorsal lateral hinge points (Colas and Schoenwolf, 2001; Greene and Copp, 2009). Importantly, fusion of the fold causes a subset of neuroectodermal cells to detach between the newly fused region and dorsal surface ectoderm. These cells are referred to as the neural crest (Griffith et al., 1992). Neural crest cells (NCCs) are not contributed to the neural tube, rather they remain their own distinct population that

resides between the epidermis and neural tube until directed to migrate (Griffith et al., 1992)

Cells of the neural crest are transient, highly migratory and pluripotent. It provides the organism with a variety of cell types which contributes vastly to adult tissue (Dupin et al., 2006). NCCs migrate dorso-ventrally from the dorsal most aspect of the neural tube, and coalesce to form dorsal root ganglions (DRG). DRG are located laterally adjacent to the edges of the SC at the level of each somite (Marmigere and Ernfors, 2007). Somites are block like segments of mesoderm lining the vertebral column that give rise to sclerotome, myotome and dermatome (Ordahl and Le Douarin, 1992). NCCs are instructed by specific pathways mediated by secreted, diffusible, and cell surface molecular signals which induce their differentiation into diverse cell types (Hall and Ekanayake, 1991; Garcia-Castro et al., 2002; Knecht and Bronner-Fraser, 2002; Cheung et al., 2005). As a result, NCCs give rise to several progeny including a number of non-neural structures such as pigment cells, cartilage, and bone. Additionally, they contribute to neurosecretory endocrine cells and importantly, sensory neuron and glial cells of the peripheral nervous system (Sieber-Blum, 1989; Anderson, 1997; Anderson et al., 1997). These peripheral cell types are involved in the perception of different sensory stimuli for the propagation of appropriate motor reflex responses.

SPINAL CORD DEVELOPMENT

The CNS is the processing center of the organism that responds to consequences of motor acts relayed as proprioceptive sensory signals (Hantman and Jessell, 2010). It is responsible for integrating sensory information from the peripheral nervous system and responding to it efficiently and accurately. It consists of two parts:

the brain and the SC. These structures are particularly sensitive to the differential expression of TFs which confer distinct identities to neurons that compose each structure (Wilson and Maden, 2005).

The brain is derived from the anterior portion of neural tube, which begins as three primary divisions: prosencephalon (forebrain), mesencephalon (midbrain), and rhombencephalon (hindbrain) (Altmann and Brivanlou, 2001). The caudal most portion of the neural tube gives rise to the SC, which is involved in sensory reception, generation of certain local spinal reflexes and controlling movement for locomotion. It also serves as the highway by which peripheral sensory impulses are conducted to the brain and returned as motor messages to the rest of the body. These functions make the SC chief executor of all motor responses (Gillespie and Walker, 2001; Julius and Basbaum, 2001; Caspary and Anderson, 2003). Thus, exchange of information between the external environment and brain is critical for normal functioning of sensorimotor circuits.

Homeodomain (HD) TFs are largely responsible for the initiation of neurogenesis in the developing SC (Jessell, 2000). Transcription factors differentially expressed along the dorsal-ventral axis identify eleven spinal progenitor domains (pd) that give rise to unique populations of spinal neurons. Subsequent proliferation, specification, and differentiation of progenitor cells is also regulated by TFs expressed in each domain. For the formation of sensorimotor circuits, TFs confer distinct functional characteristics to spinal neurons. This allows them to elicit differential responses to distinct sensory stimuli and enables them to form a synaptic network (Shirasaki and Pfaff, 2002; Helms and Johnson, 2003; Del Barrio et al., 2013).

1.3 CELL PROLIFERATION

Early SC patterning along the dorsoventral (DV) axis is mediated by the graded expression of secreted signaling molecules from the transforming growth factor β (TGFβ/BMP) family and sonic hedgehog (Shh), respectively (Jessell, 2000; Goulding et al., 2002). However, it has become clear that many essential aspects of the developmental programming are directed by the restricted expression profiles of TF in a cell type specific manner (Briscoe et al., 2000; Gross et al., 2002; Muller et al., 2002; Caspary and Anderson, 2003). The efficiency of the CNS relies, in part, on the number of functionally distinct neurons generated during embryonic development. Accordingly, mechanisms have evolved to control plasticity of the cell cycle to ensure sufficient rates of proliferation (Artus and Cohen-Tannoudji, 2008).

Proliferation of neural precursor cells, also called progenitors, occurs rapidly after formation of the neural tube. This is followed by specification and extensive differentiation, resulting in the vast number of specialized cell types that populate the mature SC. Cell proliferation occurs within the epithelial layer surrounding the lumen, or the ventricular zone (VZ) of the SC (Smart, 1972; Weiss et al., 1996). Newly generated and terminally differentiated cells begin migrating laterally outward from the ventricular zone forming atri-layer neural tube consisting of (i) a columnar epedymal layer which surrounds the central canal of the hollow neural tube, (ii) a densely packed medial layer, or mantle zone which becomes the gray matter of the CNS and (iii) an outer layer, or external marginal zone which becomes the white matter of the CNS. Regulation of this event is the function of several morphogenic signaling families, including FGFs and Wnts (Reviewed in (Ulloa and Briscoe, 2007)).

Cell proliferation begins after the neural tube is formed and continues at a rapid rate in a defined spatial-temporal manner until spinal neurons become terminally differentiated. Once cells begin to differentiate, proliferation decreases as cells become arrested during the cell cycle. To replace cells that have been lost as a result of injury or cell death, most cells have the ability to resume proliferation (Johansson et al., 1999; Bareyre, 2008). Thus, cell proliferation is meticulously balanced with cell death in order to manage neural cell population sizes (Oppenheim, 1991; Jacobson et al., 1997).

1.4 CELL DEATH

Programmed cell death (PCD), or apoptosis, is an essential and normal part of development (Buss et al., 2006). It is a process regulated by several genetic factors, allowing for easy scientific manipulation to determine developmental repercussions in the absence of cell death (Reviewed in (Baehrecke, 2002)). This has led to the widely accepted notion that all vertebrate organisms require controlled death of cells for normal development (Burek and Oppenheim, 1996). Several studies have demonstrated this necessity for several developmental purposes including: management of neural population sizes, deletion of unnecessary structures and the elimination of abnormal cells (Jacobson et al., 1997; Meier et al., 2000; Luo and O'Leary, 2005).

The most highly studied aspect of PCD is the property that selected cells are "programmed" to die, such that in the absence of growth or differentiation factors these cells are already pre-destined to commit suicide (Burek and Oppenheim, 1996; Jacobson et al., 1997). In developing animals, studies have been aimed to elucidate the biochemical mechanisms underlying the control of PCD (Hengartner, 2000; Shi, 2002).

PCD is initiated by a number of stimuli which activate caspase proteases, the core cell-death machinery (Shi, 2002). The stimulation of caspase activity by members of the tumor necrosis factor superfamily and Bcl-2 protein family, commits cells to death pathways that fragment DNA with subsequent degradation (Adams and Cory, 1998).

Many types of spinal neurons die by apoptosis as a result of normal developmental patterning to modify neural connectivity (Yuan and Yankner, 2000; Yuan et al., 2003). Notably, regressive events that occur during embryonic development also cause neurons to die for this purpose (Low and Cheng, 2006). An alternative strategy to apoptosis to manage the synapses formed by neurons and their post-synaptic targets is synaptic pruning. Phenomena associated with this regressive event have become synonymous with PCD and play a key role in synaptic refinement including, elimination of supernumerary synapses and disassembly of aberrant connections (Purves and Lichtman, 1980; Meier et al., 2000; Luo and O'Leary, 2005; Low and Cheng, 2006). Apoptosis and Pruning during early SC neurogenesis refines synaptic connections like those used for locomotion (Purves and Lichtman, 1980; Burek and Oppenheim, 1996; Hyman and Yuan, 2012). A normal level of apoptosis occurs during the developmental stages in which neural constituents of sensorimotor circuits begin establishing connection amongst each other (E16-E18). Cell death initiates in ventral spinal neural populations during the first wave of synaptogenesis primarily between E14.5-E17.5. It then proceeds in a wave-like manner towards IN populations in the dorsal SC after postnatal day (P) 0 when the remainder of synapses are being formed and refined (Lowrie and Lawson, 2000; Prasad et al., 2008). The postnatal survival of spinal MNs and INs is partly regulated by input connections from other locomotor components and

functional synapses made with muscle targets. Cell death in the postnatal SC indicates size matching of synaptically linked neuronal populations and the establishment of appropriate synaptic connections (Yuan et al., 2003)

1.5 SPINAL CORD PATTERNING

Patterning along the anteroposterior (AP) and dorsoventral (DV) axes is essential to confer anatomical and functional organization of the developing SC. An established pattern of gene expression regionalized along the midline (Figure 1.1) initiates the formation of distinct neural classes, which are important constituents of sensorimotor circuits. Neurons that process sensory stimuli are predominately positioned in the dorsal SC, whereas INs and MNs that modulate and elicit motor output are found ventrally (Caspary and Anderson, 2003; Helms and Johnson, 2003; Stepien and Arber, 2008)

Patterning along the AP axis is regulated by the spatially-confined, combinatorial expression of FGFs, Hox genes, Lim HD proteins, Wnt proteins and retinoic acid. Whereas, patterning along the DV axis is initiated by two secreted morphogenic factors that impart positional cues to neural progenitor cells within the ventricular zone beginning at embryonic (E) day E9.0. The roof plate and overlying epidermal layer secretes bone morphogenetic proteins (BMPs) while the notochord and floor plate secrete sonic hedgehog (SHH), to instruct fate acquisition of dorsal and ventral progenitors, respectively. This results in the spatially-confined induction of cross-repressive HD TFs that divide spinal neuron populations into eleven distinct dorsoventral domains (dI1–dI6, V0–V3, vMN) by E11, and the subsequent generation of

fourteen distinct classes of postmitotic neurons (Figure 1.1) (Ladle et al., 2007; Goulding, 2009; Gosgnach, 2011).

1.5.1 DORSAL INTERNEURON DEVELOPMENT

Sensory INs in the dorsal SC are required to relay information from the periphery associated with touch, pain, and body position (Helms and Johnson, 2003). Specification and patterning of dorsal progenitor cells requires the differential expression of basic helix-loop-helix (bHLH) and HD-containing TFs in response to graded BMP/TGF-β and Wnt signaling from the roof plate (Liem et al., 1997; Lee et al., 2000). Following their specification, dorsal progenitors differentiate into different classes of dorsal INs (dI1-d16, DILA and DILB) distinguished on the basis of a proneural TF code (Helms and Johnson, 2003; Zhuang and Sockanathan, 2006).

Development of dorsal INs occurs in two waves of neurogenesis (Gross et al., 2002; Muller et al., 2002). Six pd's positioned along the ventricular zone (pd1 - pd6) give rise to early-born classes of sensory dorsal INs (dI1-dI6) (Helms and Johnson, 2003). The six types of dorsal INs that emerge during the first wave can be divided into two classes: Class A (dI1-dI3) relay neurons that are induced in response to BMP signaling, and Class B (dI4-dI6) neurons that develop independent of BMP and express the HD TF *Lbx1* (Gross et al., 2002). Of the early-born classes of INs, the dI4 domain generates inhibitory GABAergic sensory neurons that express *Gsh1/2*, *Lbx1*, *Ptf1a* and *Pax2*. The dI5 domain develops into glutamatergic excitatory sensory INs that express *Gsh1/2, Lbx1, Tlx1/3* and *Lmx1b* (Gross et al., 2002; Muller et al., 2002; Cheng et al., 2004; Glasgow et al., 2005; Mizuguchi et al., 2006).

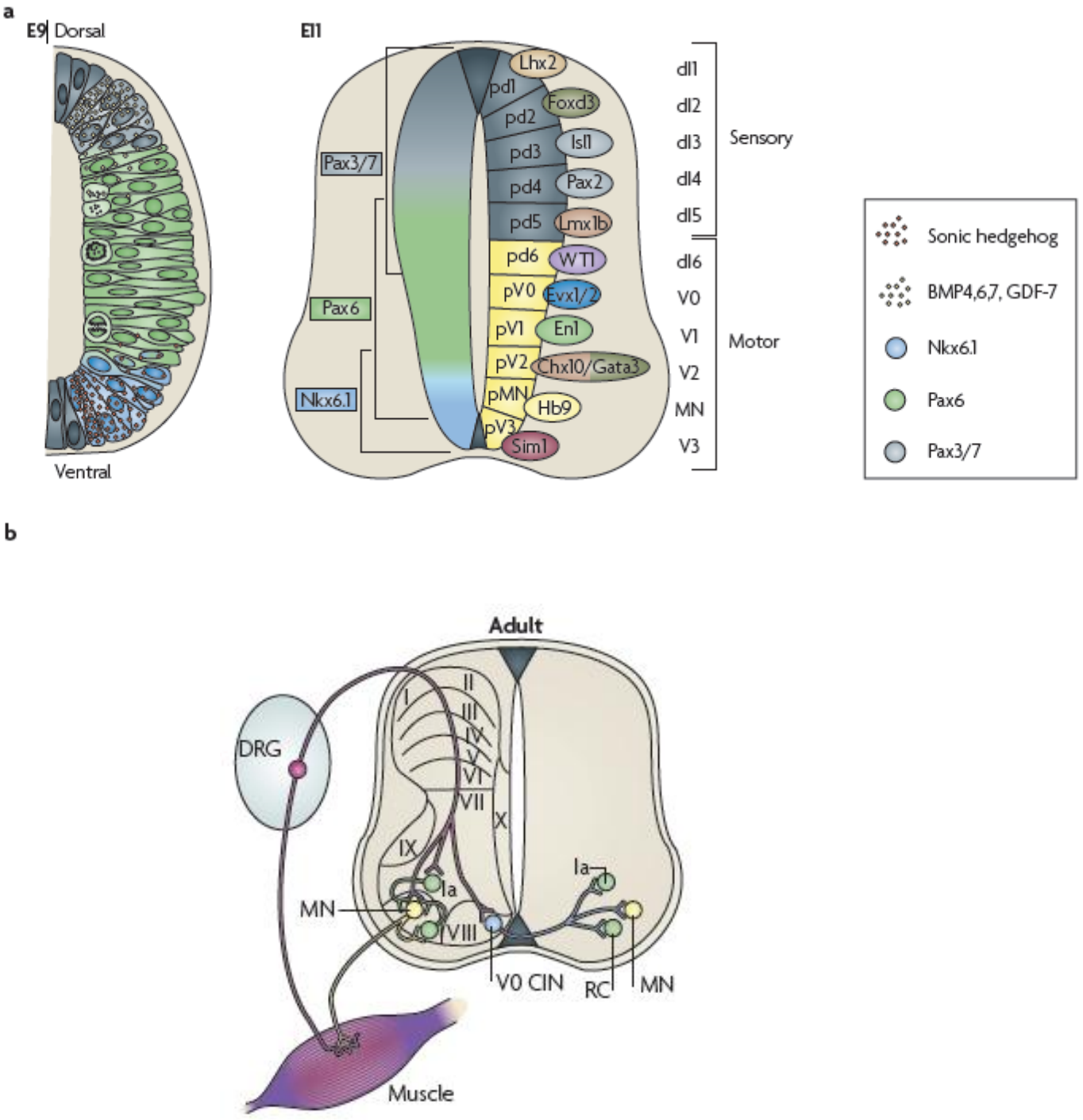
a
E9
Dorsal
Ventral
E11
Lhx2
pd1
Foxd3
pd2
Isl1
pd3
Pax2
pd4
Lmx1b
pd5
WT1
pd6
Evx1/2
pV0
En1
pV1
Chx10/Gata3
pV2
pMN
Hb9
pV3
Sim1
Pax3/7
Pax6
Nkx6.1
dI1
dI2
dI3
dI4
dI5
dI6
V0
V1
V2
MN
V3
Sensory
Motor
Sonic hedgehog
BMP4,6,7, GDF-7
Nkx6.1
Pax6
Pax3/7
b
Adult
DRG
I
II
III
IV
V
VI
VII
VIII
IX
X
Ia
MN
V0 CIN
RC
Muscle

Figure 1.1

Figure 1.1 - Early spinal cord development. (a) Schematic representation of the patterning and specification of neural populations in the developing mouse SC. At embryonic (E) day 9, a gradient of sonic hedgehog (SHH) (ventral, red) and bone morphogenetic protein (BMP) (dorsal, blue) impart positional cues to proliferating progenitor cells in the ventricular zone. This activates the expression of TFs within restricted domains along the dorsal-ventral axis, resulting in the presence of eleven early-born classes of postmitotic neurons by E11. Dorsal progenitors give rise to dI1-dI5 and are primarily involved in sensory spinal networks relayed to the ventral SC, whereas ventral progenitors give rise to MN and V0-V3 neurons involved in execution of locomotor circuitry. The TFs that identify the postmitotic neurons are indicated to the right of each domain. (b) Schematic cross-section of an adult mouse SC showing the topographic positioning of some neurons involved in locomotor circuitry within various laminae (roman numerals): motor neurons (MN) (yellow), renshaw cells (RC) and Ia inhibitory interneurons (Ia) (green) and V0 commissural interneurons (CINs) (blue). DRG, dorsal root ganglion. This figure was originally published in Goulding, M. (2009). "Circuits controlling vertebrate locomotion: moving in a new direction." Nat Rev Neurosci 10(7): 507-518. The host-manuscript can be accessed with the URL: http://www.nature.com/nrn/journal/v10/n7/full/nrn2608.html.

During the second phase of neurogenesis, E11-E13.5, changes in transcription factor expression profiles in a subset of (*Gsh1/2*$^{+}$, *Lbx1*$^{+}$, *Ptf1a*$^{+}$) progenitor cells occurs, resulting in a common pool of late-born progenitors, the dIL domain. dIL progenitors generate either inhibitory GABAergic dILA INs that express *Gsh1/2*, *Lbx1*, *Ptf1a*, and *Pax2* or excitatory glutamatergic dILB INs that express *Gsh1/2*, *Lbx1*, *Ptf1a*, and *Tlx1/3*. Notably, the TF code for inhibitory or excitatory neurons of the early- and late-born class is similar. dILA and dILB INs develop into association INs that emerge from deep layers of the dorsal horn to populate laminae I-III of the dorsal horn (Gross et al., 2002; Mizuguchi et al., 2006).

1.5.2 VENTRAL INTERNEURON DEVELOPMENT

The ventral SC houses INs (V0-V3) that modulate output elicited by MNs (Table 1) (Goulding, 2009; Alaynick et al., 2011; Gosgnach, 2011; Arber, 2012; Francius et al., 2013). Interneurons in the ventral SC are specified and patterned by a gradient of SHH protein secreted by the floorplate and notochord (Ericson et al., 1997). Similar to dorsal INs, ventral IN precursors are consolidated by the restricted expression of HD proteins expressed in a graded response to exposure of secreted SHH between E10-E13 (Ericson et al., 1997; Briscoe et al., 2000; Jessell, 2000). Each domain resident to ventral INs is comprised of cells capable of differentiating into molecularly and functionally distinct neuronal subtypes as a result of TF induction during differentiation, demonstrating that mechanisms in addition to SHH signaling are involved in acquisition of ventral fate (Matise, 2013).

The progenitor domain that gives rise to V0 INs, pd0, is defined by the expression of *Dbx1/Dbx2*. Postmitotic V0 INs express *Evx1/Evx2* and develop into three

distinct subpopulations of commissural and ipsilaterally projecting neurons: $V0_D$, $V0_V$, $V0_C$ (Matise and Joyner, 1997; Moran-Rivard et al., 2001; Pierani et al., 2001). Inactivation of *Dbx1* in mice, which ablates all V0 subtypes, lead to the conclusion that V0 INs establish the alternating left-right pattern of locomotion. These mutants display bilateral synchrony rather than alternating motor output (Lanuza et al., 2004).

Engrailed1 (*En1*) expressing V1 INs marked by the expression of *Pax2* and *FoxD3* are derived from pd1 and give rise to two inhibitory subtypes: renshaw cells (RCs) and 1a INs. The V1 IN population is important in the propagation of the proprioceptive modality necessary for locomotion. They play a major role in regulating the speed of locomotor output by modulating the activity of MNs through presynaptic inhibition (Gosgnach et al., 2006).

The V2 IN population is derived from *Lhx3*-expressing progenitors within pd2, and can be divided into two subtypes. V2 derivatives are distinguished by their postmitotic molecular expression profiles, V2a cells selectively express *Chx10* (Peng et al., 2007) whereas, V2b cells express *Gata2/3* (Ericson et al., 1997). Furthermore, marked differences in the V2 population appear with the acquisition of their neurotransmitter phenotypes as $Chx10^+$ cells are excitatory and $Gata2/3^+$ cells are inhibitory (Lanuza et al., 2004; Lundfald et al., 2007). Studies have yet to thoroughly characterize the role of V2b cells in locomotion, however extensive examination of V2a cells have demonstrated their importance in coordinating left-right alternation, like V0 INs, but primarily at high speeds (Crone et al., 2009; Zhong et al., 2010).

Lastly, $Sim1^+$ V3 INs are generated from $Nkx2.2^+$ and $Nkx2.9^+$ pd3 progenitors cells (Briscoe et al., 1999). They originate from the most ventral aspect of the SC and

are primarily excitatory where they make monosynaptic connections to contralateral MNs (Zhang et al., 2008). In mice lacking V3 cells, there was a marked irregularity of locomotor rhythm, suggesting that V3 cells balance the rhythmic output of locomotion from either side of the SC (Zhang et al., 2008).

Table 1 - **Genetically-defined interneuron populations currently thought to be involved in locomotor activity.**

Cell Population	Subpopulations	Molecular Marker	Neurotransmitter phenotype	Axonal Projection	Knockout Phenotype	Primary Refrences
dI6		BhlhB5	Some inhibitory	Some cells commissural	Not determined	Goulding 2009
V0	$V0_D$	Dbx1/Evx1$^-$	Inhibitory	Primarily commissural	Loss of left-right coordination	Pierani et al. 2001
	$V0_v$	Dbx1/Evx1$^+$	Inhibitory	Primarily commissural		Lanuza et al. 2004
	$V0_{C/G}$	Evx2/Pitx2	Excitatory	Ipsilateral		Zagoraiou et al. 2009
V1		En1	Inhibitory	Ipsilateral	Slow rhythm	Sapir et al. 2004; Gosgnach et al. 2006
V2	V2a	Chx10	Excitatory	Ipsilateral	Left-right synchrony at high speeds	Zhong et al. 2010; Lundfald et al. 2007; Crone et al. 2008; Crone et al. 2009
	V2b	Gata2/3	Inhibitory	Primarily Ipsilateral	Not determined	Lundfald et al. 2007; Lanuza et al. 2007
V3		Sim1	Excitatory	Ipsilateral and commissural	Unbalanced rhythm	Zhang et al. 2008
Hb9			Excitatory	Ipsilateral	Not determined	Kwan et al. 2009; Hinkley et al. 2005; Wilson et al. 2005

Table 1 - Genetically-defined interneuron populations currently thought to be involved in locomotor activity. Table listing spinal cell populations along with their subpopulations that derive as a result of the differential expression of postmitotic molecular markers. Description of their neurotransmitter phenotype, axonal projection and knockout phenotype are also defined. Primary references for data represented are provided. Adapted from (Gosgnach, 2011).

1.5.3 VENTRAL MOTOR NEURON DEVELOPMENT

In addition to the vast number of locomotor-related IN populations that are generated in the ventral SC, MNs are also derived ventrally and are critically involved in all motor output. MNs are the earliest born cell type in the SC and originate from a single progenitor domain, pMN, expressing *Olig2* and *Lhx3* (Arber et al., 1999; Thaler et al., 1999; Thaler et al., 2004; Lee et al., 2005). Postmitotic MNs are generated between E9.5-E11.5, and are distinguished by the co-expression of *Hb9* and *Islet1* (ISL1) (Thaler et al., 2004; Liang et al., 2011). MN birth is followed by the acquisition of distinct MN identities between E11.0-E12.5, based on the anatomical position of their cell bodies within stereotypical motor groups and columns that form as a result of selective expression of LIM-HD, and ETS TFs (Tsuchida et al., 1994; Lin et al., 1998).

Following their birth, MN cell bodies form motor columns and cluster by stereotypic positioning during migration into motor pools. Resident MNs of each pool innervate individual skeletal muscles in the periphery (Jessell, 2000). To account for differences in peripheral muscle targets of distinct sensorimotor circuits, MN cell number, class, and connectivity are varied along the rostro-caudal axis of the SC (Arber, 2012). For example, the lateral motor column (LMC) only exists at brachial and lumbar levels of the SC and project axons to forelimb and hindlimb muscles, respectively. Thus, a molecular program that provides MNs with the intrinsic competence to differentiate into discrete subpopulations is customized at each axial level (Dalla Torre di Sanguinetto et al., 2008).

Initially all post-mitotic spinal MNs express the LIM-HD factor *Islet1*, but as a subset of the MNs begin their medial-lateral migration they downregulate *Islet1* and

upregulate other members of the LIM-HD family (*Lhx3, Lhx1, Isl2*) to begin their organized sorting process (Tsuchida et al., 1994; Jessell, 2000; Shirasaki and Pfaff, 2002; Price and Briscoe, 2004; Dalla Torre di Sanguinetto et al., 2008). It is well noted that neurons within distinct motor pools project axons to individual muscles in the periphery. MN cell bodies positioned in a more dorsal motor pool project to the most distal muscle targets. Conversely, MN cell bodies positioned more ventrally extend towards the most proximal muscle targets. Specific pools of MNs also express members of the ETS family of TFs, *Er81* and *Pea3* (Lin et al., 1998; Livet et al., 2002). Interestingly, there is a close correlation between the expression of ETS TFs within motor groups and the type of sensory afferent with which it synaptically connects.

The number of skeletal muscle fibers innervated by a given motor pool depends on the number of MNs that distinctly populate MN pools. This relationship is contingent upon the generation of appropriate MN cell numbers initially, and the subset lost through developmental cell death, a concept referred to as regressive neurogenesis(Cowan et al., 1984). The highest occurrence of normal MN cell death at E13.5, coincides with the stage in which MNs depend on target-derived signals from the periphery. If this retro-grade target signaling becomes interrupted, the incident of abnormal cell death increases due to the loss of cell survival factors protecting the MNs from normal cell death (Kablar and Rudnicki, 1999).

DEVELOPMENT OF SENSORIMOTOR CIRCUITS

The dorsal and ventral regions of the SC are functionally and anatomically distinct, interacting through complex neuronal circuits. Assembly of neuronal circuits in the SC depends on specification and patterning of distinct neurons that reside within

both regions. In addition, it relies on the generation of several peripheral sensory neuron cells types with the ability to process and transmit distinct sensory modalities (Caspary and Anderson, 2003). During assembly, afferents of sensory neuron cell bodies that reside within DRG project into the dorsal SC, and establish precise connections with INs and MNs in distinct laminae along the DV axis. In turn, these MNs innervate target muscles in the periphery to elicit motor reflexes in response to the sensory stimulus received. The precise connectivity of sensory afferents with subpopulations of dorsal INs or ventral MNs is critical for processing sensory information from the periphery (Garcia-Campmany et al., 2010). Thus, to better understand how locomotion is controlled and elicited by the activity of sensorimotor circuits, we must first understand the mechanisms that control functional connectivity between peripheral sensory neurons and spinal MNs.

1.6 PERIPHERAL SENSORY NEUROGENESIS

The DRG houses sensory neuron cell bodies that perceive and translate many types of stimuli (Caspary and Anderson, 2003). They are derived from a heterogeneous population of multipotent NCCs that delaminate from the dorsal neural tube between E8.5-E10, following induction by TGFβ/BMP and Wnt signaling (Marmigere and Ernfors, 2007). The influence of these signals causes neural crest to undergo an epithelial-to-mesenchymal transition, accompanied by massive cytoskeletal rearrangements and the dynamic expression of cell adhesion molecules that allow these cells to become highly motile. With a ventral-lateral trajectory, the NCCs initiate migration and merge into the DRG, where they undergo massive proliferation and subsequent specification and

differentiation. The expression of proneural factors with bHLH TFs in NCCs correlates with differentiation of sensory neurons and generation of distinct sensory subtypes (Lallemend and Ernfors, 2012). As a result of differentiation, three major types of sensory neurons are established: mechanoreceptive that perceive touch, nociceptive that perceive pain and proprioceptive that provide information about limb positioning for self-orientation (Figure 1.2) (Caspary and Anderson, 2003). After the completion of differentiation by E11, sensory neurons are distinguished by their differential expression of tyrosine kinase (*Trk*) neurotrophin receptors. Mechanoreceptors express *TrkB*, nociceptors express *TrkA* and proprioceptors express *TrkC*, which specifically mediates the activity of its ligand, neurotrophin-3 (NT3). Trk receptor signaling controls many aspects of late DRG neuron differentiation and survival, and has been shown to participate in laminar target selection by sensory afferents (Klein et al., 1994; Lin et al., 1998).

The axons of distinct DRG sensory neuron subtypes begin innervating the dorsal SC as early as E13.0 (Caspary and Anderson, 2003). The afferents project along a common pathway through the dorsal root entry zone (DREZ), but upon innervating the dorsal SC they pursue distinct trajectories towards their target zones (Golding and Cohen, 1997). Afferents terminate in different laminar target zones depending on the type of sensory stimuli being transmitted. Nociceptive and mechanoreceptive neurons terminate in the dorsal SC where they make synapses with sensory IN groups. Conversely, the afferents of proprioceptive neurons extend towards the intermediate SC and are then distinguished by the extent of the ventral trajectory. Group 1a afferents project to the ventral horn where they make monosynaptic connections directly with

locomotor MNs (Chen et al., 2003). The selection of laminar termination made by sensory afferents is highly important to establish the proper sensory connectivity necessary to process the appropriate sensory stimulus (Chen et al., 2006).

1.7 REGULATION OF PROPRIOCEPTIVE SENSORIMOTOR CIRCUIT ASSEMBLY

Locomotion is facilitated by the activity of proprioceptive sensorimotor circuits, which integrate, process and respond to anatomical and positional cues provided by proprioceptors in the periphery (Dietz, 2002). The selective expression of a vast number of molecular factors, including neurotrophic factors, TFs and target-derived retrograde signals are essential for the cell survival of proprioceptive sensory neurons and proper innervation of peripheral target muscles (Figure 1.5) (Klein et al., 1994; Lin et al., 1998; Arber et al., 2000; Inoue et al., 2002; Usui et al., 2012).

Genetic studies in mice provide evidence that projection of 1a afferents to the SC and establishment of sensorimotor connections is controlled by the differential expression of TFs (Arber et al., 2000; Levanon et al., 2002). A Runt class transcription factor, *Runx3*, is selectively expressed by proprioceptive DRG neurons [103]. It regulates circuit assembly by contributing to the cell survival of proprioceptive neurons in the DRG (Levanon et al., 2002). Selectivity by which 1a afferents project to different cellular target zones in the SC is regulated by response to gradations in levels of *Runx3* activity (Inoue et al., 2002; Chen et al., 2006). Inactivation of *Runx3* severely disrupts projection of 1a afferents to the ventral SC, instead they remain in the dorsal SC (Levanon et al., 2002). These studies show that *Runx3* has a primary role in directing the projection of proprioceptive sensory afferents.

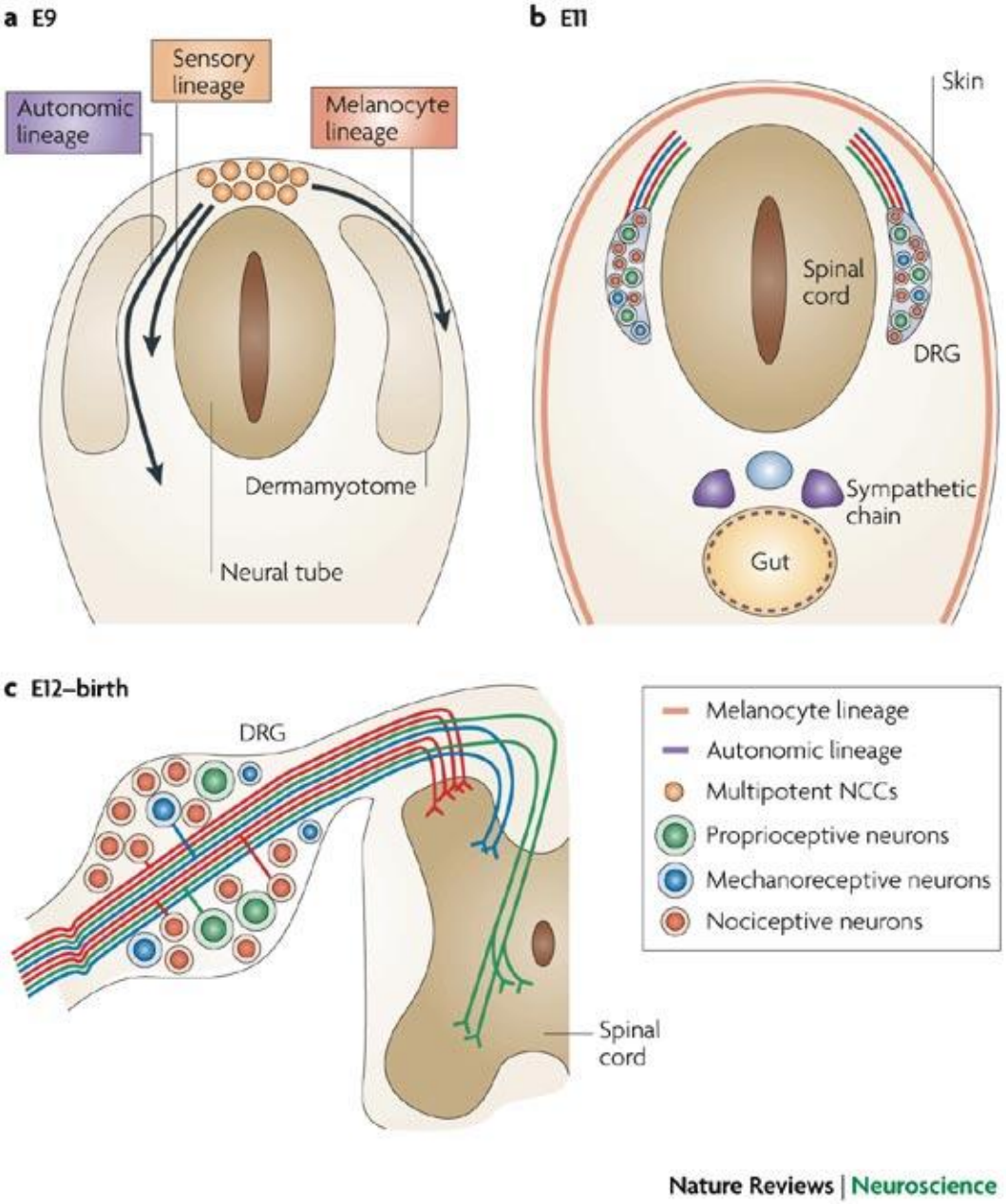
a E9
Sensory lineage
Autonomic lineage
Melanocyte lineage
Dermamyotome
Neural tube
b E11
Skin
Spinal cord
DRG
Sympathetic chain
Gut
c E12–birth
DRG
Spinal cord
Melanocyte lineage
Autonomic lineage
Multipotent NCCs
Proprioceptive neurons
Mechanoreceptive neurons
Nociceptive neurons
Nature Reviews | Neuroscience

Figure 1.2

Figure 1.2 - Peripheral Sensory Neurogenesis. (a) Neural crest cells (NCCs) from the trunk delaminate from the dorsal-most aspect of the neural tube and migrate ventrally before they begin to coalesce to generate cells of the dorsal root ganglion (DRG; sensory lineage), and sympathetic and enteric neurons (autonomic lineage). Otherwise, NCC take a dorsolateral pathway to colonize the skin with melanocytes. (b) During NCC development, the cells commit to a sensory neuron fate and differentiate into three principal subpopulations: nociceptive, mechanoreceptive and proprioceptive neurons. (c) Laminar termination in the spinal cord is determined after the specification of DRG sensory neurons. The axons of nociceptive neurons terminate in superficial layers of the dorsal spinal cord, mechanoreceptors in deep layers of the dorsal spinal cord, and proprioceptive terminate in the intermediate zone and ventral spinal cord. E, embryonic day. This figure was originally published in Marmigere, F. and P. Ernfors (2007). "Specification and connectivity of neuronal subtypes in the sensory lineage." Nat Rev Neurosci 8(2): 114-127. The manuscript can be accessed with the URL: www.nature.com/nrn/journal/v8/n2/full/nrn2057.html.

A member of the ETS TF family, *Er81,* functions indirectly to enhance the activity of Runx3. It has also been shown to regulate axonal entry of 1a afferents into the ventral horn. *Er81* expression is required for differentiation of muscle spindles and induced by skeletal muscle derived *NT3*. *NT3* expressed by developing muscle spindles also induces broad expression of *Er81* in proprioceptive neurons and along the length of their afferents. *Er81* deficient mice lack differentiated muscle spindles and display premature termination of axons in the intermediate SC, nearly disrupting all monosynaptic connections with α-MNs. As a consequence, mice carrying the *Er81*-null mutation develop ataxia, a defect in motor coordination (Arber et al., 2000).

Neurotrophins are a family of proteins that are potent factors for sensory neuron survival in the CNS and PNS (Liu and Jaenisch, 2000; Ernfors, 2001; Chen et al., 2002). In turn, these proteins are important for the establishment of sensorimotor connections. In proprioceptive neurons, the activity of *NT3* is mediated through its receptor, *TrkC*. *NT3* is expressed by muscle spindles, and induces *ER81* in proprioceptive sensory neurons which is crucial for central connectivity within the SC. In *NT3* deficient mice, proprioceptive DRG neurons die before their axons are able to invade muscles to initiate the differentiation of muscle spindles. Thus, these mutants lack functional muscle spindles and SC sensory innervation (Ernfors et al., 1994). Similarly, limb ablation studies in the chick result in the elimination of $TrkC^{+}$ proprioceptive neurons and decreased innervation of ventral MNs (Oakley et al., 1995; Oakley et al., 1997). This demonstrates expression of *TrkC* in proprioceptive DRG neurons is necessary for their survival and to mediate the activity of its ligand *NT3* in the periphery to initiate spindle formation. Thus, *TrkC* not only consolidates the

differentiation program for proprioceptive neurons, but it is also important for the assembly of a functional proprioceptive circuit (Klein et al., 1994). Furthermore this exemplifies the importance of target-derived trophic factors from muscles like *NT3*, for the establishment of sensorimotor connectivity.

Recently, elegant genetic studies have demonstrated the involvement of axonal guidance molecules in development of sensorimotor circuitry in the SC (Gagliardini and Fankhauser, 1999; Ben-Zvi et al., 2008; Ben-Zvi et al., 2008; Maro et al., 2009). Members of the plexin family are important receptors mediating the activity of secreted semaphorins. Both are differentially expressed in the SC. *PlexinA1* and *PlexinD1* are expressed by proprioceptive 1a afferents. Whereas, *Sema6c* and *Sema6d* are dynamically expressed in the dorsal SC and *Sema3e* is expressed in a subset of ventral MNs (Cohen et al., 2005). Upon genetic inactivation of *PlxnA1* signaling, proprioceptive axons follow an aberrant trajectory through the dorsal SC disrupting innervation of cutaneous axons. Although the afferents are misguided, they still appear to make monosynaptic connections with their intended ventral MN targets (Yoshida et al., 2006). Furthermore in a study manipulating the signaling of S*ema3e* or *PlxnD1*, the pattern of monosynaptic sensorimotor connections is perturbed while having no effect on the segregation of MNs into motor pools (Pecho-Vrieseling et al., 2009). These data revealed that semaphorin-plexin signaling is a crucial determinant of sensorimotor circuitry in the developing SC. Recently, a study characterizing the expression of another plexin family member, *PlxnA4*, found that it localized with α-bungarotoxin at the NMJ, implying an as of yet unknown role in synaptic function between locomotor MNs and target muscles in the periphery (Gutekunst et al., 2012).

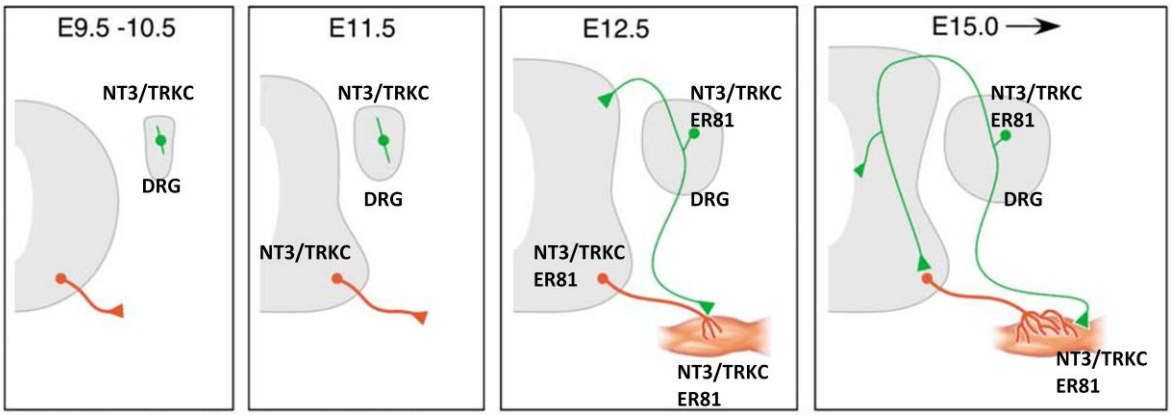

Adapted from Koo et al. *Neuron* **26** (2002)

Figure 1.3

Figure 1.3 - Molecular Regulation of Proprioceptive Circuit Formation. (a) Between E9.5-E10.5, the axons of MNs born in the ventral SC begin extending into the periphery to innervate muscle targets at later stages. In the DRG, expression of *TrkC* and *NT3* specifies proprioceptive sensory neurons. (b) At E11.5, The axons of proprioceptive sensory neurons start projecting dorsally and ventrally. *NT3* and *TrkC* expression in MNs helps to establish synaptic connections in the periphery. (c) By E12.5, both motor and sensory axons have establish function synapses with muscle targets in the periphery due to the expression of *NT3* and *TrkC*. Expression of *NT3* induces the onset of *Er81* expression in sensory neurons, MNs and muscle spindles. The combinatorial expression of these genes helps guide sensory axons to the dorsal SC. (d) At E15, the sensory axon has established functional synapses with ventral MNs. This figure was originally published in Koo, S. J. and S. L. Pfaff (2002). "Fine-tuning motor neuron properties: signaling from the periphery." Neuron 35(5): 823-826. The original figure is shown here in full and has been modified by the inclusion of text. The host-manuscript can be accessed with the URL: http://www.sciencedirect.com/science/article/pii/S089662730200870X.

In the SC, MNs with similar muscle targets or input from sensory afferents are grouped together in distinct motor columns and motor pools. Therefore, in addition to the expression of molecular factors important for circuit assembly, the matching of 1a afferents with MNs is also controlled anatomically by the post-migratory topographic positioning of MN subtypes in the ventral SC (Levine et al., 2012; Tripodi and Arber, 2012). Similar to other constituents of the proprioceptive sensorimotor circuit, MNs contain combinatorial genetic expression profiles of neurotrophic factors and ETS TFs, which regulate molecular mechanisms underlying the sorting of MNs into distinct motor pools and connective patterning of their efferent and afferent projections (Lin et al., 1998; Dalla Torre di Sanguinetto et al., 2008). *Er81* is expressed by a subset of MNs in the LMC and has been proposed to control central connectivity through this expression. The onset of *Er81* expression within distinct MN populations correlates with the developmental stage (E12.5) in which their motor axons innervate their muscle targets, which also express *ER81* (Arber et al., 2000; Livet et al., 2002). Following limb ablation studies, *Er81* fails to be induced in MNs (Oakley et al., 1997). This likely occurs due to the retrograde transport of target-derived neurotrophic signals from within the muscle such as NT3, which is necessary to induce the activity of *Er81* (Patel et al., 2003). This mechanism facilitates proper NMJ formation between motor axon collaterals and target flexor/extensor muscles in the periphery. This data shows that ETS factor *Er81* has the ability to control late stages of proprioceptive sensorimotor connectivity. The expression profile for this gene implicates its importance in the assembly of each component of the proprioceptive sensorimotor circuit.

1.8 MONOSYNAPTIC STRETCH REFLEX (MSR) CIRCUIT

The simplest sensorimotor circuit mediating proprioception and facilitating locomotion is the MSR circuit (Chen et al., 2003; Kiehn, 2006; Kiehn, 2011). While the synaptic connections made are highly precise, the constituents of the MSR circuit are easily accessible for genetic and anatomic investigation and provide an excellent system to study developmental events of neural circuit formation (Grillner and Jessell, 2009). It consists of two functional units: a sensory unit and a motor unit (Figure 1.3) (Goulding et al., 2002; Chen et al., 2003; Kiehn, 2006; Goulding, 2009; Kiehn, 2011). The proprioceptive sensory unit relays information about the position, tension and length of limb muscles to the CNS (Chen et al., 2003). It is composed of proprioceptors embedded in the muscle (muscle spindles), and DRG proprioceptive neurons which peripherally innervate muscle spindles then subsequently translate the message along its axon (Ia afferent) to the motor unit. Muscle spindles are proprioceptive sensory structures that perceive changes in muscle tension and length during motor activity and are essential for accurate reflex responses.

The motor unit controls muscle reflexes according to the sensory signal it receives. It consists of α-MNs in the ventral horn of the SC and receives direct excitation from the proprioceptive Ia afferent through a monosynaptic (single synaptic) connection. α-MNs target the same muscle in the periphery it received the sensory message from, conjoining the two units and completing the stretch-reflex circuit (Chen et al., 2003). To ensure specificity in the synaptic connections that propagate the MSR, a vast number of TF families, cell guidance molecules and target derived retrograde signals (neurotrophic factors) are required (Arber et al., 2000; Goulding et al., 2002; Goulding, 2009).

Sensory Unit	Motor Unit
Muscle Spindle	α – motor neuron
1a afferent	

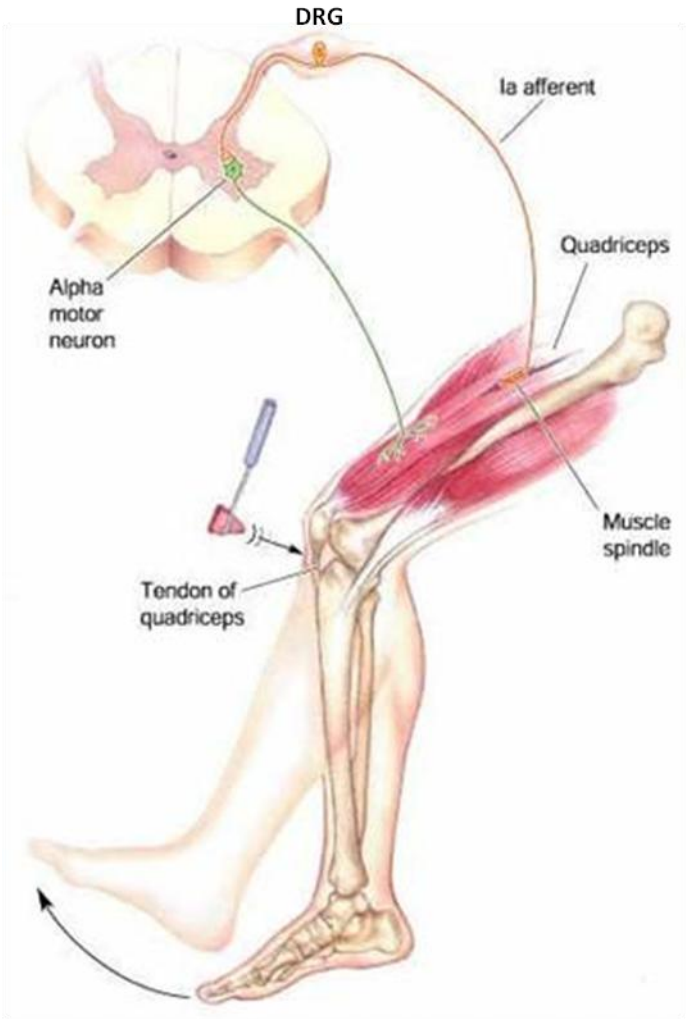

Figure 1.4

Figure 1.4 - Monosynaptic Stretch Reflex Circuit. The MSR circuit is comprised of two functional units: a sensory unit and a motor unit. The sensory system relays information about the length of a muscle to CNS, whereas the motor unit controls muscle contractions as a form of reflex. The sensory unit is composed of stretch-sensitive receptors embedded within muscle known as muscle spindles, which are innervated by axons of proprioceptive sensory neurons housed in the dorsal root ganglion. The proprioceptive neuron also extends an axon into the CNS called the 1a afferent which makes a single or monosynaptic connection directly with the motor unit. The motor unit consists of alpha motor neurons in the ventral SC, each of which projects back into the periphery to innervate the same muscle group in which it received its sensory input from. The anatomical drawing used in this figure can be located with the URL: http://grants.hhp.coe.uh.edu/clayne/6397/unit7.htm

GASTRULATION BRAIN HOMEOBOX GENES

The gastrulation brain homeobox (*Gbx*) genes encode two closely related and evolutionarily conserved HD-containing TFs, GBX1 and GBX2 (Murtha et al., 1991). Amino acid sequences between members of the Gbx family are largely conserved, with highest homology occurring in proline-rich regions and the HD (Matsui et al., 1993; Matsui et al., 1993; Chapman and Rathjen, 1995). The most defining feature of the Gbx family is a highly conserved 60 amino acid DNA-binding domain, which differs by just three amino acids, accounting for 97% sequence identity (Waters et al., 2003). In addition to having highly conserved functional domains, *Gbx1* and *Gbx2* expression domains overlap in several areas of the developing CNS, including the forebrain, anterior hindbrain and SC. Observation of overlapping expression domains implicate possible overlapping functional roles.

Using *in situ* hybridization assays, comparative mRNA expression patterns for *Gbx1* and *Gbx2* have been well characterized throughout murine embryonic development (Waters et al., 2003; Rhinn et al., 2004; John et al., 2005). Transcripts for both genes are first detected in the embryo proper at embryonic day 7.5 (E7.5). While *Gbx1* expression is confined to the mesodermal and ectodermal layers, *Gbx2* is expressed throughout all three germ layers, including the endodermal layer. By E8.5, their expression is broadly detected in the neural folds, with *Gbx1* extending caudally from rhombomere (r) 3 and *Gbx2* extending caudally from the mid-hindbrain boundary. At E9.0, *Gbx1* is expressed within neural crest cell populations emanating from r4 and r6/r7, the pericardio-peritoneal canal and the optic vesicle. At E10.5, *Gbx1* is also detected in the medial ganglionic eminence forebrain structure, genital primordium and

broadly along the SC ventricular zone. At E10.5,*Gbx2* is additionally expressed in fore- and hind-limb buds, diencephalon, and in dorsal and ventral SC (Waters et al., 2003). By E12.5, *Gbx2* also becomes expressed in the medial ganglionic eminence forebrain structure.

It is important to note a dynamic change of *Gbx* gene expression in the SC throughout embryonic development. At E9.0, *Gbx1* mRNA transcripts are broadly detected within the ventricular zone of the developing SC. At E10.5, *Gbx2* is heavily expressed in the dorsal ventricular and mantle zones and two ventral lateral stripes corresponding to engrailed-1 expressing domains. The expression of *Gbx1* becomes restricted to the dorsal mantle zones by E12.5, overlapping significantly with the *Gbx2* expression remaining in the dorsal mantle zones. Interestingly, as *Gbx1* expression persists throughout the remainder of development, *Gbx2* mRNA expression in the SC is rapidly downregulated after E12.5 (John et al., 2005).

1.9 FUNCTIONAL ROLES OF GBX WITHIN THE DEVELOPING CENTRAL NERVOUS SYSTEM

While the domains of expression for *Gbx1* and *Gbx2* overlap in many instances throughout development of the CNS, so far, overlapping functional roles have only been identified in the anterior hindbrain, and have yet to be investigated in the SC. Interestingly, there is accumulating evidence demonstrating that many closely related DNA-binding TFs with overlapping expression domains are genetically redundant and able to functionally compensate for family members having reduced levels of expression due to hypomorphic or inactivation mutations (Hanks et al., 1995; Urbanek et al., 1997; Tourtellotte et al., 2000; Relaix et al., 2004). This notion was recently demonstrated in a

zebrafish study, in which Gbx genes function redundantly in morphogenesis and subsequent differentiation (Su et al., 2014). Hence, the transient, partially overlapping expression domains of *Gbx1* and *Gbx2* in the developing SC raises the possibility that genetic and/or functional redundancy between *Gbx* genes may also occur in this region of the CNS. Both GBX proteins co-localize with $PAX2^+$ INs in the dorsal mantle zones beginning at E12.5 (John et al., 2005; Luu et al., 2011; Del Barrio et al., 2013; Meziane et al., 2013). In the ventral SC, it has been shown through fate mapping analyses that $Gbx2^+$ cell lineage gives rise to a subset of MNs (Luu et al., 2011). Importantly, *Gbx* loss-of-function mutants display a marked depletion of subsets of $ISL1^+$ MNs (Luu et al., 2011; Buckley et al., 2013). However, like homologs of many transcription factor families, homozygous inactivation of *Gbx1* or *Gbx2* in mice, reveal very different consequences (Wassarman et al., 1997; Buckley et al., 2013; Meziane et al., 2013)

The *Gbx* genes have been shown through recent studies, as essential for correct patterning and maintenance of neurons and MNs along the AP axis of the developing neural tube (Wassarman et al., 1997; Liu and Joyner, 2001; Li et al., 2002; Waters and Lewandoski, 2006; Burroughs-Garcia et al., 2011; Luu et al., 2011; Roeseler et al., 2012; Buckley et al., 2013). The most characterized member of the *Gbx* family, *Gbx2*, has a defined role in CNS development where it is indispensible for the establishment and maintenance of the mid-hindbrain organizer, and proper formation of anterior hindbrain rhombomere (r)1-r3 (Wassarman et al., 1997; Joyner et al., 2000; Li et al., 2002; Waters and Lewandoski, 2006; Roeseler et al., 2012). However, it was not until recently that the lineage and function of *Gbx2* in SC development was studied. Fate mapping studies have demonstrated that a subset of $ISL1^+$ ventral MNs as well as

PAX2^{+} dorsal and ventral INs of the SC are derived from the *Gbx2* lineage (Luu et al., 2011). Furthermore, inactivation of *Gbx2* reveals a requirement for correct SC patterning by maintaining the proliferative status of dorsal progenitors (Luu et al., 2011).

In comparison, the functional necessity of *Gbx1* in CNS development has only began to be elucidated. The most thorough characterization for GBX1 demonstrates colocalization of GBX1 with a set of TFs unique to dILA inhibitory dorsal spinal INs, LBX1, LHX1/5 and PAX2 (John et al., 2005). Recently, a functional study of *Gbx1* has demonstrated a requirement in the maturation of the late-born GABAergic neuronal subtype, dILA sensory INs (Meziane et al., 2013).

One of the most elegant methods to study the role of a gene is to genetically manipulate it *in vivo* for loss-of-function studies. Our data has provided evidence for a novel requirement for *Gbx1* in promoting normal locomotor output through analysis of a murine mutant null for the *Gbx1* allele (Buckley et al., 2013; Meziane et al., 2013). Herein, we show that genetic inactivation of this gene disrupts the two major components of proprioceptive locomotor circuits, the innervation of proprioceptive sensory afferents into the dorsal SC and number of ventral MNs (vMNs) during mid-developmental stages (Figures 2.6 and 2.8). Collectively these studies demonstrate the importance of *Gbx1* in development of INs and MNs within the dorsal and ventral SC that are constituents of locomotor neural circuits.

CHAPTER 2

CHARACTERIZATION OF THE *Gbx1*$^{-/-}$ MOUSE MUTANT: A REQUIREMENT FOR *Gbx1* IN NORMAL LOCOMOTION AND SENSORIMOTOR CIRCUIT DEVELOPMENT

[This work was published in PLoS ONE, 2013, Vol. 8(2), p. 1-16]

Desirè M. Buckley[1,2,4], Jessica Burroughs-Garcia[1,2,4], Mark Lewandoski[3], Samuel T. Waters[1,2]

1 Division of Biological Sciences, University of Missouri, Columbia, Missouri, USA, **2** Christopher S. Bond Life Sciences Center, University of Missouri, Columbia, Missouri, USA **3** Cancer and Developmental Laboratory, National Cancer Institute, National Institutes of Health, Frederick, Maryland, USA **4** Equal contribution to manuscript

2.1 ABSTRACT

The Gbx class of homeobox genes encodes DNA binding transcription factors involved in regulation of embryonic central nervous system (CNS) development. *Gbx1* is dynamically expressed within spinal neuron progenitor pools and becomes restricted to the dorsal mantle zone by embryonic day (E) 12.5. Here, we provide the first functional analysis of *Gbx1*. To identify the function of *Gbx1* in development of the nervous system, we created a conditional *Gbx1* (floxed) allele in which exon 2 that contains the functional homeodomain is flanked with loxP sites, enabling us to convert it to a null allele via Cre-mediated recombination. In contrast to mice homozygous for a loss-of-function allele of Gbx2, mice homozygous for the *Gbx1* null allele, $Gbx1^{-/-}$, are viable and reproductively competent. However, $Gbx1^{-/-}$ mice display a profound locomotive defect that specifically affects hindlimb gait. Analyses of embryos homozygous for the *Gbx1* null allele reveal abnormal projection of proprioceptive sensory afferents into the dorsal SC suggesting a disorganized assembly of proprioceptive sensorimotor circuitry within the SC. Moreover, we show a marked loss of $ISL1^{+}$ ventral MNs beginning at E14.5. The generation of this null allele has enabled us to functionally characterize a novel role for *Gbx1* in development of the SC. Taken together, these data demonstrate that *Gbx1* function contributes to the development of the neural network that contributes to normal locomotion.

Keywords: *Gbx1*; sensorimotor circuit; proprioceptive; Isl1; motor neuron; development; CNS; spinal cord; movement disorder

2.2 RESULTS

Gbx1$^{-/-}$ mice exhibit a profound locomotive defect

To study the role of *Gbx1* in development of neural networks, we generated mice carrying a conditional *Gbx1* allele (*Gbx1*^{flox}), by flanking exon 2 that contains the sequence encoding the functional DNA-binding homeodomain with *lox*P sequences (Fig. 2.1A, materials and methods). Accurate recombination of the short and long homology arms into the endogenous *Gbx1* locus of embryonic stem (ES) cells was confirmed through Southern blotting using XbaI and NdeI/XbaI digested genomic DNA, respectively, (Fig. 2.1B) and PCR (Fig. 2.1C). Germline transmission of the *Gbx1*^{flox} allele was determined by PCR and *Gbx1*$^{flox/+}$ heterozygotes were intercrossed to obtain mice homozygous for the *Gbx1*$^{flox/flox}$ allele. Unlike *Gbx2*$^{neo/neo}$ mice, which die at the day of birth (Wassarman et al., 1997; Waters et al., 2003), *Gbx1*^{flox} homozygotes are viable and do not display any overt behavioral phenotypes. Therefore, to eliminate *Gbx1* function, *Gbx1flox/flox* mice were mated with transgenic mice that express a DNA recombinase gene in the early embryo under the control of human β *-actin* regulatory elements (Lewandoski et al., 1997). This resulted in mice with the genotype *Gbx1*$^{-/+}$. *Gbx1*$^{-/+}$ heterozygotes were then intercrossed to generate *Gbx1* null mutants (*Gbx1*$^{-/-}$). We examined if mRNA expression in exon 2, which encodes the functional DNA-binding homeodomain is absent in *Gbx1*$^{-/-}$ mice. We analyzed wild-type and *Gbx1*$^{-/-}$ embryos by in situ hybridization at E 9.5, using *Gbx1* full-length and *Gbx1* exon 2-specific probes. A comparison in wild-type embryos shows that expression of full-length (Fig. 2.2A and 2.2D) and exon 2-specific probes (Fig. 2.2B and 2.2E) are identical. Exon 2 expression is absent in *Gbx1*$^{-/-}$ embryos, indicating that the

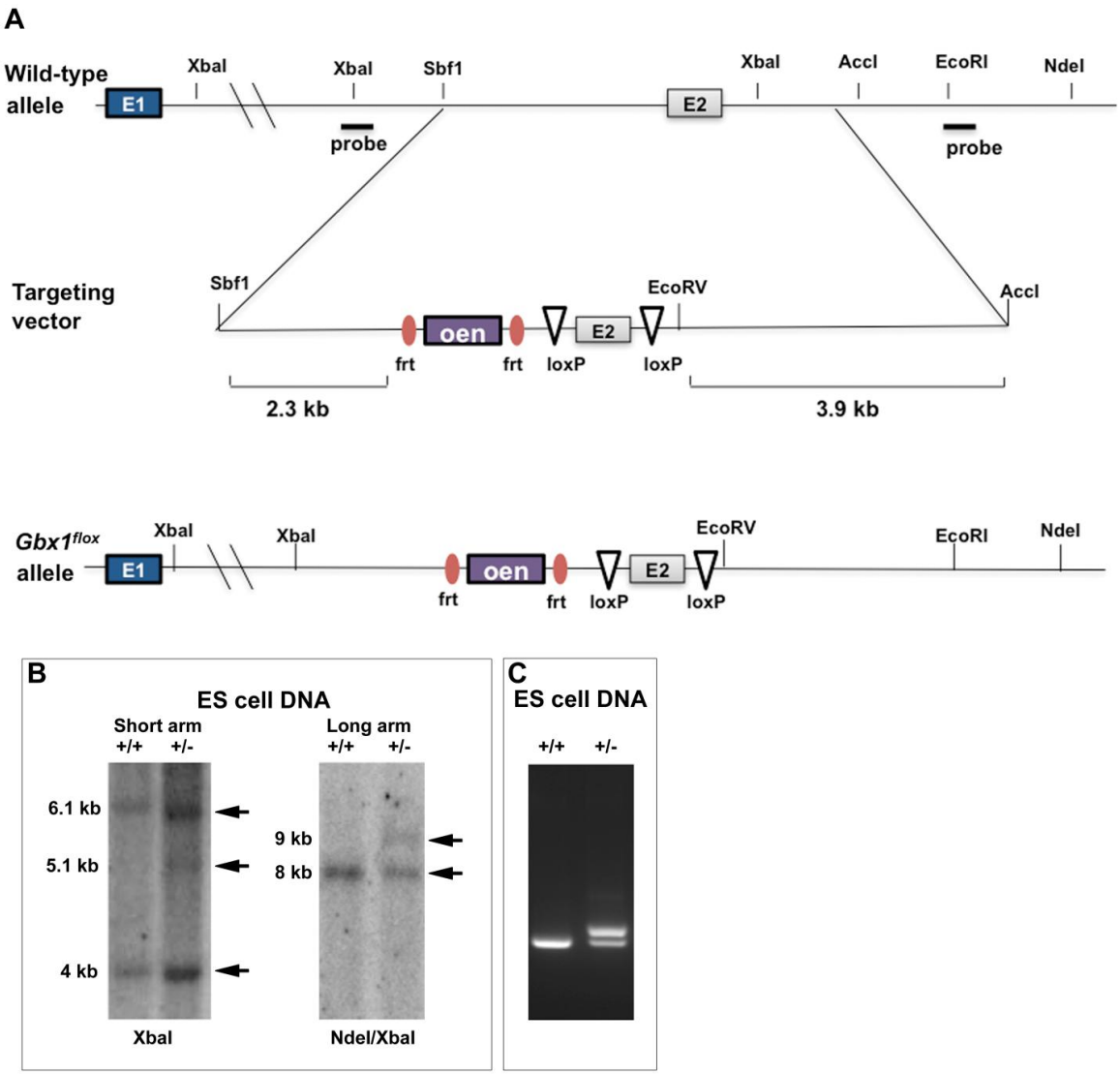
A
Wild-type allele
XbaI
XbaI
Sbf1
XbaI
AccI
EcoRI
NdeI
E1
E2
probe
probe
Targeting vector
Sbf1
EcoRV
AccI
oen
E2
frt
frt
loxP
loxP
2.3 kb
3.9 kb
Gbx1flox allele
XbaI
XbaI
EcoRV
EcoRI
NdeI
E1
oen
E2
frt
frt
loxP
loxP
B
ES cell DNA
Short arm
+/+ +/-
Long arm
+/+ +/-
6.1 kb
5.1 kb
4 kb
9 kb
8 kb
XbaI
NdeI/XbaI
C
ES cell DNA
+/+ +/-

Figure 2.1

Figure 2.1 - Generation of *Gbx1* mutant mice. (A) For the construction of the conditional *Gbx1*-null, *loxP* sites were inserted flanking exon 2 and a neomycin expression cassette was inserted 5' to the flanked region as depicted in the schematic. Deletion of exon 2, thereby rendering the endogenous gene null, is mediated by the mating of a mouse containing the targeted allele with a mouse ubiquitously expressing β-actin Cre. (B) To identify ES cells that properly underwent homologous recombination, the long and short homology arms were screened by Southern Blot of restriction digested genomic DNA. (C) The presence of wild-type and targeted alleles in the progeny derived from targeted ES cells were confirmed by PCR of genomic DNA using specific primer sets. Arrow in (A) represents direction of neo transcription; Arrowheads in (A) represent the location of PCR primers used in (C); Gray box indicates exon 2 (E2), which encodes the *Gbx1* homeodomain; Purple box indicates the *neo* cassette flanked by FRT sites (orange circles); White triangles represent the position of *loxP* sites; ES, embryonic stem cell.

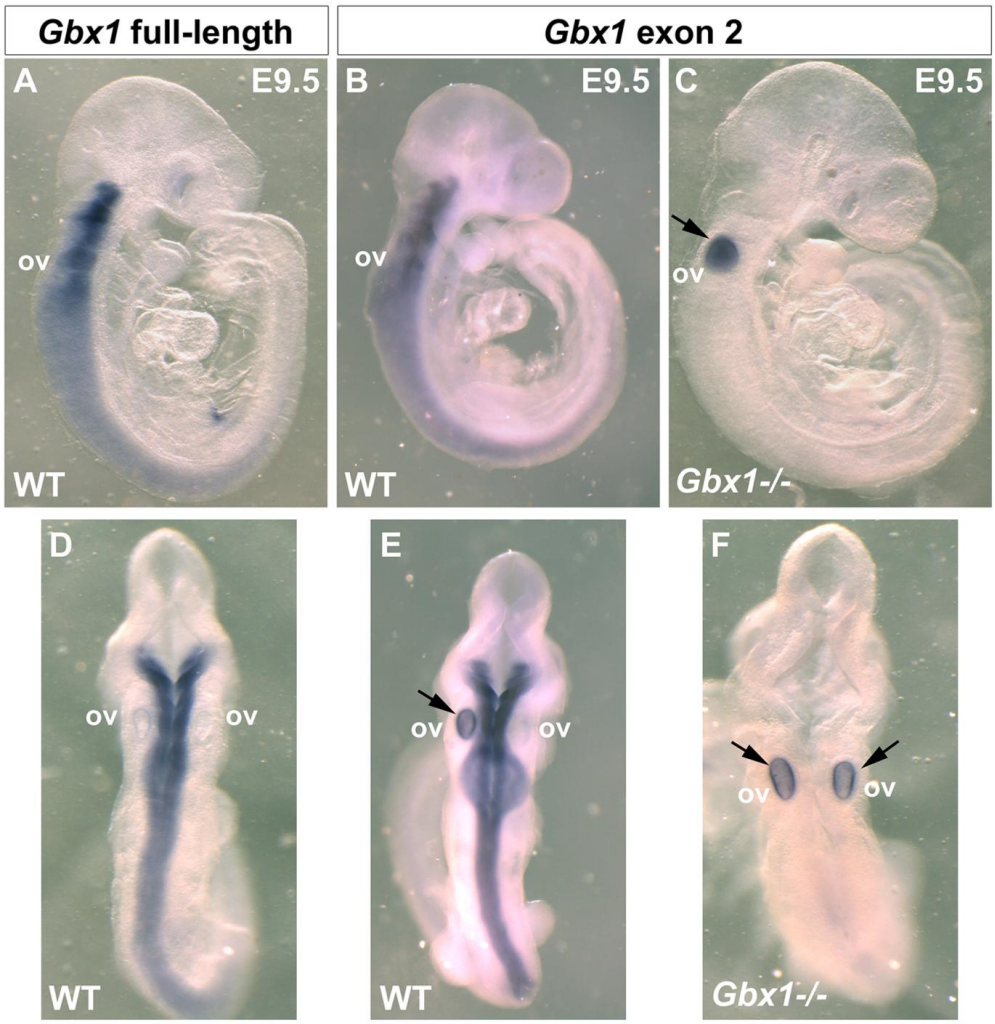
Gbx1 full-length
Gbx1 exon 2
A
E9.5
ov
WT
B
E9.5
ov
WT
C
E9.5
ov
Gbx1-/-
D
ov
ov
WT
E
ov
ov
WT
F
ov
ov
Gbx1-/-

Figure 2.2

Figure 2.2 - The functional homeodomain of *Gbx1* is deleted in *Gbx1*$^{-/-}$ mutants. Wholemount in situ hybridization for *Gbx1* full-length or *Gbx1* exon 2 mRNA at embryonic (E) day 9.5 (A-F). Lateral view, dorsal is to the left (A-C). Dorsal view *Gbx1* (D-F). Full-length expression in a *Gbx1* wild-type embryo. Strong *Gbx1* expression detected within the anterior hindbrain with a lessening gradient as expression extends caudally. Expression not detected within the otic vesicles (A, D). *Gbx1* exon 2 expression in a *Gbx1* wild-type embryo. Expression of sequence encoding the functional HD of GBX1 recapitulates the pattern detected using the full-length RNA probe. Otic vesicle staining observed within the dorsal view is nonspecific (arrow) (B and E). *Gbx1* exon 2 expression in a *Gbx1*$^{-/-}$ embryo. No specific staining observed throughout the entire embryo, demonstrating deletion of the GBX1 functional domain. Otic vesicle staining observed is nonspecific (arrows) (C and F). ov, otic vesicle.

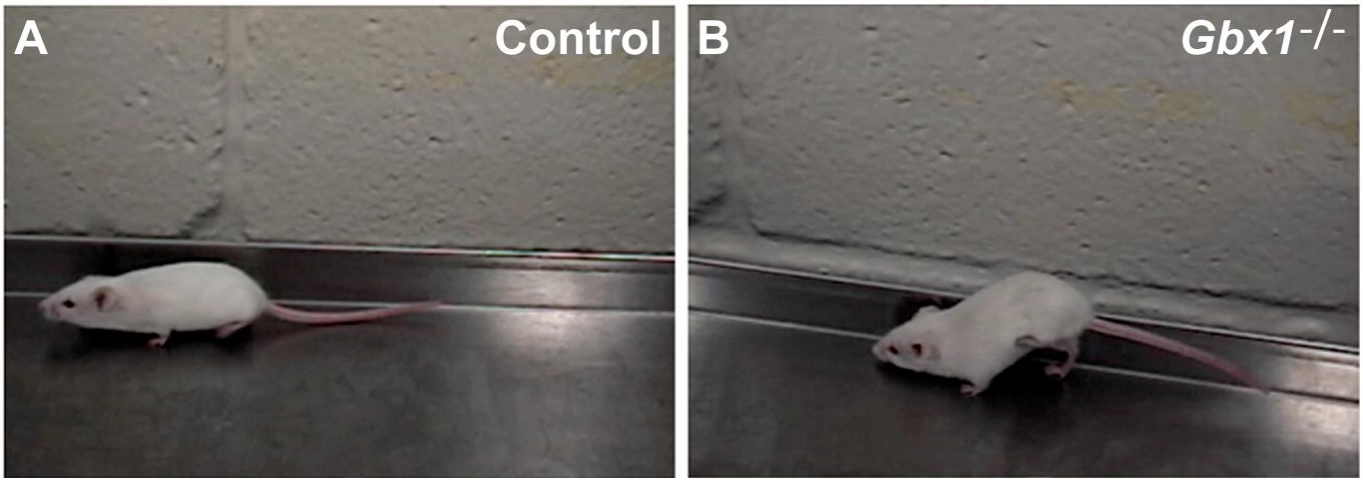

Figure 2.3

Figure 2.3 - *Gbx1*$^{-/-}$ mice display a profound locomotive defect severely affecting hindlimb gait. (A) Photograph depiction of the locomotive phenotype observed in *Gbx1*$^{-/-}$ 3-month-old mouse compared to a (B) *Gbx1*$^{-/+}$ age-matched control embryo.

functional DNA-binding domain has been deleted (Fig. 2.2C and 2.2F). The staining observed in the otic vesicle was due to unspecific trapping of the color precipitate (Fig. 2.2C, E, F). *Gbx1*$^{-/-}$ mice are obtained in a ratio in accordance with mendelian genetics, are fertile, and are as viable through postnatal maturation, as their normal littermate counterparts.

Mice heterozygous for the null mutation displayed no overt behavioral abnormalities. Surprisingly, in *Gbx1*$^{-/-}$ mice, we observe a locomotive defect that specifically, and bilaterally, affects hindlimb gait (Fig. 2.3B). Descriptively, the phenotype is characterized as a prolonged step cycle period with overall increased amplitude of the locomotive rhythm. The abnormal gait is observed as early as P15 and persists at a constant level of severity until death of the animal. While the locomotive defect does not progressively exacerbate in mutant mice, the degree to which the phenotype affects different animals varies, ranging from mild to severe.

Ventral spinal motor neurons appear specified in *Gbx1*$^{-/-}$ embryos

The early onset of *Gbx1* expression in the dorsal and ventral ventricular zone of the SC at E9.0 - E10.5, suggests a role for *Gbx1* in the specification and generation of defined spinal neuronal subpopulations (Waters et al., 2003). We performed a series of immunohistochemical analyses to examine the expression of a panel of molecular markers including, basic helix-loop helix and homeodomain transcription factors, normally expressed within distinct precursor cell populations throughout the dorsal and ventral SC (Purves and Lichtman, 1980). Comparison of *Gbx1*$^{-/+}$ and *Gbx1*$^{-/-}$ embryos at E10.5 did not reveal any apparent differences in expression of these markers (Fig.

2.4A-J). The execution of motor response from sensory stimuli is the result of activated MNs within the ventral SC and subsequent transmission of that signal through axonal projections that target muscles in the periphery. The homeobox gene *Hb9*, is expressed at the onset of motor neurogenesis, E9.5, where it is essential for the specification of MN cell fate and is maintained postmitotically as a critical factor for MN differentiation (Thaler et al., 1999). A key indicator of motor neuron differentiation is the expression of a LIM-homeodomain transcription factor, Islet1 (ISL1), just after exiting the cell cycle which consolidates MN cell fate from pMNs (Pfaff et al., 1996; Lee and Pfaff, 2003)

To address the defective locomotive phenotype exhibited by *Gbx1*$^{-/-}$ mutants, we analyzed the molecular composition of MN populations within the ventral SC using immunohistochemical analyses during several developmental stages of neural generation. At E10.5 - E11.5, no significant difference in expression of HB9 (Fig. 2.5A, 2.5B) and ISL1 (Fig. 2.5C, D) in ventral motor neurons was observed between *Gbx1*$^{-/+}$ and *Gbx1*$^{-/-}$ mice (Figure 2.5I and J). By E11.5 greater than (85%) of the total pMN population has differentiated into motor neurons (Arber et al., 1999). Therefore, these results indicate that the pre-mitotic pMNs that gave rise to the observed postmitotic HB9^{+} and ISL1^{+} ventral spinal MNs at these stages were likely properly specified. Taken together, these data suggest no apparent disruption in the generation of the neuronal population which functions to relay motor output signals to the periphery.

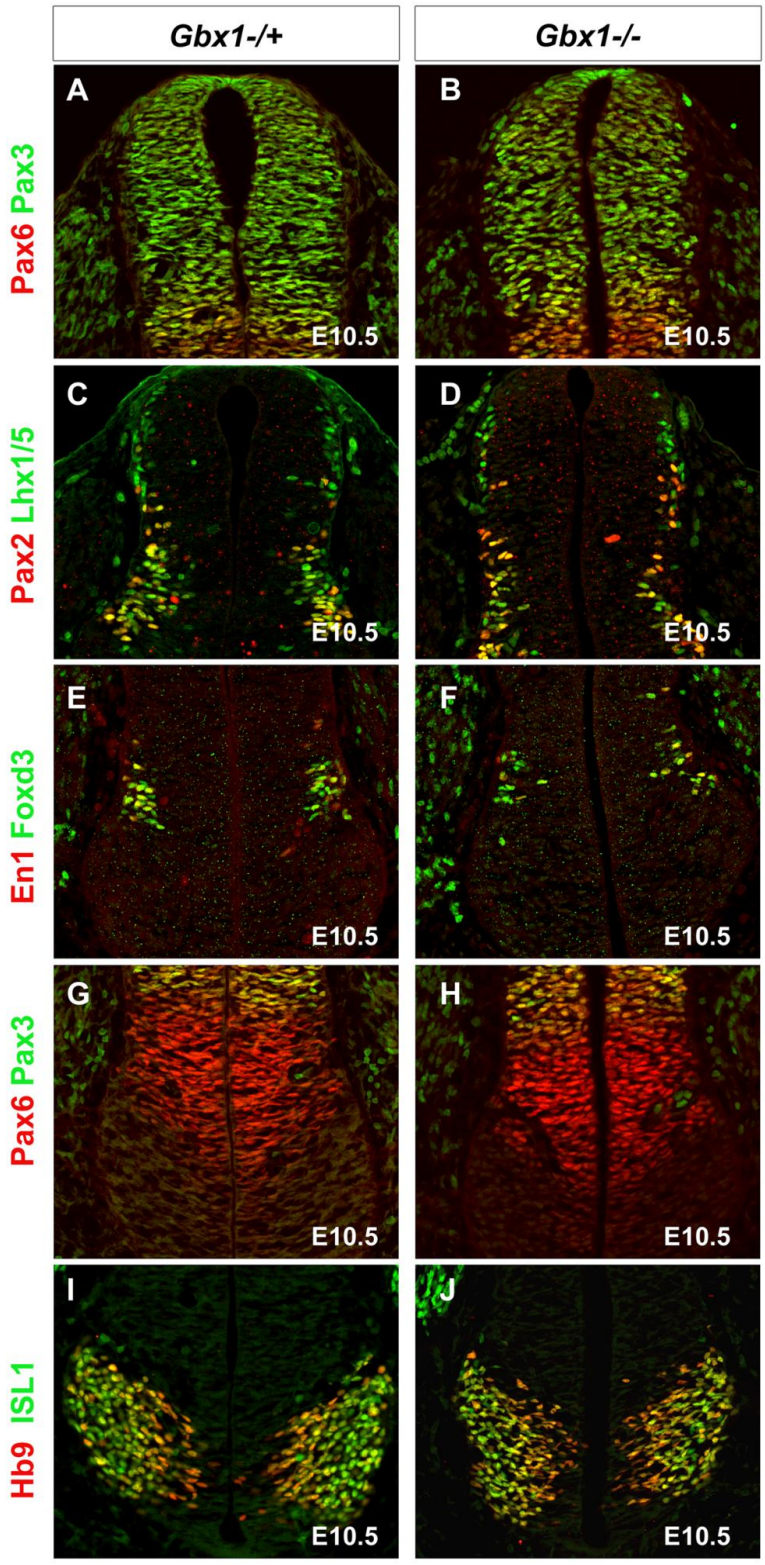
Gbx1-/+
Gbx1-/-
Pax6 Pax3
Pax2 Lhx1/5
En1 Foxd3
Pax6 Pax3
Hb9 ISL1
A
B
C
D
E
F
G
H
I
J
E10.5

Figure 2.4

Figure 2.4 - Deletion of *Gbx1* does not affect the patterning of embryonic developmental markers that direct specification of progenitor cell identity within the neural tube. Immunostaining of E10.5 spinal cords to detect localization of proteins required for the acquisition of distinct spinal neuron progenitor populations: Pax6 [dI4-pMN] and Pax3 [dI1-dI6] (A-B and G-H); Pax2 [dI4, dI6-v1] and Lhx1/5 [dI2, dI4, dI6-v1] (C-D); En1 [v1] and Foxd3 [dI2,v1] (E-F); HB9 [pMN] and ISL1 [pMN] (I-J). The expression domains, including the dorsal and ventral boundaries of the various genetically distinct populations of cells are not perturbed in *Gbx1*$^{-/-}$ mutants (panels in right column), when compared to heterozygous (*Gbx1*$^{-/+}$) age matched controls (panels in left column).

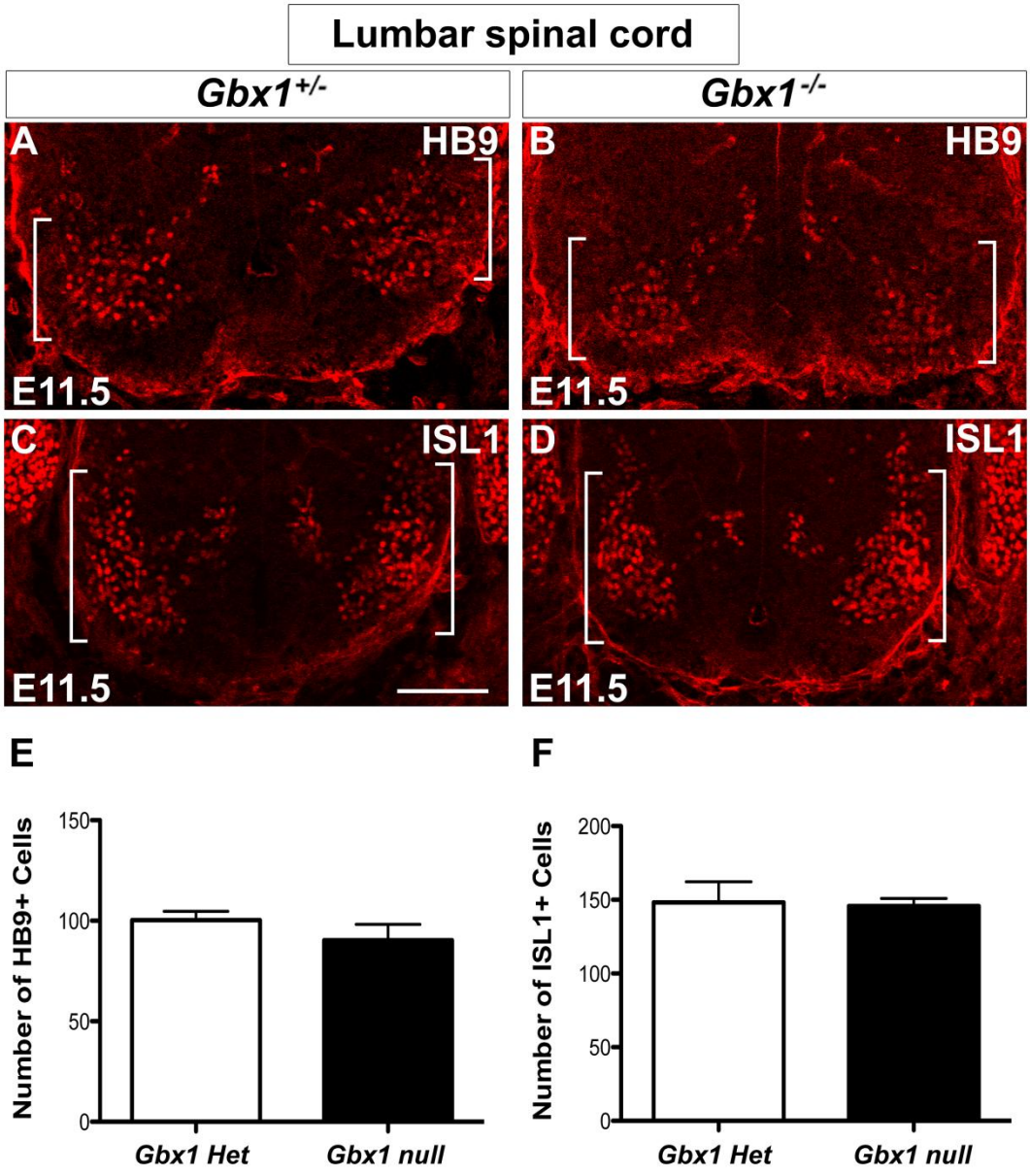
Lumbar spinal cord
Gbx1+/-
Gbx1-/-
A
HB9
E11.5
B
HB9
E11.5
C
ISL1
E11.5
D
ISL1
E11.5
E
Number of HB9+ Cells
150
100
50
0
Gbx1 Het
Gbx1 null
F
Number of ISL1+ Cells
200
150
100
50
0
Gbx1 Het
Gbx1 null

Figure 2.5

Figure 2.5 - Deletion of *Gbx1* does not affect the generation of ventral spinal cord motor neurons. Immunostaining to detect $HB9^{+}$ (A-B) and $ISL1^{+}$ (C-D) motor neurons (indicated by white brackets) at E11.5 in lumbar spinal cord sections. Specification of *Gbx1* null motor neurons appears unaffected (B and D) when compared with normal embryos (A and C). Quantification of $HB9^{+}$ (E) and $ISL1^{+}$ (F) ventral motor neurons in $Gbx1^{-/-}$ embryos at E11.5, reveals no significant differences in the number of immunopositive cells when compared to heterozygous ($Gbx1^{-/+}$) age-matched control embryos. Scale bar represents 100mm. 20X magnification.

Gbx1$^{-/-}$ embryos display abnormal projection of proprioceptive sensory axons and a decrease in Peripherin^{+} ventral motor neurons

Since there was no major difference in molecular composition or gross morphological assembly observed of the motor neuron populations in our *Gbx1* null mutant when compared to the heterozygous (*Gbx1*$^{-/+}$) control at E11.5, we sought to examine the neural systems that synchronize somatosensory stimuli and that might address the locomotive phenotype. Peripherin is a type III intermediate filament protein that is abundantly expressed within developing spinal motor neurons and primary proprioceptive afferent axonal projections in the dorsal spinal cord (Brody et al., 1989; Escurat et al., 1990). To examine anatomical constituents of the proprioceptive modality, we analyzed the expression of peripherin by immunohistochemistry in transverse sections of the lumbar SC during mid-embryonic stages. At E14.5, peripherin expression is observed along the length of primary sensory afferents projecting into the dorsal SC through the dorsal root entry zone (DREZ) and marks a subset of ventral motor neurons, in *Gbx1*$^{-/+}$ embryos (Fig. 2.6A). This expression profile is altered in *Gbx1*$^{-/-}$ embryos at E14.5. While peripherin expression persists within the axonal afferents they appear disorganized with several axons extending ectopically (compare white arrow in Fig.2.6B and 2.6A). In addition, we observed a considerable decrease in peripherin expression within the subset of ventrally marked motor neurons (brackets in Fig. 2.6B). By E15.5, the perturbed assembly of the proprioceptive sensory axon afferents become significantly disarrayed in mutant embryos, displaying a premature termination of ingrowth to their intended target zone and interneural connection, the Ia interneurons (compare white arrow in Fig. 2.6D and 2.6C). Additionally, further

examination of peripherin expression within ventral motor neurons of *Gbx1*$^{-/+}$ and *Gbx1*$^{-/-}$ embryos demonstrates that the significant decrease in expression persists through E15.5 (Fig. 2.6D).

The data shown above through mid-embryonic stages, strongly suggest that components of the proprioceptive system are disrupted in SCs of *Gbx1* null embryos during early stages of motor circuit assembly. However, it is important to note that synaptogenesis and the ontogeny of motor development are not completed until early postnatal stages. To determine if change in the projection of proprioceptive sensory afferent axons persist during late-embryonic and postnatal stages, we assessed the axonal expression of parvalbumin (PV) a marker of proprioceptive neurons. At E17.5 the projection of proprioceptive afferents into the ventral termination zone characteristic of group Ia afferents was nearly absent in *Gbx1*$^{-/-}$ mutants when compared to *Gbx1*$^{-/+}$ embryos (Fig. 2.7A and B). The first phase of postnatal maturation and synaptogenesis occurs between postnatal day (P) 0 and P8 (Siembab et al., 2010). Importantly, we show that the dramatic reduction of proprioceptive afferents into the ventral horn of *Gbx1* mutants persist through P5, a stage when synaptogenesis and proliferation of proprioceptive synapses occurs (Siembab et al., 2010) (Fig. 2.7C and D). Taken together, these data demonstrate that essential components of the proprioceptive system are disrupted in *Gbx1* null embryos, which may serve as a contributing factor to the locomotive phenotype.

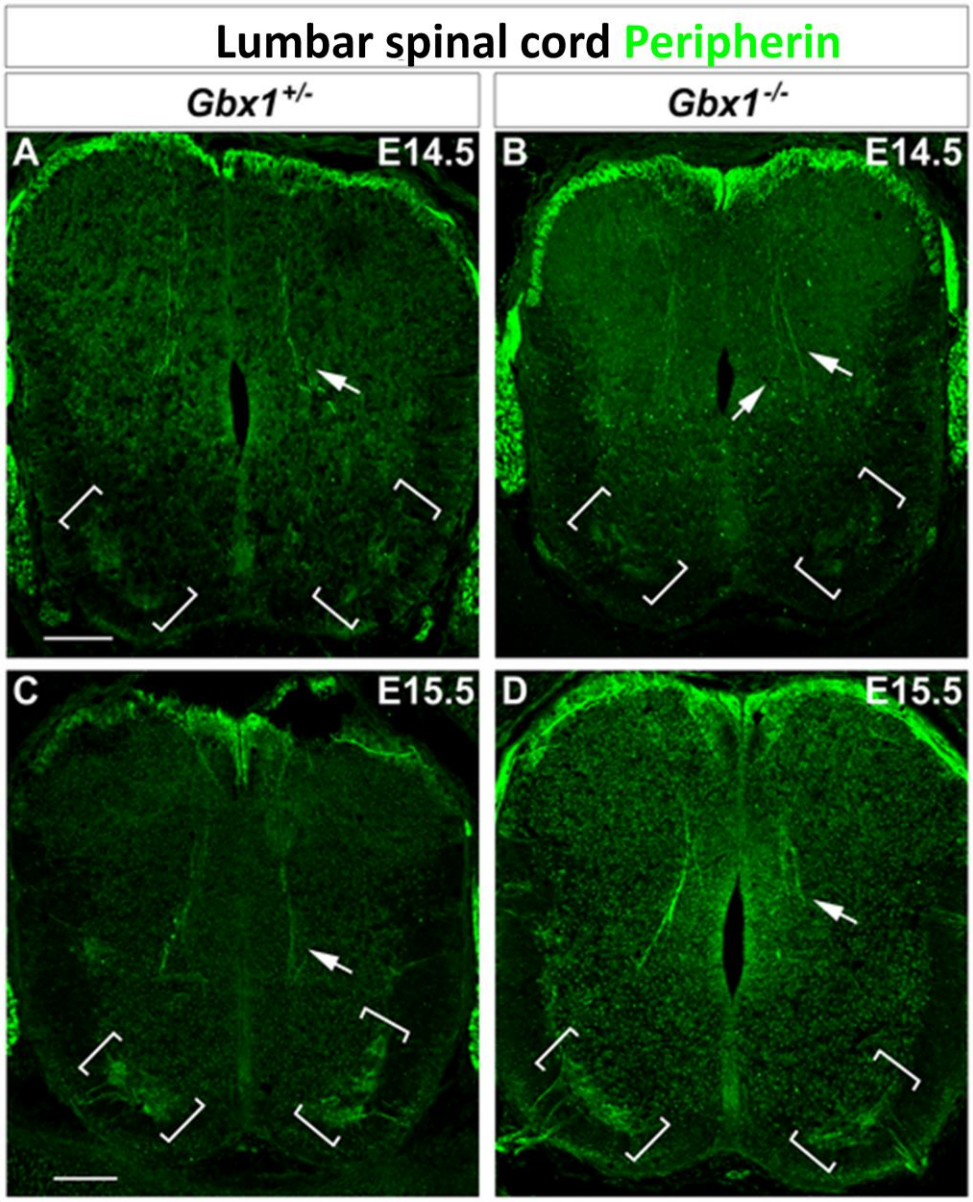
Lumbar spinal cord Peripherin
Gbx1+/-
Gbx1-/-
A
E14.5
B
E14.5
C
E15.5
D
E15.5

Figure 2.6

Figure 2.6 - *Gbx1*$^{-/-}$ embryos display abnormal projection of proprioceptive afferents and decrease in peripherin^{+} ventral motor neurons. Peripherin immunolabeling in lumbar spinal cord sections at E14.5 and E15.5. Arrows indicate proprioceptive afferents extending into the spinal cord. Heterozygous (*Gbx1*$^{-/+}$) control embryos show normal projection of afferents into the intermediate spinal cord (A) and ventral termination zone (C). Many of the proprioceptive afferents fail to project into the ventral spinal cord of *Gbx1*$^{-/-}$ mice (B and D). *Gbx1*$^{-/-}$ embryos also show a marked decrease in the expression of peripherin^{+} ventral motor neurons (brackets) in (B and D) when compared to *Gbx1*$^{-/+}$ embryos (A and C). Scale bars represent 100mm. 10X magnification.

Gbx1$^{-/-}$ embryos display a decrease in both ISL1^{+} and ISL1^{+}/Peripherin^{+} ventral MNs

Since we observed a decrease in the population of peripherin-immunoreactive ventral motor neurons at a later stage of spinal neural development, we chose to revisit and further examine those populations for ISL1, at comparable developmental stages (E14.5 - 15.5). At both stages examined, there is a dramatic reduction in ISL1-immunoreactive ventral motor neurons in *Gbx1*$^{-/-}$ embryos when compared to *Gbx1*$^{-/+}$ embryos (Fig. 2.8A - D). Quantified measurement of the ISL1 immunohistochemical assay reveals a significant reduction in the total number of ISL1^{+} cells in the ventral SC (Figure 2.9B; $P < 0.0001$).

This observation prompted us to investigate whether the subset of motor neurons which lose peripherin immunoreactivity between E14.5-E15.5 are the same subset of motor neurons that lose ISL1 immunoreactivity at the same developmental stage. Thus, we examined SC sections of *Gbx1*$^{-/+}$ (control) and *Gbx1* null embryos co-stained with ISL1 and peripherin. The results show co-localization of ISL1 and peripherin in a subset of ventral motor neurons, in mutant and *Gbx1*$^{-/+}$ control embryos (Figure 2.8E-H). We observed a comparable loss in the expression of ISL1 and peripherin co-immunopositive motor neurons in the vMN pool to that of our single staining analyses. This suggests that the reduced population of ventral cell bodies observed in our previous immunohistochemical assays is the same subset of ISL1^{+} and peripherin^{+} motor neurons. This conclusion is supported by quantification of the ISL1 $^{+}$ peripherin immunopositive cell bodies, which affirms a marked attenuation of the ventral motor neurons in embryos lacking functional *Gbx1* (Figure 9B; $P < 0.0001$). Furthermore, we

show that the significant reduction in ventral ISL1^{+} cells persists through E17.5 in *Gbx1*$^{-/-}$ embryos (Supp. figure 2.1). Together, these results indicate that *Gbx1*$^{-/-}$ embryos suffer from a severe reduction in the number of vMNs expressing the hallmark motor neuron marker, ISL1, and which also express the axonal growth factor peripherin (Portier et al., 1993), likely contributing to the locomotive phenotype.

The population of proprioceptive sensory neuron cell bodies within the dorsal root ganglion remains unaffected in *Gbx1*$^{-/-}$ mutants

Currently, there are no studies identifying a role for *Gbx1* in NC cell development. Recent studies in *Xenopus*, however, indicate that *Gbx2* is the earliest factor in the genetic cascade of NC induction regulated by Wnt signaling (Li et al., 2009). The perturbation of constituents that mediate the internal transmission of the proprioceptive modality in *Gbx1*$^{-/-}$ embryos prompted us to analyze the NC-derived components that initiate proprioceptive perception. We have previously shown that *Gbx1* is expressed in the r4 and r6 NC streams of the anterior hindbrain at E9.0 (Waters et al., 2003). To determine if NC cells are specified and migrate correctly in *Gbx1*$^{-/-}$ embryos, we examined the expression of the NC marker *Sox10* in wild-type and *Gbx1*$^{-/-}$ embryos at E9.5. We observed no apparent differences in *Sox10* expression between wild-type and mutant embryos in the r4/r6 streams or trunk DRG at this stage (Fig. 2.10A-D). The NC-derived cell bodies functionally responsible for integrating spatial orientation of the organism reside in the DRG. Thus, we examined the DRG for the neurotrophic factor TrkC, which is the molecular marker for proprioceptive sensory neuron cell bodies. TrkC^{+} neurons are generated during the first two, of three waves of sensory neuron genesis occurring between E9.5 - E14.5 (Ma et al., 1999). Furthermore, the

diversification of sensory subtypes generated during the first and second waves to those that functionally implement proprioceptive stimuli occurs at E14.5, through the co-expression of the RUNX family transcription factor *Runx3* and TrkC (Levanon et al., 2002). Our immunohistochemical analysis showed no overt differences to the morphology of the $TrkC^{+}$ pool of neurons between our mutant and $Gbx1^{-/+}$ control animals (Fig. 2.11A, B). Quantification of the total number of individual $TrkC^{+}$ cell bodies reinforced the notion that the proprioceptive sensory neuron pool is unaffected in $Gbx1^{-/-}$ mutant embryos (Fig. 2.11C). This data provides evidence that the population that defines the origin of the proprioceptive modality is properly established in early stages of development in mutant embryos. This implies that disruption to downstream elements of the proprioceptive system is likely the source of molecular and anatomical manipulation that causes hindrance to the neural network that facilitates normal locomotion in $Gbx1^{-/-}$ mice.

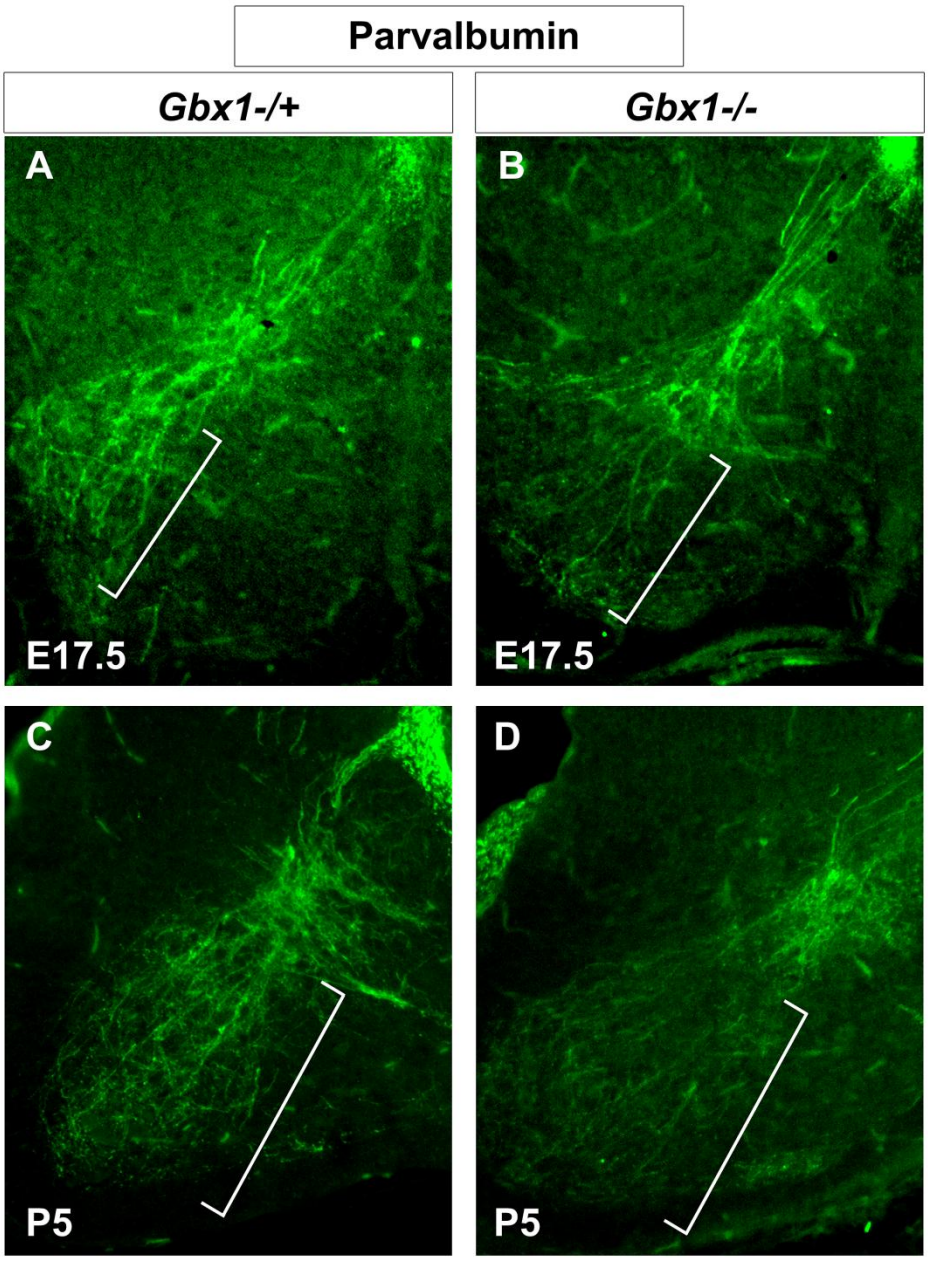

Figure 2.7

Figure 2.7 - *Gbx1*$^{-/-}$ embryos continue to display abnormal projection of proprioceptive afferents at late embryonic and early postnatal stages in development. Parvalbumin immunolabeling in transverse lumbar spinal cord sections at E17.5 and P5. Brackets indicate the innervation of proprioceptive afferents into the intermediate and ventral spinal cord where they are destined to make synaptic connections with their interneuron or motor neuron targets, respectively. *Gbx1*$^{-/+}$ mice show normal projection of afferents to their intermediate and ventral termination zones (A and C). Many of the proprioceptive afferents fail to fully project to their ventral termination zones in the spinal cord of *Gbx1*$^{-/-}$ mice (B and D), while maintaining their proper termination in the intermediate spinal cord. 10X magnification.

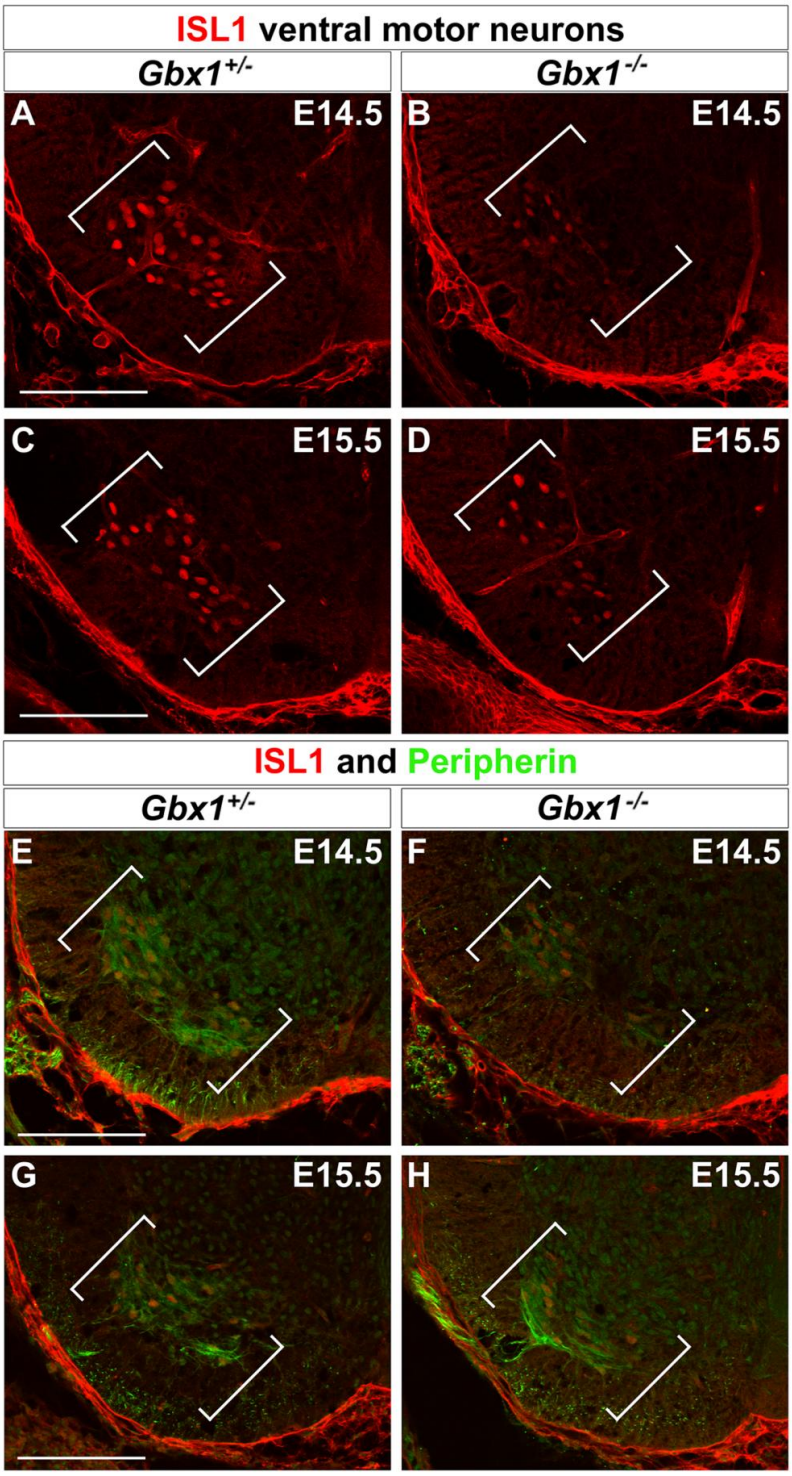
ISL1 ventral motor neurons
Gbx1+/-
Gbx1-/-
A
E14.5
B
E14.5
C
E15.5
D
E15.5
ISL1 and Peripherin
Gbx1+/-
Gbx1-/-
E
E14.5
F
E14.5
G
E15.5
H
E15.5

Figure 2.8

Figure 2.8 - ISL1^{+} and ISL1^{+}/peripherin^{+} co-expressing motor neurons are reduced in *Gbx1*$^{-/-}$ ventral spinal cord. Immunohistochemical analysis for ISL1 (A-D) and ISL1^{+}/peripherin^{+} co-expressing cells (E-H) in lumbar spinal cord sections at E14.5 and E15.5. Expression of ISL1^{+} motor neurons (A and C) and ISL1^{+}/peripherin^{+} co-expressing cells (E and G) in the ventral spinal cord of *Gbx1*$^{-/+}$ embryos. *Gbx1*$^{-/-}$ embryos show a significant reduction in the number of ISL1 ventral motor neurons at E14.5 and E15.5 (B and D) and motor neurons coexpressing ISL1/peripherin (F and H). Scale bars represent 100mm. 20X magnification.

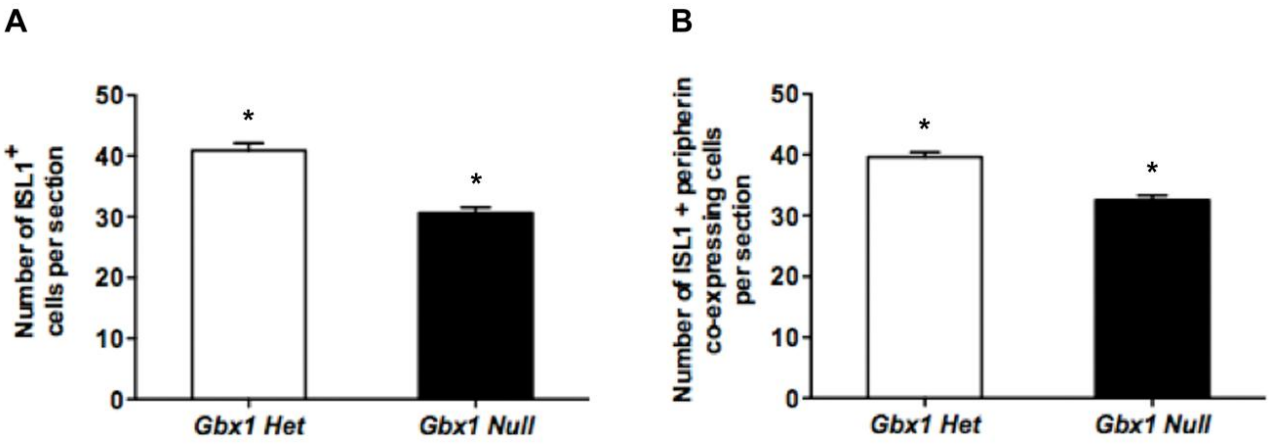
A
Number of ISL1+ cells per section
50
40
30
20
10
0
*
*
Gbx1 Het
Gbx1 Null
B
Number of ISL1 + peripherin co-expressing cells per section
50
40
30
20
10
0
*
*
Gbx1 Het
Gbx1 Null

Figure 2.9

Figure 2.9 - Quantification of ISL1^{+} and ISL1^{+}/peripherin^{+} ventral motor neurons in *Gbx1*$^{-/-}$ embryos. Quantification of ISL1 expressing motor neurons (A) and ISL1/peripherin coexpressing motor neurons (B) in the lumbar ventral spinal cord of E14.5 and E15.5 embryos. Each bar represents the average from 10 sections (n = 4) for null and (n = 4) for heterozygotes; *P < 0.0001.

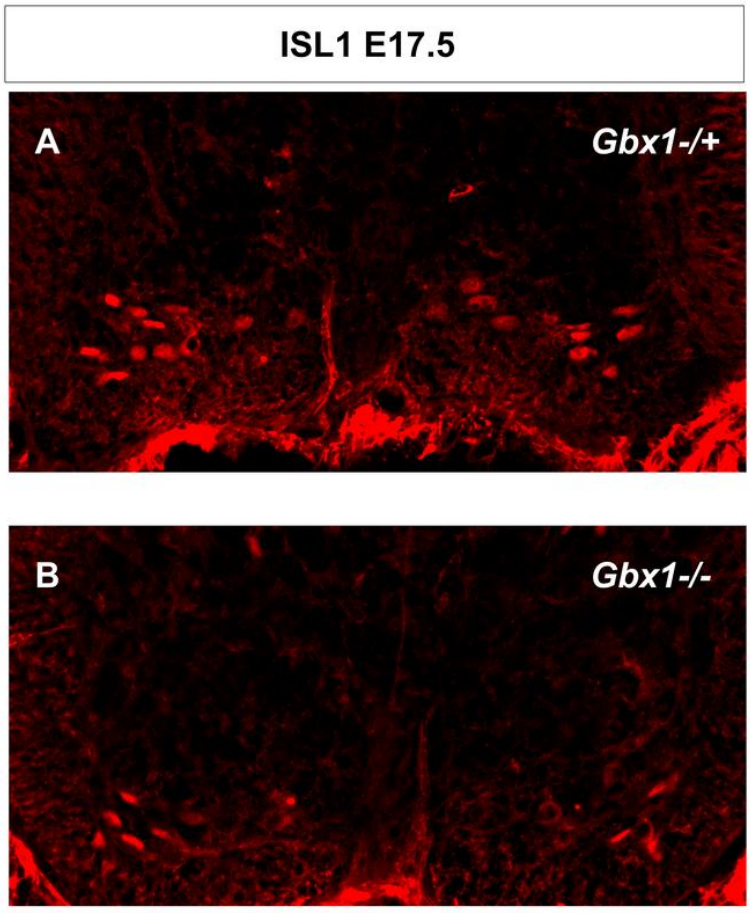

Supplemental Figure 2.1

Supplemental Figure 2.1 - Reduction of ISL1^{+} motor neurons in *Gbx1*$^{-/-}$ ventral spinal cord persists at a late stage in embryonic development.

Immunohistochemical analysis for ISL1^{+} cells in lumbar spinal cord sections at E17.5 Expression of ISL1^{+} motor neurons (A) in the ventral spinal cord of *Gbx1*$^{-/+}$ control embryos. *Gbx1*$^{-/-}$ embryos show a qualitatively observable significant reduction in the number of ISL1^{+} ventral motor neurons (B). 20X magnification.

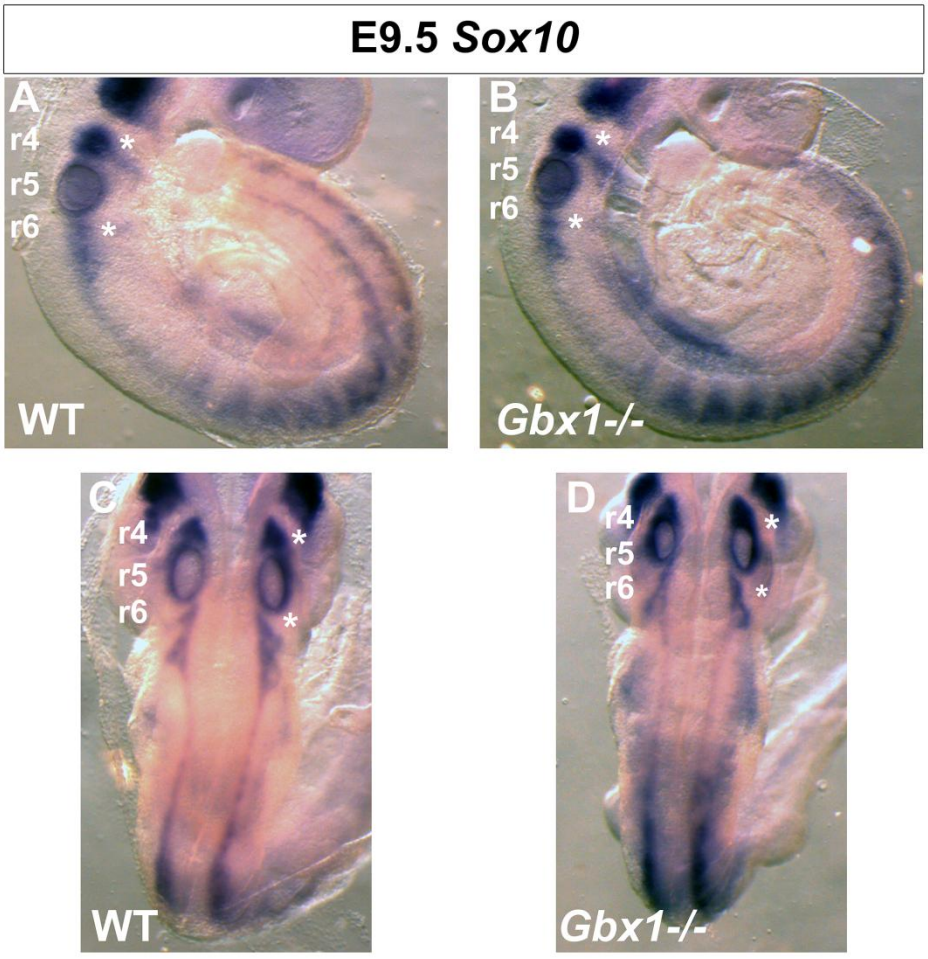

Figure 2.10

Figure 2.10 - Expression analysis of *Sox10* in *Gbx1*$^{-/-}$ embryos. (A-D) Whole-mount in situ hybridization for *Sox10* expression at E9.5. (A-B) Lateral view, dorsal is to the left. (C-D) Dorsal view. *Sox10* expression detected in the r4/r6 hindbrain neural crest streams (asterisks) and within the dorsal root ganglia in the trunk adjacent to the developing spinal cord, is largely unaffected in a *Gbx1*$^{-/-}$ mutant embryo (B) compared to a littermate *Gbx1*$^{-/+}$ control embryo (A). r,rhombomere.

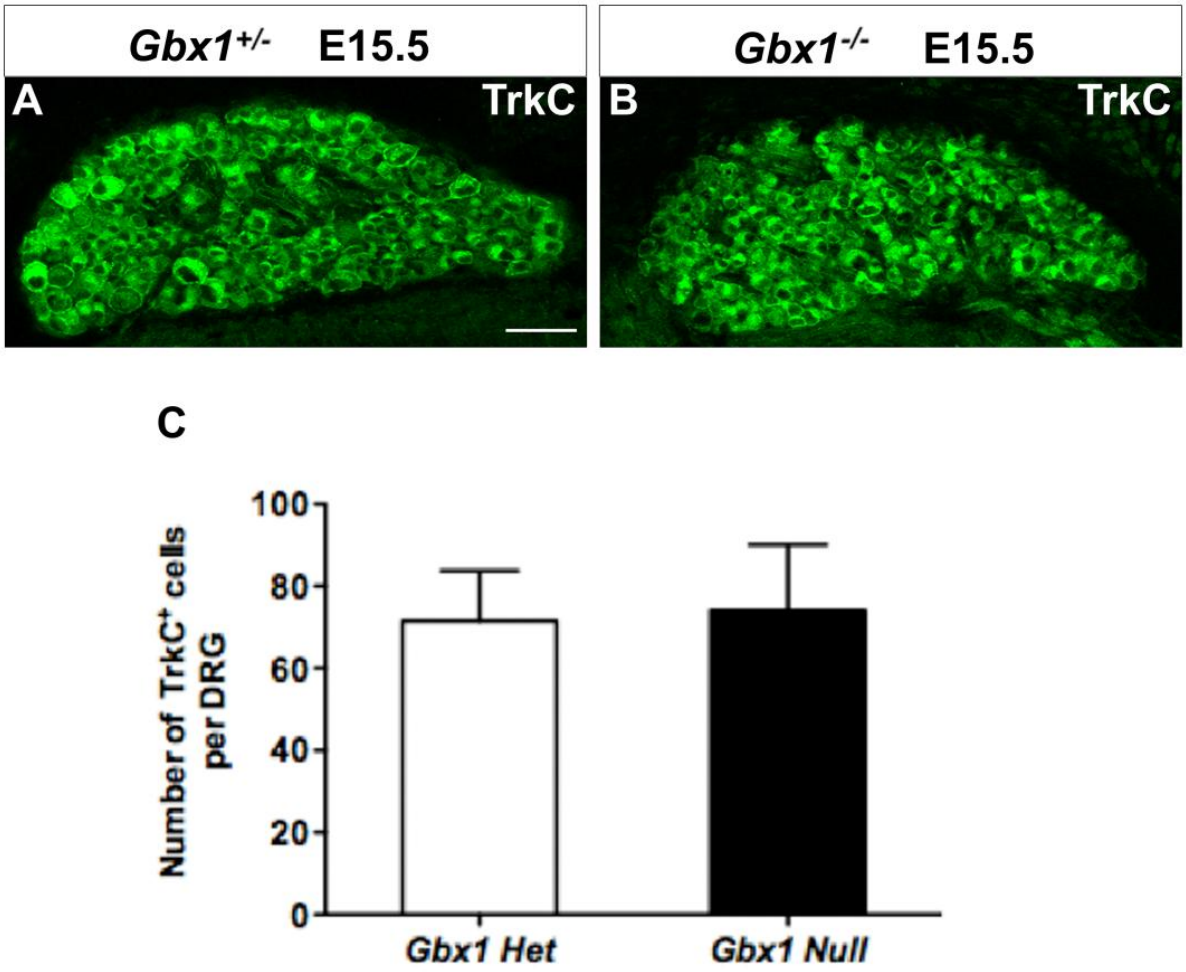
Gbx1+/- E15.5
A
TrkC
Gbx1-/- E15.5
B
TrkC
C
Number of TrkC+ cells per DRG
100
80
60
40
20
0
Gbx1 Het
Gbx1 Null

Figure 2.11

Figure 2.11 - The number of proprioceptive neurons in the DRG is not affected in *Gbx1*$^{-/-}$ mice. The distribution of proprioceptive neurons marked by the expression of TrkC antibody in the DRG of embryos at E15.5 (A and B). The proprioceptive neurons show no difference in the expression between the *Gbx1*$^{-/-}$ (B) and *Gbx1*$^{-/+}$ control embryos (A). Quantification of TrkC expressing neurons in the DRG (C). Each bar represents the average of six DRGs from (n = 3) heterozygous controls and (n = 3) for *Gbx1*$^{-/-}$ embryos; $P < 0.8107$, non-significant; Scale bar represent 100mm. 20X magnification.

2.3 DISCUSSION

Gbx1 is dynamically expressed during embryogenesis, particularly within the CNS. In this study, we have focused our analysis on the functional role(s) *Gbx1* plays in the developing nervous system. By producing mice homozygous for a *Gbx1* loss-of-function allele, we demonstrate that *Gbx1* function is a key regulatory component in assembly of neuronal circuitry controlling normal locomotion. In contrast to mice homozygous for the *Gbx2*$^{-/-}$ allele, *Gbx1* mutants are viable. However, as consistent with *Gbx2* mutant embryos, *Gbx1*$^{-/-}$ embryos display severe developmental defects impacting CNS organization and function. Our data show a disruption in the growth of proprioceptive afferents towards the intermediate zone and ventral termination zone in SCs of E14.5 - E15.5 *Gbx1* mutant embryos when compared to normal embryos. In addition, we show a significant loss of ISL1^{+} and ISL1^{+}/peripherin^{+} coexpressing ventral motor neurons. These abnormalities are detected at E14.5 and become more apparent at E15.5. Furthermore, we show that the reduction of proprioceptive afferent projection into the ventral horn of *Gbx1* mutants persist through P5, when synaptogenesis of proprioceptive synapses occurs. Collectively, the results from our analysis of *Gbx1*$^{-/-}$ mutants from E14.5 - P5 provide strong evidence that *Gbx1* function is required in aspects key to the formation, interconnection and maintenance of sensorimotor circuits in the SC. In addition, the data provide new genetic insights towards the elucidation of the molecular mechanisms underlying somatosensory-related gait disorders.

Loss of *Gbx1* function impacts the late stages of sensorimotor circuit development

During development, sensory neurons of the DRG send axons to the CNS and to sensory receptors in the periphery (Goulding et al., 2002; Inoue et al., 2002; Chen et al., 2003). Several classes of transcription factors have been implicated in the early developmental processes of specification, patterning, and selection of early axonal trajectories of different classes of sensory neurons (Arber et al., 2000; Jessell, 2000; Goulding et al., 2002; Inoue et al., 2002; Shirasaki and Pfaff, 2002; Chen et al., 2003). For example, the generation of all DRG sensory neurons requires the combinatorial expression of basic helix loop- helix proteins Neurogenin 1 and Neurogenin 2 (Wolpert). More recent studies show that *Runx3*, a member of the Runt family of transcription factors, regulates development and survival of proprioceptive afferents. In addition, *Runx3*-deficient mice display severe motor discoordination and limb ataxia (Inoue et al., 2002; Levanon et al.). Unlike mice harboring mutations for the above stated transcription factors, we detected no change in the total number of $TrkA^+$, $TrkB^+$ or $TrkC^+$ DRG sensory neurons in *Gbx1*$^{-/-}$ embryos when compared to normal embryos (Fig. 11, data not shown). Thus it is unlikely that *Gbx1* expression has a significant role in the establishment or diversification of DRG sensory neurons.

DRG sensory axons and motor axons reach their peripheral target areas prior to the entry of DRG sensory afferents into to the SC (Hollyday, 1980; Ozaki and Snider, 1997). Depending on their sensory modality, sensory neurons of the DRG send axons to superficial layers of the dorsal horn (nociception and thermoception), or the deep layers of the dorsal horn, lateral horn and ventral horn, (mechanoreceptive and

proprioceptive) (Goulding et al., 2002; Marmigere and Ernfors, 2007; Todd, 2010). The early onset of *Gbx1* expression in the dorsal and ventral ventricular zone of the SC at E9.0 - E10.5, is consistent with the specification and generation of defined spinal neuronal subpopulations, suggesting a possible role for *Gbx1* in their integration into neuronal circuits (Waters et al.). In contrast to that theory, our immunohistochemical analyses of *Gbx1*$^{-/-}$ embryos at E10.5 did not uncover any abnormal expression of a panel of molecular markers including, basic helix-loop-helix and homeodomain transcription factors, normally expressed within the distinct precursor cell populations throughout the dorsal SC (Fig. 4). Collectively, these data strongly suggest that *Gbx1* expression does not impact the early steps underlying the formation of sensorimotor circuits. Nevertheless, recent studies have shown that *Gbx1* expression in the SC is dynamic and becomes restricted to the dorsal mantle zones at E12.5. Immunohistochemical analyses of wild-type embryonic and adult SCs demonstrate that *Gbx1* is expressed in late-born LBX1^{+} (class B) neurons from E12.5 - E16.5, distinguishes a distinct subpopulation of GABAergic dorsal spinal neurons and could function in the late steps of spinal circuit assembly (Waters et al., 2003; John et al., 2005).

Proprioceptive neurons begin to project afferents into the dorsal SC at E14.0, before cutaneous afferents terminate in the dorsal horn, and into the deep dorsal horn by E15.0 (Ozaki and Snider, 1997). Establishment of connections between Ia afferents and ISL1^{+} motor neurons in the ventral horn begins at E15.5 and continues until P8 (Ozaki and Snider, 1997; Arber et al., 2000). In *Gbx1*$^{-/-}$ embryos, projection of proprioceptive afferents into the intermediate and ventral SC terminates prematurely

(Figs. 6 and 7). As a result, these mutant mice lack many of the direct synaptic connections normally formed with motor neurons in the ventral termination zone, correlating well to the severe hindlimb motor discoordination. Interestingly, the late neuronal and behavioral phenotypes observed in *Gbx1* null mutants resembles mild forms of the motor control defects seen in mutant mice with major alterations in proprioceptive neuronal circuitry (Ernfors et al., 1994; Inoue et al., 2002; Levanon et al., 2002). For example, *Er81*, a member of the ETS transcription factor family is expressed in both developing motor neurons and proprioceptive sensory neurons. Results from studies of *Er81* mutant mice exhibit a failed formation of a discrete termination zone between Ia proprioceptive afferents and motor neurons in the ventral SC. However, specification of motor neurons and induction of muscle spindles in *Er81* mutant mice occurs normally. Furthermore, it is interesting to note that similar to *Gbx1*$^{-/-}$ mice, *Er81* mutants display severely uncoordinated limb movements (Arber et al., 2000).

In addition to projection of proprioceptive afferents into the intermediate and ventral SC, our data demonstrate a requirement of *Gbx1* for normal patterning of ISL1^{+} ventral motor neurons, another key component of sensorimotor circuits in vertebrates. Motor neurons are within the earliest born neurons of the ventral SC (Hollyday and Hamburger, 1977; Nornes and Carry, 1978). The first postmitotic motor neurons in the mouse SC are detected at E9 - E9.5, and the generation of motor neurons is complete by E11.0 (Nornes and Carry, 1978). We and others have shown that *Gbx1* is expressed in the prospective SC at E9.0 and in the ventral ventricular zone at an anatomical level that coincides with motor neuron progenitor cells by E10.5 (Waters et al., 2003; Rhinn et al., 2004). Consistent with our analysis of dorsal SC precursor cells of *Gbx1*$^{-/-}$ embryos,

our immunohistochemical analyses at E10.5 did not uncover any abnormal expression of ISL1, HB9 or a panel of transcription factors expressed within the distinct precursor cell subtypes throughout the ventral SC (data not shown). Furthermore, no apparent difference in the total number of postmitotic $ISL1^{+}$ and $HB9^{+}$ ventral motor neurons was observed in *Gbx1* mutant embryos at E11.5 when compared to normal *Gbx1*$^{-/+}$ control embryos (Fig. 5).

Intriguingly, we observed a marked reduction in the total number of $ISL1^{+}$ and $ISL1^{+}$/peripherin^{+} motor neurons at later stages in development, E14.5 - 15.5, in *Gbx1*$^{-/-}$ embryos compared to normal embryos. These results further support a role for *Gbx1* in establishment of sensorimotor connections. However, our results raise two distinct issues concerning the mechanism underlying the loss of motor neurons at this late stage of development of *Gbx1* mutant embryos. First, a considerable amount of neuronal loss occurs amongst differentiated, post-migrational neurons that are in the process of establishing connections between afferents and target neurons (Burek and Oppenheim, 1996). We have shown that premature termination of proprioceptive afferents occurs in the intermediate zone of *Gbx1*$^{-/-}$ SCs from E14.5 - P5 mutants. As a consequence, functional connections with motor neurons in the ventral target zone may not be made, resulting in a loss of motor neurons through programmed cell death (Posada and Clarke, 1999). In contrast, recent studies in mice have demonstrated that reduced levels of Islet protein favors the generation of V2a interneurons at the expense of motor neuron formation (Song et al., 2009). In support of this notion, cell-fate conversion of motor neurons occurs in zebrafish upon knockdown of *isl1* and *isl2* (Hutchinson and Eisen, 2006). Our previous *in situ* hybridization analyses show that

Gbx1 expression coincides with a population of motor neurons in the ventral SC at E10.5 (Waters et al., 2003). In this study we show that inactivation of *Gbx1* does not result in a failure to specify $ISL1^{+}$ motor neurons. Yet, we observed a significant decrease in the total number of motor neurons in *Gbx1* mutant embryos. While our study does not address this question directly, it presents the hypothesis that *Gbx1* can play a role in the maintenance of ISLI1 expression in a subset of motor neurons, preventing their conversion into V2a interneurons. However, this possibility remains to be determined empirically.

Abnormal locomotion in *Gbx1* mutants

Our analysis of $Gbx1^{-/-}$ mice has revealed a novel role for Gbx transcription factors in regulating the assembly of sensorimotor circuits and motor behavior. Unlike *Gbx2* mutant mice, *Gbx1* mutants display a striking gait disorder, which specifically affects the hindlimbs. Since $Gbx2^{-/-}$ mice do not survive beyond birth, we cannot determine the manifestation of a gait disorder. However, *Gbx2* mutants do display cranial nerve V motor neuron and motor control defects during embryogenesis that severely impact hindbrain development and the ability to suckle (Waters and Lewandoski, 2006; Burroughs-Garcia et al., 2011). In addition, a recent lineage-tracing study using $Gbx2^{CreER\text{-}ires\text{-}eGFP}$ mice has demonstrated a requirement for *Gbx2* expression in early progenitor cells of the neural tube (E8.5) for normal development and patterning of ventral motor neurons in the SC to occur (Luu et al., 2011). It is also intriguing that *Gbx2* mutant embryos develop with severe inner ear defects affecting vestibular function, which could contribute to impairment of movement and coordination (Lin et al., 2005). Our examination of *Gbx1* mutant mice did not reveal any apparent

musculoskeletal or peripheral nervous system defects. And, since *Gbx1*$^{-/-}$ mice do not display any abnormal head movements or circling behavior, it is highly unlikely that the phenotype is a result of impaired vestibular function (Vidal et al., 2004). While our data do not rule out a possible requirement for *Gbx1* expression in regions outside of the SC for normal locomotion, we did not observe changes in other components of the major systems that govern posture and locomotion. Moreover, while *Gbx1* is expressed in the medial ganglionic eminence, which contributes to the formation of the basal ganglia, expression has not been detected in other major components of the motor system outside of the SC, such as the, brainstem, or cerebellum (Waters et al., 2003). Movement disorders are caused by a variety of neurological conditions, which manifest into a broad clinical spectrum that includes dystonia, ataxia and gait disorders. Nevertheless, all movement disorders share common features in neural circuits which impair the planning, control or execution of movement (Klein, 2005). One of the simplest and best understood neuronal circuits in the vertebrate CNS is the spinal monosynaptic stretch reflex circuit, in which connections are formed between a sensory unit and an effecter unit (Chen et al., 2003). The precise coordination of movement by this circuit is carried out by connections formed between two main classes of neurons, proprioceptive Ia sensory neurons and ventral spinal motor neurons. Therefore, it is very intriguing that *Gbx1* directly impacts both proprioceptive afferent projection and ventral motor neuron development in the SC. Furthermore, the function of *Gbx1* parallels several transcription factors that control the establishment of connections within the spinal monosynaptic stretch reflex circuit (Chen et al., 2003). Group Ia afferents innervate muscle spindles in the periphery and form direct connections with ventral motor neurons in this circuit. We

have shown a marked reduction of the group Ia proprioceptive afferents in *Gbx1* mutants. Whereas the group Ib afferents, which project to the intermediate SC and do not make synaptic contact with motor neurons appear normal in *Gbx1* mutants. In summary, our studies revealed a novel role for *Gbx1* in regulating key components involved in the integration of sensorimotor circuitry affecting motor behavior. A challenge now is to further define the mechanisms impacted by a loss of *Gbx1*. Future investigations should be conducted to identify and analyze the direct molecular targets of GBX1. Insight into these factors will provide greater understanding of transcriptional control of the distinct subpopulations of motor and sensory neurons by *Gbx1*.

CHAPTER 3

Gbx1 AND *Gbx2* ARE ESSENTIAL FOR NORMAL PATTERNING AND DEVELOPMENT OF INTERNEURONS AND MOTOR NEURONS IN THE EMBRYONIC SPINAL CORD

[This work was submitted and reviewed by *Developmental Neurobiology*, 2014]

[1,2] Desirè M. Buckley, [1,2] Jessica Burroughs-Garcia, [3]Sonja Kriks and [1,2] Samuel T. Waters[*]

1 Division of Biological Sciences, University of Missouri, Columbia, Missouri, USA, **2** Christopher S. Bond Life Sciences Center, University of Missouri, Columbia, Missouri, USA **3** The Salk Institute for Biological Studies, La Jolla, California, USA

3.1 ABSTRACT

The molecular mechanisms regulating neurogenesis involve the control of gene expression by transcription factors. *Gbx1* and *Gbx2*, two members of the Gbx family of homeodomain-containing transcription factors, are known for their essential roles in central nervous system development. The expression domains of mouse *Gbx1* and *Gbx2* include regions of the forebrain, anterior hindbrain and SC. In the SC, *Gbx1* and *Gbx2* are expressed in $PAX2^{+}$ interneurons of the dorsal horn and ventral motor neuron progenitors. Based on their shared domains of expression and instances of overlap, we investigated the functional relationship between *Gbx* family members in the developing SC using $Gbx1^{-/-}$, $Gbx2^{-/-}$ and $Gbx1^{-/-}$;$Gbx2^{-/-}$ embryos. In situ hybridization analyses of embryonic SCs show up-regulation of *Gbx2* expression in $Gbx1^{-/-}$ embryos and up-regulation of *Gbx1* expression in $Gbx2^{-/-}$ embryos. Additionally, our data demonstrates that *Gbx* genes regulate patterning of a subset of $PAX2^{+}$ dorsal inhibitory interneurons. While we observe no difference in overall proliferative status of the developing ependymal layer, expansion of proliferative cells into the anatomically defined mantle zone occurs in *Gbx* mutants. Lastly, our data shows a marked increase in apoptotic cell death, specifically in $ISL1/2^{+}$ ventral motor neurons of *Gbx* mutants during mid-embryonic stages. Although our studies reveal that both members of the *Gbx* gene family are involved in patterning subsets of $PAX2^{+}$ dorsal interneurons and survival of ventral motor neurons, the genes are not sufficient to genetically compensate for the loss of one another. Thus, our data provide novel insight to the relationship harbored between *Gbx1* and *Gbx2* in SC development. **Key words:** *Gbx1*, *Gbx2*, spinal cord, mouse, development

3.2 RESULTS

Increase in embryonic spinal cord expression of *Gbx1* and *Gbx2* in homozygous null counterparts

A significant role for *Gbx* transcription factors in neural development has been recently established. However, while their mRNA expression in the SC overlap spatially and temporally, they are not biochemically identical. Whereas both *Gbx1* and *Gbx2* are heavily expressed in the dorsal mantle zone at E12.5, *Gbx2* expression diminishes after E13.5 (John et al., 2005) (Fig. 1), while *Gbx1* expression persists through postnatal stages. Key in understanding phenotypic differences and similarities in *Gbx* homozygous null mutants and relative functions of *Gbx1* and *Gbx2* in SC development (Wassarman et al., 1997; Byrd and Meyers, 2005; Lin et al., 2005; Waters and Lewandoski, 2006; Buckley et al., 2013), is whether the observed loss-of-function phenotypes are determined by differences in spatial and temporal expression or biochemical differences between the proteins.

We have previously demonstrated using whole-mount in situ hybridization that *Gbx1* expression is not overtly up-regulated outside the CNS in the absence of *Gbx2* (Waters et al., 2003). In addition, we and others, have shown that *Gbx2* is robustly expressed in the dorsal mantle zones of wild-type control embryos and is then rapidly down-regulated beginning at E12.5 (Waters et al., 2003; John et al., 2005). Therefore to examine if any genetic interaction occurs between *Gbx* genes, we first sought to determine if the loss of *Gbx1* impacts expression of *Gbx2* in the SC. Surprisingly, we observed a striking increase of *Gbx2* expression in the dorsal mantle zones of *Gbx1*$^{-/-}$

embryos when compared to wild-type (*Gbx1*$^{+/+}$) control embryos at E13.5 (Fig. 3.1A, B). Further examination at later developmental stages, E14.5 - E16.5 (Fig. 3.1C–H), demonstrates that elevated levels of *Gbx2* expression persists in the dorsal SC of *Gbx1*$^{-/-}$ embryos at E14.5 and E15.5 (Fig. 3.1D, F). However, *Gbx2* expression in *Gbx1* mutants is nearly absent at E15.5. While we observed increased levels of *Gbx2* mRNA throughout the superficial dorsal horn of *Gbx1*$^{-/-}$ embryos, the predominant expression appears localized in laminae (III – IV) (Fig. 3.1, asterisk). The apparent qualitative increase of *Gbx2* mRNA is consistent with our recent quantitative assessment of *Gbx2* expression in *Gbx1* mutants using quantitative real-time PCR, revealing a marked increase of *Gbx2* transcripts at E13.5 (Villalon et al., 2014).

We next examined if *Gbx1* expression is altered in *Gbx2*$^{-/-}$ SCs. Recent studies have indicated that *Gbx1* expression is down-regulated in the ventricular zone of the SC at E11.5 and is up-regulated specifically in the dorsal mantle zones at E12.5 where its expression persists through birth. We analyzed *Gbx1* expression by in situ analysis in wild-type (*Gbx2*$^{+/+}$) and *Gbx2*$^{-/-}$ SCs at E13.5 and E14.5 (Fig. 3.1I - L). Our results show that like *Gbx2*, there is a notable increase of *Gbx1* expression in the dorsal SC of its null counterpart at both stages examined (Fig, 3.1J, L). Taken together, these observations show that loss-of-function of one *Gbx* family member invokes higher levels of expression in its counterpart.

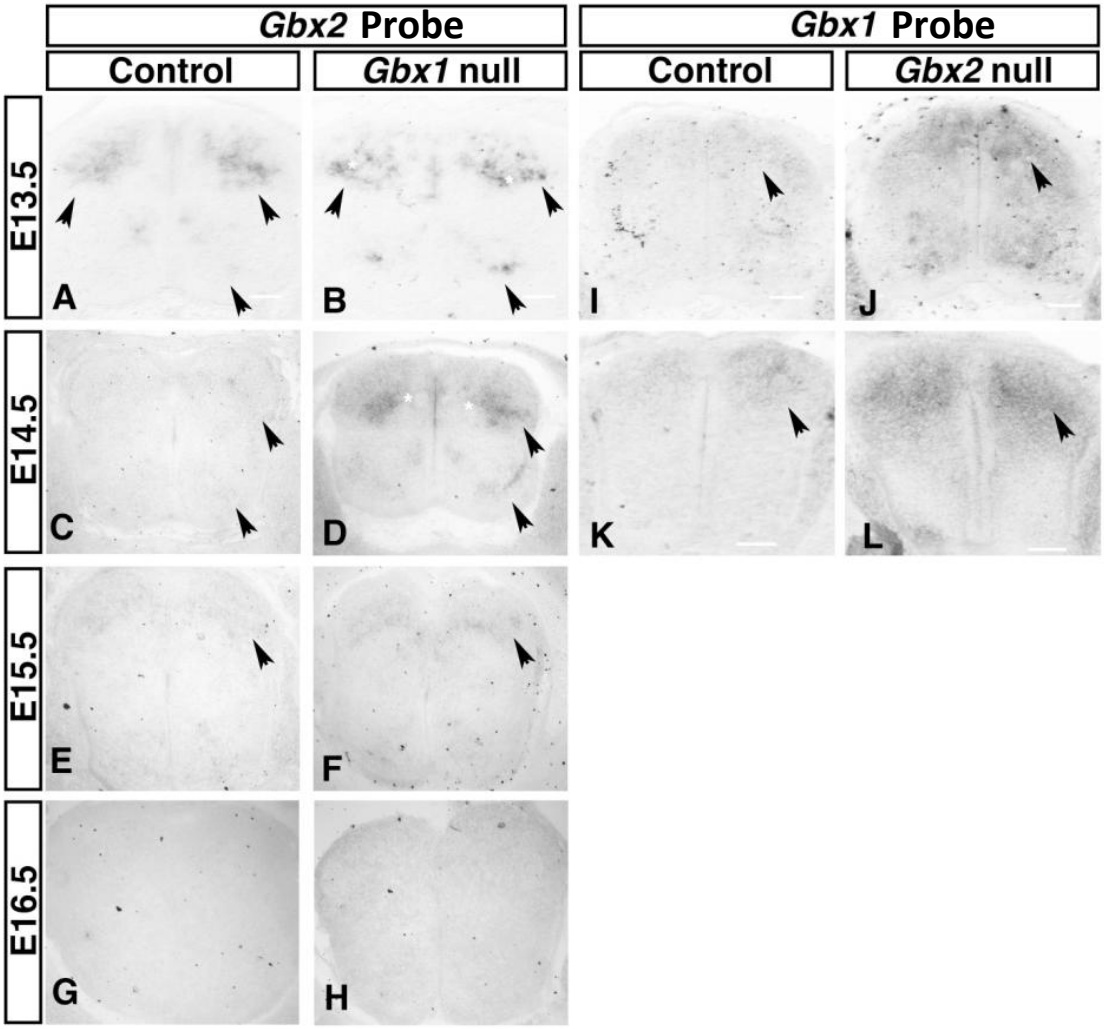
Gbx2 Probe
Gbx1 Probe
Control
Gbx1 null
Control
Gbx2 null
E13.5
E14.5
E15.5
E16.5
A
B
I
J
C
D
K
L
E
F
G
H

Figure 3.1

Figure 3.1 - *Gbx* mRNA expression is transiently up-regulated in null counterparts during mid-embryonic stages. *Gbx2* and *Gbx1* mRNA expression analysis between E13.5-E16.5 in *Gbx2*$^{-/-}$,*Gbx1*$^{-/-}$ and age-matched control (*Gbx2*$^{+/+}$ or *Gbx1*$^{+/+}$) lumbar spinal cord sections (A-L). Section *in situ* hybridization was performed using the *Gbx2* probe that is designed to recognize the full-length sequence encoding *Gbx2* mRNA (A-H). *Gbx2* is expressed within neural populations of the developing dorsal mantle zone in wild-type (*Gbx1*$^{+/+}$) embryos at E13.5, (A; black arrowhead). *Gbx2* expression pattern remains consistent in *Gbx1*$^{-/-}$ embryos at E13.5, however *Gbx2* is expressed to a greater extent throughout laminae (III-IV) (B; asterisk). Persistent up-regulation of *Gbx2* expression in the spinal cords of *Gbx1*$^{-/-}$ embryos occurs through E14.5, when compared to the control embryo (compare D with C; white asterisk). *Gbx2* expression is barely observable in the control embryo at E15.5 (E), and this intensity is comparable in the mutant spinal cord (F), which marks the stage in which up-regulation of *Gbx2* terminates. By E16.5, *Gbx2* expression is absent from the spinal cord of control and mutant embryos (G-H, black arrowhead). Section *in situ* hybridization was performed using the *Gbx1* probe that is designed to recognize the full-length sequence encoding *Gbx1* mRNA (I-L). *Gbx1* expression pattern recapitulates that of the wild-type (*Gbx2*$^{+/+}$) embryo at E13.5 (I), however, *Gbx1* is expressed more broadly and intensely throughout the dorsal horn in *Gbx2*$^{-/-}$ mutants (J). Increased *Gbx1* expression persists in the spinal cord of *Gbx2*$^{-/-}$ mutants through E14.5 (L). Scale bars represent 100 μm. (n=3) for each genotype and embryonic stage examined.

Loss of *Gbx1* and *Gbx2* results in abnormal patterning of developing dorsal spinal cord neurons

Gbx1 is expressed in a subset of late-born GABAergic interneurons of the developing dorsal horn, the class B dILA interneurons (John et al., 2005). The *Gbx2* lineage has also been shown to contribute to $PAX2^+$ inhibitory dILA interneurons, and maintenance of the proliferative status of dorsal progenitors (Luu et al., 2011). Therefore, to investigate the role of the *Gbx* family in development of inhibitory interneurons in the dorsal SC, we analyzed $Gbx1^{-/-}$ and $Gbx2^{-/-}$ embryos. Transverse, lumbar SC sections from $Gbx1^{-/-}$, $Gbx2^{-/-}$ and wild-type ($Gbx1^{+/+};Gbx2^{+/+}$) control embryos were examined at E13.5 (Fig. 3.2A-D) and E14.5 (Fig. 3.2E-H) by immunohistochemistry examining PAX2, the cell-type specific marker of dorsal inhibitory interneurons (Gross et al., 2002; Cheng et al., 2004). At both stages, the pattern and distribution of PAX2 is perturbed in $Gbx1^{-/-}$ and $Gbx2^{-/-}$ mutants when compared to control embryos. In wild-type embryos at E13.5, $PAX2^+$ cells span the medio-lateral axis of the dorsal SC as they migrate into the various laminae (Fig. 3.2A). This forms the characteristic horn morphology of the dorsal SC, where the early-born (dI4) interneurons populate the deep medial region of the superficial dorsal horn (laminae III-IV) and later-born (dILA) interneurons populate the most peripheral regions throughout laminae (II – IV) (Caspary and Anderson, 2003). At E13.5, the superficial layers of the dorsal horn appear less-densely populated with $PAX2^+$ cells in $Gbx1^{-/-}$ and $Gbx2^{-/-}$ mutant SCs (Fig. 3.2B, C). By E14.5, the reduction in PAX2 expression within the most peripheral regions of the superficial laminae becomes even more apparent in both mutants, when compared to the age-matched wild-type control embryo (Fig. 3.2E – G).

The loosely packed and scattered distribution of PAX2^{+} cells in the superficial laminae of *Gbx1* mutants severely disturbs the characteristic horn cytoarchitecture observed in wild-type control embryos. Notably, the apparent abnormal patterning of PAX2^{+} cells appears to span not only the peripheral, but also the medial regions of laminae II – IV (asterisk, Fig. 3.2A-C), affecting the overall presence of PAX2^{+} expression in the entire dorsal SC when compared to wild-type. We further analyzed the observed differences in PAX2 expressing cells between wild-type embryos and *Gbx* single mutants quantitatively. Consistent with our qualitative assessment, quantification of PAX2^{+} cells reveals a significant decrease in the number of inhibitory interneurons within the superficial laminae of the dorsal horn in *Gbx1*$^{-/-}$ and *Gbx2*$^{-/-}$ mutants (Fig. 3.2I, J). Moreover, our observed reduction of PAX2^{+} cells in *Gbx1*$^{-/-}$ SCs is consistent with results from recent studies (Meziane et al., 2013).

The observation that null mutations for either gene of the *Gbx* family results in the loss of PAX2^{+} cells within the superficial layers of the dorsal SC, prompted us to examine the effects of inactivating both genes simultaneously on maintenance of PAX2 in dorsal inhibitory interneurons. Transverse sections of the lumbar cords of *Gbx* dKO embryos were assessed in the same manner as the single mutants for comparison. At E13.5 and E14.5, *Gbx* dKO embryos display similar reduction in PAX2 expression as in each of the single mutants, when compared to age-matched wild-type embryos (Fig. 3.2A, D). Quantification of cells immunopositive for PAX2 in the superficial layers of *Gbx* dKO embryos at E13.5 and E14.5, confirms our qualitative observations as for each of the single *Gbx* mutants, and shows that there is a significant diminution in the number of PAX2^{+} cells (Fig. 3.2I, J). These data show that the inactivation of *Gbx* gene members

individually, is sufficient to induce a significant loss of PAX2 expression in neurons of the superficial dorsal SC, and the simultaneous inactivation of both *Gbx* genes results in the same defect. Taken together these data suggest that members of the *Gbx* gene family share a functionally similar role in the development of late-born $PAX2^+$ interneurons that settle into the most superficial layers of the dorsal SC.

Our observation that *Gbx* mutants have reduced numbers of $PAX2^+$ cells in the superficial layers of the dorsal horn at E13.5 and E14.5, prompted us to investigate possible mechanisms to explain the phenotype. Based on previously reported involvement of *Gbx2* in cell proliferation, we sought to examine the proliferative capacity of neural progenitors in SCs of wild-type, $Gbx1^{-/-}$, $Gbx2^{-/-}$ and *Gbx* dKO littermate embryos. Immunohistochemistry was performed on transverse sections of lumbar segments of the SC for each genotype, using an antibody specific for phosphorylated Histone H3 (H3P), a marker for mitotically active cells (Waters and Lewandoski, 2006). We assessed the proliferative status of SCs at E10.5 and E12.5, the major developmental stages of neurogenesis for early-born and late-born classes of interneurons within the dorsal horn, respectively. Interestingly, we observed a striking difference, in which *Gbx* mutants appear to have an expanded zone of proliferation (Fig. 3.3). Qualitative and quantitative analyses did not reveal a major difference in the uniformity or number of mitotically active cells constituting the ependymal/ventricular layer (EL) along the surface of the central canal between wild-type and *Gbx* mutant SCs at either stage of development (Fig. 3.3A-H, I, K). However, at E10.5, we observed a significant expansion of $H3P^+$ cells outside the normal zone of proliferation, into the

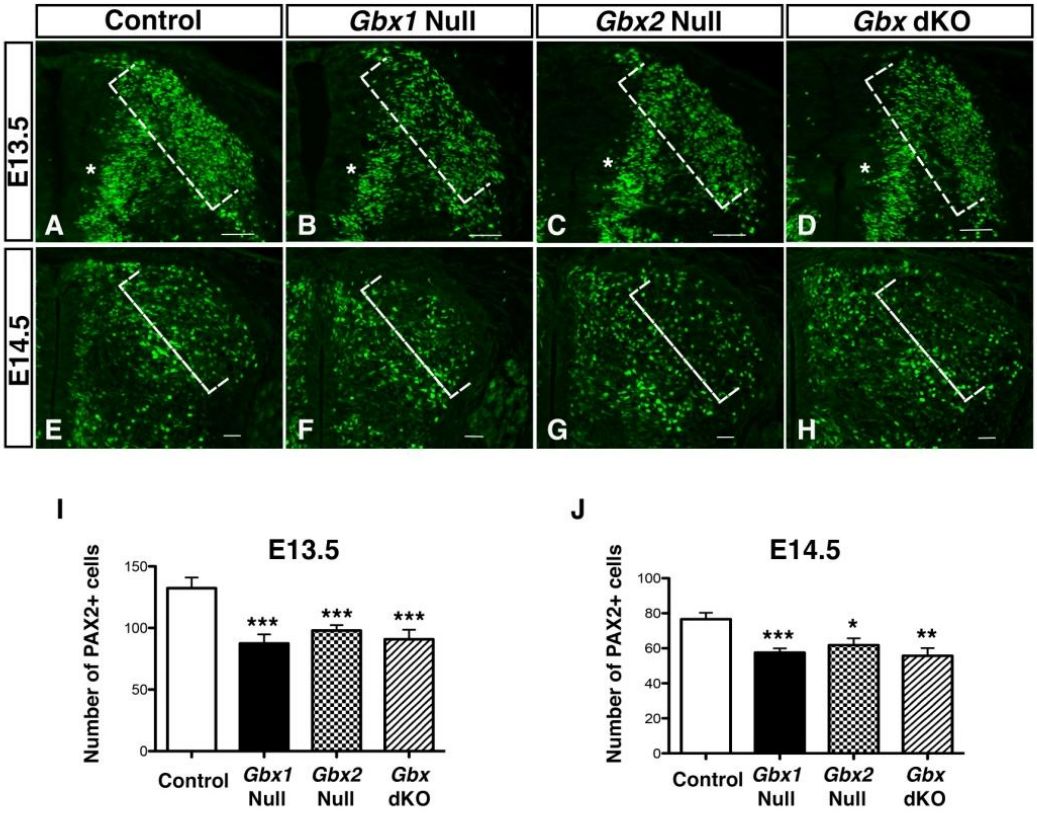
Control
Gbx1 Null
Gbx2 Null
Gbx dKO
E13.5
E14.5
A
B
C
D
E
F
G
H
I
E13.5
Number of PAX2+ cells
150
100
50
0
***
***
***
Control
Gbx1 Null
Gbx2 Null
Gbx dKO
J
E14.5
Number of PAX2+ cells
100
80
60
40
20
0
***
*
**
Control
Gbx1 Null
Gbx2 Null
Gbx dKO

Figure 3.2

Figure 3.2 - Loss of *Gbx1* and/or *Gbx2* expression results in reduction of PAX2^{+} cells in the superficial dorsal horn. Expression analysis of PAX2, a marker of inhibitory interneurons at E13.5 (A-D) and E14.5 (E-H) in lumbar spinal cords of control, *Gbx1*$^{-/-}$, *Gbx2*$^{-/-}$, and *Gbx* dKO mutants. In control embryos at E13.5, the characteristic morphology of the dorsal spinal cord begins to emerge as interneurons populate the deep and superficial layers of the dorsal horn (A; white bracket). Proliferative progenitor cells of late-born class B interneurons within the deep dorsal horn (A; white asterisk). Analysis at E13.5 reveals loss of PAX2 immunoreactivity in the most superficial layers of the dorsal horn in *Gbx1*$^{-/-}$ (B); *Gbx2*$^{-/-}$ (C), and *Gbx* dKO embryos (D), accompanied by additional loss in PAX2 immunoreactivity within progenitor cells (A –D; white asterisk). Quantification of PAX2^{+} cells in the lateral regions of the superficial dorsal laminae reveals a significant decrease in PAX2^{+} cells for all *Gbx* mutants when compared to age-matched controls at E13.5 (I) and E14.5 (J). Samples considered statistically significant have a value of $*P < 0.05$, $**P < 0.005$, $***P < 0.0005$. Scale bars represent 100 µm. (n= 3-5) for each genotype and embryonic stage examined.

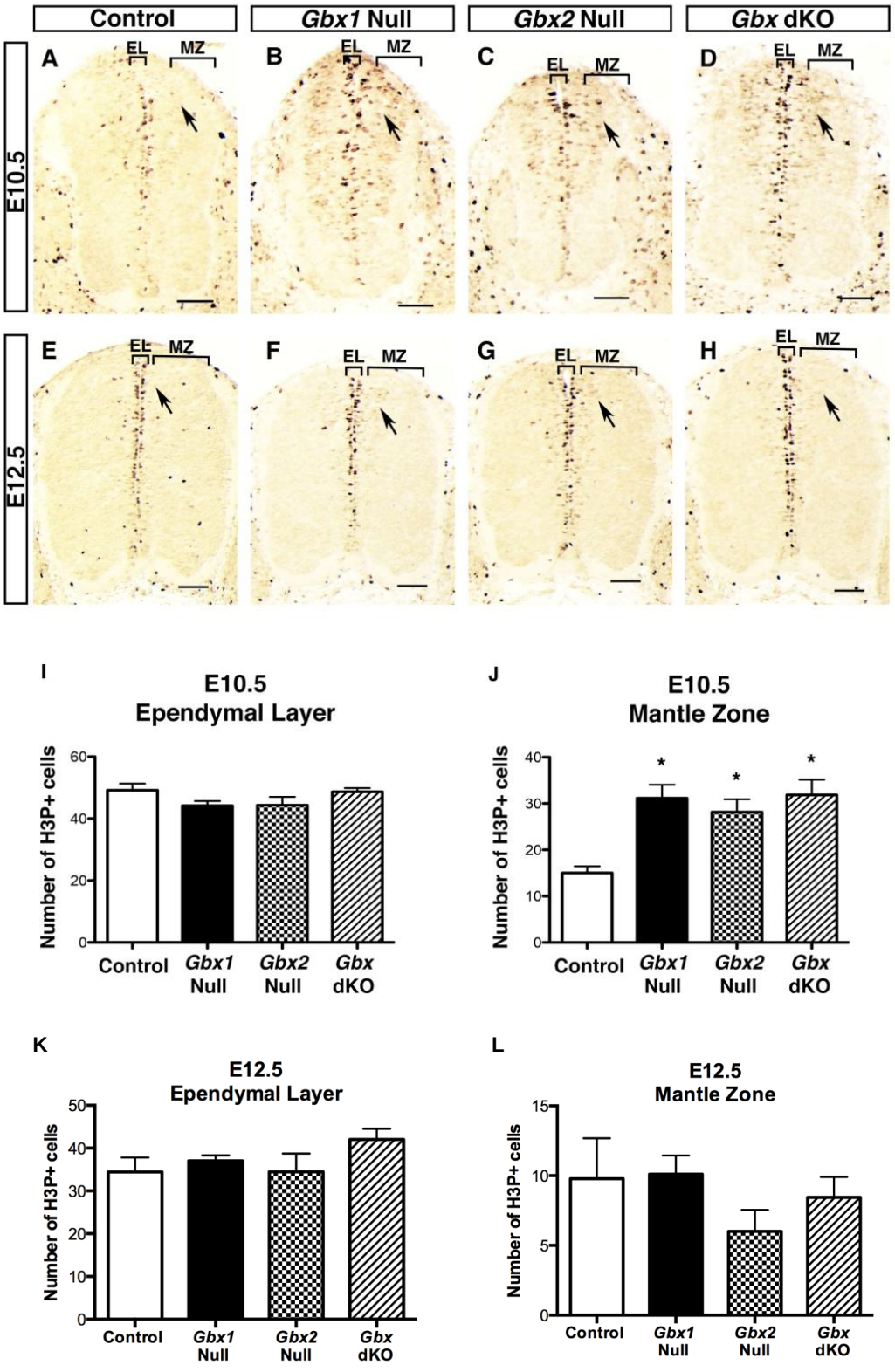
Control
Gbx1 Null
Gbx2 Null
Gbx dKO
E10.5
E12.5
A
B
C
D
E
F
G
H
EL
MZ
I
E10.5
Ependymal Layer
J
E10.5
Mantle Zone
K
E12.5
Ependymal Layer
L
E12.5
Mantle Zone
Number of H3P+ cells
Control
Gbx1 Null
Gbx2 Null
Gbx dKO

Figure 3.3

Figure 3.3 - **Absence of *Gbx* gene expression results in aberrant patterning of proliferative cells in the dorsal spinal cord of *Gbx* mutants**. Immunolabeling of proliferative cells with phosphorylated histone H3 (H3P). At E10.5, during the earliest stages of spinal neuron proliferation, we observe a striking expansion of $H3P^+$ cells in *Gbx* mutants (compare B-D to A). While the level of proliferation remains consistent within the ependymal layer (EL), the number of labeled cells increased significantly within the mantle zone (MZ) at E10.5 5 (black arrowhead). This expansion continues at E12.5 to a lesser degree (E-H). Quantification of $H3P^+$ cells within the EL (I) and MZ (J) reveal a significant increase in the number of cells within the MZ but not EL of all *Gbx* mutants at E10.5. However, repeated quantification at E12.5 demonstrates that the expansion of $H3P^+$ cells into the MZ observed at E10.5 does not persist (L) and no difference exists within the EL (K). Each bar represents the average of three lumbar SC sections from three samples of each genotype analyzed (i.e. nine sections each for $Gbx1^{+/+}$;$Gbx2^{+/+}$ (control), $Gbx1^{-/-}$, $Gbx2^{-/-}$, $Gbx1^{-/-}$;$Gbx2^{-/-}$ (dKO)). Samples considered statistically significant have a value of $*P < 0.05$. Scale bars represent 100 µm. Arrows indicate cells labeled with H3P.

mantle zone (MZ) (Fig. 3.3B-E, J) ($P < 0.05$) in all *Gbx* mutants. However, the expansion of H3P+ cells does not persist through E12.5 within the remaining psuedostratified epithelium of *Gbx* mutants (Fig. 3.3 F – H, L) (Smart, 1972). Similar to the anterior hindbrain of *Gbx* mutants, these results strongly suggest that the proliferative capacity of dorsal neural progenitor cells is affected in *Gbx* mutants. Furthermore, the reduction in $PAX2^{+}$ cells in the dorsal superficial layers of *Gbx* mutants may be a result of mis-patterning of mitotically active cells within the ventricular and mantle zones.

Loss of *Gbx* transcription factor function results in increased apoptosis in the ventral spinal cord

We next examined the impact of *Gbx* function on cell survival. Recent studies have provided intriguing evidence supporting a role for *Gbx* genes in motor neuron development. Results from our studies show that pMNs are specified correctly in *Gbx1*$^{-/-}$ embryos. However, a significant decrease in the number of $ISL1^{+}$ motor neurons in the SC occurs at E14.5 in *Gbx1*$^{-/-}$ embryos (Buckley et al., 2013). In addition, we have shown that *gbx2* knockdown in zebrafish results in disorganization of anterior hindbrain, cranial nerve V motor neurons (Burroughs-Garcia et al., 2011). More recent *Gbx2* lineage studies in mouse embryos have also demonstrated that a subset of $ISL1^{+}$ ventral motor neurons derived from *Gbx2* expressing cells at E8.5 are absent in the SC by E12.5 in *Gbx2*$^{-/-}$ embryos (Luu et al., 2011).

Therefore, to gain insight into the possible function of *Gbx* genes in cell survival, possible mechanism(s) underlying the loss of motor neurons in single *Gbx* mutants and

if the level of ISL1^{+} cell loss increases in *Gbx* dKO embryos, we examined SC sections for immunoreactivity to caspase-3 at E12.5, E13.5 and E14.5 in *Gbx* single and dKO embryos. Caspase-3 is a cysteine-aspartic acid protease that is used to identify cells entering into the apoptotic signaling cascade (Alnemri et al., 1996). We did not observe any difference in apoptotic activity in the dorsal or ventral SCs of wild-type control and *Gbx* mutant at E12.5 (Fig. 3.4A – D). Interestingly, however, we observed an apparent increase in activated caspase-3 in the ventral SCs of both *Gbx* single mutants when compared to wild-type control embryos at E13.5 (Fig.3. 4E – G). We also noted an increase in caspase-3 activity in E13.5 *Gbx* dKO embryos. Surprisingly, the level of caspase-3 activity appears augmented in *Gbx* dKO embryos at this stage when compared to each single *Gbx* mutant (Fig. 3.4F – H). Increased apoptotic activity persists in *Gbx1*$^{-/-}$ and *Gbx* dKO embryos through E14.5 (Fig. 3.4I, J, L). However, we did not detect any apoptotic activity above that observed in wild-type control embryos in *Gbx2* mutants at E14.5 (Fig. 3.4I, K). The fact that these data show a marked increase in the amount of caspase-3^{+} cells in *Gbx* single mutants, and that apoptotic activity is enhanced in *Gbx* dKO mutants when compared to single mutants at E13.5 (Fig. 3.4B – D), strongly suggests that cooperation between *Gbx1* and *Gbx2* in survival of ventral neurons occurs at this stage.

We next sought to determine if the dying cells observed in *Gbx* mutant SCs are indeed motor neurons. We co-stained transverse, lumbar SC sections from *Gbx1*$^{-/-}$, *Gbx2*$^{-/-}$, *Gbx* dKO, and wild-type littermate control embryos by immunohistochemistry with ISL1 and caspase-3 at E13.5 (Fig. 3.5A - D) and E14.5 (Fig. 3.5E - H). At E13.5, very little apoptotic cell death occurs in the ventral horn of control embryos (Fig. 3.4E,

3.5A). Moreover, very few caspase-3^{+} cells in the ventral horn of wild-type control embryos co-localize with ISL1^{+} motor neurons (Fig.3.5A arrowheads). In contrast, we observed extensive (ISL1/caspase-3) co-localization in *Gbx1*$^{-/-}$ embryos at E13.5 (Fig. 3.5B arrowheads, inset). Only a few of the caspase-3^{+} cells in *Gbx2*$^{-/-}$ embryos (Fig. 3.4G) co-localize with ISL1^{+} cells at E13.5 (Fig. 3.5C arrowheads, inset). While to a lesser degree than at E13.5 (Fig. 3.4M), increased caspase-3 activity is sustained in *Gbx1* and *Gbx* dKO mutants at E14.5 (Fig. 3.4J, L, N). However, the majority of caspase-3 positive cells in these mutants do not appear to co-localize with ISL1^{+} motor neurons, like that observed in wild-type (Fig. 3.5E, F, H). The results of these data show that loss of *Gbx* gene function results in increased apoptotic activation, which is co-localized with ISL1^{+} motor neurons in the ventral horn. Hence, these data support programmed cell death as the underlying mechanism resulting in motor neuron loss in *Gbx* mutants.

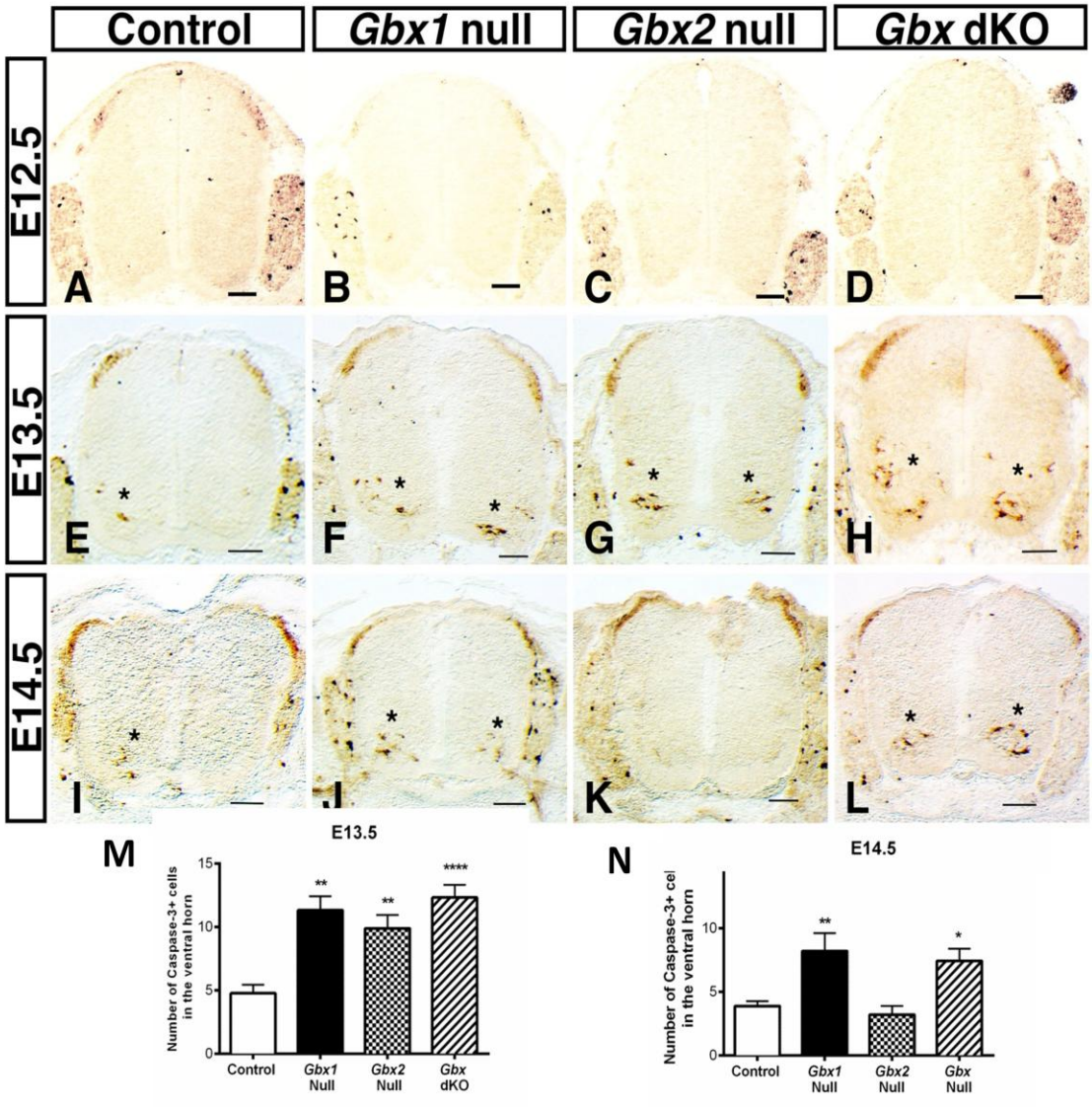
Control
Gbx1 null
Gbx2 null
Gbx dKO
E12.5
E13.5
E14.5
A
B
C
D
E
F
G
H
I
J
K
L
M
E13.5
Number of Caspase-3+ cells in the ventral horn
Control
Gbx1 Null
Gbx2 Null
Gbx dKO
N
E14.5
Number of Caspase-3+ cel in the ventral horn
Control
Gbx1 Null
Gbx2 Null
Gbx Null

Figure 3.4

Figure 3.4 - Deletion of *Gbx* genes results in apoptosis of neurons in the ventral spinal cord. Immunostaining of E12.5 (A-D), E13.5 (E-H) and E14.5 (I-L) lumbar spinal cords to detect apoptosis using caspase-3. At E12.5, no difference in the level of apoptosis is detected between any Gbx mutant when compared to the control. At E13.5, a few cells positive for caspase-3 are now observable within the ventral spinal cord of the control embryo (E), indicating a normal level of apoptosis that occurs under wild type conditions. However, this level of apoptosis appears to increase within the ventral spinal cord, upon the single or double inactivation of *Gbx* genes at E13.5: *Gbx1*$^{-/-}$ (F); *Gbx2*$^{-/-}$ (G); and *Gbx* dKO (H). Again at E14.5, a small number of cells are capsase-3^{+} in the control embryo (I). The increase in apoptosis in the ventral horn is persistently observable at this stage in *Gbx1*$^{-/-}$ (J) and *Gbx* dKO (L) embryos, however this phenomenon appears to terminate in *Gbx2*$^{-/-}$ embryos (G), as no positive cells are detected. Quantification of the number of caspase-3^{+} cells in the ventral spinal cord of each genotype examined at E13.5 (M) and E14.5 (N). Each bar represents the average of three lumbar SC sections from three samples of each genotype analyzed (i.e. nice sections each for control, *Gbx1*$^{-/-}$, *Gbx2*$^{-/-}$ *or Gbx1*$^{-/-}$;*Gbx2*$^{-/-}$). Results are represented as mean+SEM; *P < 0.0001. Black asterisks indicate cells that are caspase-3 positive. Scale bars represent 100 µm.

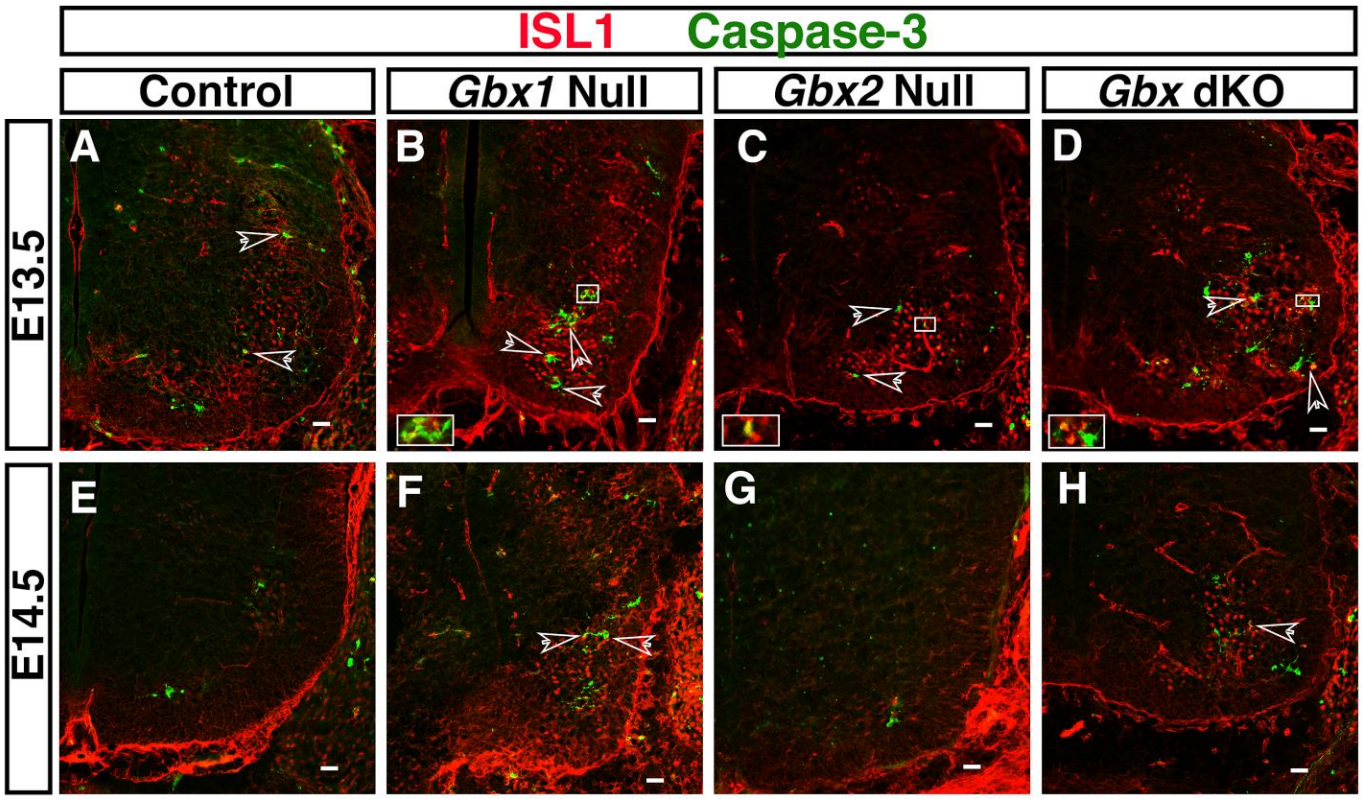
ISL1
Caspase-3
Control
Gbx1 Null
Gbx2 Null
Gbx dKO
E13.5
E14.5
A
B
C
D
E
F
G
H

Figure 3.5

Figure 3.5 - Caspase-3 co-localizes with Islet1^{+} motor neurons in the ventral spinal cord of *Gbx* mutants. Immunostaining to detect caspase-3^{+} apoptotic spinal neurons in the lumbar spinal cords of *Gbx1*$^{-/-}$, *Gbx2*$^{-/-}$ and *Gbx* dKO mutants at E13.5 (A-D) and E14.5 (E-H). Co-immunostaining with ISL1 antibody allows for the analysis of apoptotic neurons co-expressing the marker of spinal motor neurons. Upon analysis at E13.5, control embryos express a few cells immunopositive for caspase-3, however none of these cells colocalize with cell bodies expressing ISl1, indicating that under normal condition at this stage, motor neurons do not undergo apoptosis (A). In the *Gbx* mutants however, some cells immunopositive for caspase-3 colocalize with ISL1^{+} motor neurons in the ventral spinal cord (white arrows and insets in B-D). This indicates a role for *Gbx* in survival of a subset of ISL1 populations as early as E13.5. At E14.5, apoptotic cells are detectable in the ventral spinal cord of control embryos (E). This level of caspase-3 immunoreactivity is persistent *Gbx1*$^{-/-}$ and *Gbx* dKO embryos where a subset of apoptotic cells colocalize with ISL1^{+} motor neurons (F and H, white arrowhead). Notably, few to no cells are caspase-3^{+} in *Gbx2*$^{-/-}$ mutant embryos. Scale bars represent 50 µm. N=3 for each genotype, at each stage. Insets are 40x magnification of boxed regions in (B-D).

3.3 DISCUSSION

Gbx1 and *Gbx2* are dynamically expressed during embryogenesis, and display extensive overlap in the CNS, particularly in the developing SC. However, their role(s) in SC development have only recently begun to be elucidated. In this study, we have focused our analysis on possible genetic and functional redundancy between them in the developing SC. By analyzing *Gbx1*$^{-/-}$, *Gbx2*$^{-/-}$ and *Gbx1*$^{-/-}$;*Gbx2*$^{-/-}$ embryos, we demonstrate that *Gbx* function is a key regulatory component in maintenance of a subset of dorsal PAX2^{+} interneurons at E13.5 and E14.5. Furthermore, since we observed considerable motor neuron apoptosis in all *Gbx* mutants at E13.5**,** and in *Gbx1* and *Gbx* dKO embryos at E14.5, our data indicate that we have uncovered a novel mechanism through which *Gbx1* and *Gbx2* function to maintain the survival of ventral motor neurons in the developing SC. These data demonstrate that *Gbx1* and *Gbx2* are essential for normal patterning and development of spinal interneurons and motor neurons in the developing SC, which underlie the assembly of complex neural circuits within it.

Gbx1 and *Gbx2* are involved in patterning late-born inhibitory interneurons in the dorsal spinal cord

Intermingled populations of excitatory and inhibitory interneurons in the dorsal SC modulate and integrate sensory information received from the periphery. Most interneurons that populate the superficial dorsal horn are generated during the second stage of dorsal neurogenesis and are comprised of inhibitory dILA and excitatory dILB interneurons (Gross et al., 2002; Muller et al., 2002; Cheng et al., 2004; Glasgow et al.,

2005). The expression of *Gbx1* and *Gbx2* can be detected in the SC primordium as early as E9.0 and E8.5, respectively. Differences in expression patterns of each *Gbx* gene at these early stages suggest independent regulation of distinct populations of precursor cells. However, co-localization of *Gbx* mRNA expression in the dorsal mantle zones beginning at E12.5, supports possible genetic interaction during late stages of neurogenesis. We analyzed if genetic interaction between *Gbx* transcription factors occurs, with a focus on developmental stages their expression domains most heavily overlap within the dorsal SC, E12.5 - E13.5, and when *Gbx2* is significantly down-regulated in normal SCs, E14.5. This developmental period is coincident with the generation of late-born inhibitory interneurons. Our in situ hybridization analyses at E13.5 and E14.5 show that loss-of-function in a single *Gbx* gene results in increased expression of its normal counterpart. The observed marked change in *Gbx* expression profiles within the superficial dorsal horn during the late phase of neurogenesis is intriguing, and strongly support the notion that interaction between *Gbx1* and *Gbx2* occurs at a genetic level in the dorsal SC.

We observed a striking anatomical defect in the superficial dorsal horn of *Gbx* mutant embryos, where we found clear changes in the cytoarchitecture of late-born $PAX2^{+}$ cells at E13.5 and E14.5. Interestingly, recent studies have shown that GBX1 and GBX2 proteins are expressed in subsets of late-born $PAX2^{+}$ cells (John et al., 2005; Luu et al., 2011) (Del Barrio 2013, Mezianne 2013). Not surprisingly, we observed a significant loss of PAX2 expressing cells in the superficial dorsal horn in $Gbx2^{-/-}$ embryos ($P < 0.0002$, E13.5; $P < 0.01$, E14.5), as Luu et al demonstrated how *Gbx2* lineage in the dorsal SC directly gives rise to $PAX2^{+}$ interneurons as early as E8.5.

Additionally, our data shows that a significant reduction in PAX2 expressing cells also occurs in *Gbx1*$^{-/-}$ embryos ($P < 0.0001$, E13.5; $P < 0.0003$, E14.5) and is consistent with evidence demonstrating a requirement for *Gbx1* in normal expression and patterning of PAX2^{+} cells in the SC (Meziane et al., 2013). Intriguingly, the reduction of PAX2^{+} cells is not augmented in *Gbx* dKO embryos when compared to single *Gbx* mutants (Fig. 2I, J), suggesting that for this cell type, the Gbx factors do not function in a compensatory manner. One possible explanation of this paradoxical result is the traditional threshold-dependent readout model (Wolpert, 1969). Following this model, a critical threshold level of total *Gbx* gene product is required for correct development and patterning of subset(s) of late-born PAX2^{+} cells. Consequently, loss of *Gbx1*, *Gbx2* or both would result in similar cell number reductions and patterning defects. This concept is supported by recent studies showing that patterning of distinct tissues relies on how transcription factor concentration is perceived by the underlying genetic network (Liu et al., 2013). In addition, results from our recent studies demonstrate varying threshold requirements for *Gbx2* gene product in different regions of the developing anterior hindbrain (Waters and Lewandoski, 2006). While it remains to be determined if GBX1 and GBX2 proteins are co-localized in the same subpopulation(s) of PAX2^{+} cells, these data reveal remarkable parallels between *Gbx1* and *Gbx2* in development of a dorsal inhibitory interneuron population.

Reduced cell proliferation and programmed cell death are two common mechanisms that underlie loss of spinal neurons in normally developing embryos. Although we observe substantial loss of PAX2^{+} cells throughout the superficial dorsal horn at E13.5 and E14.5 (Fig. 3.5), our data shows very little apoptotic cell death, as

indicated by caspase-3 activity, occurring in the dorsal horn of *Gbx* single or dKO mutants. Importantly, this finding is consistent with prior studies demonstrating that dorsal spinal interneuron apoptosis normally begins after E17 in mice, and occurs primarily after postnatal day (P) 0 (Lowrie and Lawson, 2000; Prasad et al., 2008). Therefore, these data would support that *Gbx* genes could function in regulating the proliferative status of dorsal $PAX2^+$ inhibitory interneurons. This view is supported by results from our previous studies in mice and zebrafish demonstrating that *Gbx2* does indeed function in maintaining the proliferative status of neural progenitors in the cerebellar anlage and transient anterior hindbrain structures rhombomere (r) 2, r3, and r5 (Waters and Lewandoski, 2006; Burroughs-Garcia et al., 2011). This notion is also consistent with a recent study proposing Gbx2 to maintain the proliferative status of dorsal progenitors (Luu et al., 2011). While the present study does not exhaustively address the proliferative status of dorsal inhibitory interneurons, our data do reveal a prominent decrease in the amount of $PAX2^+$ cells in the deep dorsal horn, where dI4 and dIL progenitors reside, in *Gbx* single and dKO mutants at E13.5. It will be interesting in future studies to see if regulation of SC proliferation by *Gbx* acts by impacting the expression of morphogenic signaling molecules such as FGFs and Wnts as shown in the anterior hindbrain (Waters and Lewandoski, 2006; Su et al., 2014).

Gbx family members act to maintain ventral motor neuron populations through a shared molecular mechanism.

We also observed phenotypic parallels in the ventral SC of *Gbx* mutants. As discussed earlier, our analyses of caspase-3 activity did not uncover any abnormal programmed cell death in the dorsal SC of *Gbx* mutant embryos at E13.5 or E14.5. In

striking contrast, we observed an abundance of caspase-3 activity in the ventral horns of all *Gbx* mutant SCs at E13.5. *Gbx1*$^{-/-}$ and *Gbx* dKO embryos also display increased apoptosis at E14.5. Notably, we did observe some ventral apoptosis in wild-type embryos at these stages. Importantly, our observation of ventral apoptosis in wild-type embryos is consistent with previous results indicating that spinal interneuron apoptosis proceeds in a ventral-to-dorsal temporal gradient and correlates with the first wave of synaptogenesis in the SC between E14 and 17 (Oppenheim, 1991; Lowrie and Lawson, 2000; Mennerick and Zorumski, 2000). Our recent analysis of *Gbx1*, demonstrate that loss of *Gbx1* function results in a significant reduction in ventral ISL1^{+} motor neurons beginning at E14.5, which persists through P5. Similarly, *Gbx2* fate mapping studies in mice have shown that motor neurons derived from the *Gbx2* lineage are lost in *Gbx2* null embryos beginning at E12.5 (Luu et al., 2011). The mechanism(s) underlying the loss of motor neurons in the *Gbx* mutant SCs was not determined in those studies. In this study, we show that increased caspase-3 activity in *Gbx* mutant SCs at E13.5 co-localizes with ISL1^{+} motor neurons. Hence, these data provide first evidence demonstrating that *Gbx* gene function maintains ISL1^{+} motor neuron survival by preventing apoptotic cell death.

Whether, *Gbx1* and *Gbx2* play direct cell-autonomous or non-cell-autonomous roles in ventral motor neuron survival remains unresolved. The notion that *Gbx* genes may have non-cell-autonomous roles in motor neuron survival is intriguing. Indeed, this has been previously postulated for *gbx2* function in r2 – r3 of zebrafish hindbrain where little or no *gbx2* is expressed (Burroughs-Garcia et al., 2011). Similarly, in situ hybridization studies in several species demonstrating that *Gbx2* mRNA is barely

detectable ventral of the EN1^{+}, V1 interneuron domain in the ventral SC, also provide support for non-cell-autonomous function in motor neuron survival (Kikuta et al., 2003; Rhinn et al., 2003; Waters et al., 2003). Furthermore, several HD-containing transcription factors, EN1, EN2, PAX6 and OTX2 have been shown to function as secreted factors in shaping neural circuits (Brunet et al., 2005; Lesaffre et al., 2007; Sugiyama et al., 2008). Like *Gbx2*, our recent analysis of *Gbx1*$^{-/-}$ embryos also supports the possibility of non-cell-autonomous contributions in motor neuron survival by *Gbx* transcription factors. We have shown that projection of proprioceptive afferents into the ventral SC to establish connections with ISL1^{+} motor neurons terminates prematurely in the intermediate zone of *Gbx1*$^{-/-}$ SCs (Buckley et al., 2013). Therefore, the observed increase in apoptotic motor neurons in *Gbx1*$^{-/-}$ SCs may be due to loss of functional synapses and not cell-autonomous requirements.

We show here that heavy caspase-3 activity occurs in the SCs of both *Gbx* single mutants at E13.5, and that activity is increased in *Gbx* dKO embryos at this stage. Surprisingly, while apoptosis persists in *Gbx1* single and dKO mutants at E14.5, it is severely diminished in *Gbx2*$^{-/-}$ SCs at this stage (Fig. 4). One possible interpretation of these results is that *Gbx1* and *Gbx2* function to regulate distinct subpopulations of ISL1^{+} motor neurons undergoing apoptosis at E13.5. While at E14.5 only those ISL1^{+} motor neurons being impacted by *Gbx1* continue to undergo apoptosis. Interestingly, this view is consistent with recent fate-mapping studies suggesting that the *Gbx2* lineage contributes to ventromedial ISL1/2^{+} motor neurons that constitute the medial motor column (MMC). Whereas, our recent functional analysis strongly suggest, that motor neurons constituting the lateral motor column (LMC) are affected by the *Gbx1* null

mutation (Han et al., 2009; Luu et al., 2011; Buckley et al., 2013). Furthermore, it is noteworthy that loss of motor neurons occurs in *Gbx1*$^{-/-}$ and *Gbx2*$^{-/-}$ mutants, suggesting that neither gene functionally compensates for the loss of a family member in distinct ISL1^{+} motor neuron subpopulations. A thorough investigation through gene replacement analysis will provide more insight into this possibility. While these data do not support a potential for functional redundancy between *Gbx* genes in ventral ISL1^{+} motor neuron development, they do however demonstrate *Gbx* genes have a shared role in motor neuron survival by preventing apoptosis.

In conclusion, we have shown that the dorsal and ventral regions of the SC are affected in a remarkably parallel manner in *Gbx1*$^{-/-}$ and *Gbx2*$^{-/-}$ mouse embryos. Our results provide evidence that *Gbx1* and *Gbx2* function similarly, but not redundantly, within cellular subtypes that they together act to generate and maintain. Our observations of increased *Gbx1* and *Gbx2* mRNA expression in their null counterparts, patterning defects in PAX2^{+} dorsal interneurons, as well as increased apoptosis in ventral ISL1^{+} motor neurons of *Gbx* single and dKO mutants demonstrate that we have uncovered novel mechanisms through which *Gbx* genes pattern and maintain the survival of PAX2^{+} dorsal interneurons and ventral ISL1^{+} motor neurons, respectively, in the developing SC.

CHAPTER 4

CONCLUSIONS AND FUTURE DIRECTIONS

Locomotion is a function of motor behavior executed by the CNS, which enables an organism to move. In order to produce motor output, the organism first depends on specification and fate acquisition of genetically different SC neurons. The differential expression of HD transcription factors within progenitor and post-mitotic spinal neuron populations plays an essential regulatory role in this process (Dalla Torre di Sanguinetto et al., 2008). Next, groups of functionally distinct spinal neurons elegantly interconnect to form neural circuits, which serve as the basis for neural networks generating rhythmic locomotor patterns (Goulding and Pfaff, 2005; Arber, 2012). Integration of peripheral sensory neurons into spinal networks establishes communication between the PNS and CNS. By functioning as a mechanism to integrate the CNS and PNS, proprioceptive sensorimotor circuits are essential for locomotor output (Akay et al., 2014).

Walking is a major form of locomotion that relies on accurate and efficient locomotor output. The precision by which movement is executed during locomotor tasks is controlled by selective synaptic communication between neural constituents of proprioceptive sensorimotor circuits. The challenge in understanding mechanisms that establish neuronal connectivity in sensorimotor circuits is largely due to two reasons. (1) Several spinal neuron populations are involved in the generation of locomotion and (2)

the synapses made between them are intricate. Experiments designed to identify mechanisms involved in the development of locomotor circuits with simple synaptic connections help to circumvent the complexity of investigating complicated networks (Dasen, 2009)

The simplest locomotor circuit necessary to walk is the MSR circuit. It is a proprioceptive sensorimotor circuit operated by two functional units: proprioceptive sensory neurons (sensory unit) and MNs in the ventral SC (motor unit) (Chen et al., 2003) (Figures 2.3, 4.1A). Axons of proprioceptive neurons establish a single connection with MNs to provide the stimulus for a locomotor reflex. The simplicity of the MSR makes it useful for examining how the PNS and CNS interact systematically and how functional units of locomotor circuits work fundamentally. Advances made towards understanding development of simple circuits underlying motor control, such as the MSR, will be helpful in elucidating developmental mechanisms that establish more complex neural networks for locomotion.

The goal of the research herein was to investigate involvement of murine *Gbx1* in SC development and locomotor output. *Gbx1* is dynamically expressed in the developing SC throughout embryogenesis (Waters et al., 2003; John et al., 2005). We pursued characterization of *Gbx1* in the SC using *Gbx1*$^{-/-}$ mutants. This analysis revealed a novel requirement for *Gbx1* in development of proprioceptive locomotor circuits in the SC. We began our analysis during embryonic stages to examine the developmental requirements of *Gbx1* for locomotor output. We analyzed segments from the lumbar SC, which is populated by neurons responsible for modulating and eliciting

motor output. Through this analysis we examined independent constituents of locomotor neural circuitry, and observed perturbation of two major components in *Gbx1*$^{-/-}$ mutants (Figure 4.1B). (1) 1afferents that innervate the dorsal SC to relay information from the PNS are defasiculated and terminate innervation prematurely in the intermediate zone (Figure 2.6, Figure 4.1B). (2) Concomitantly, apoptosis drastically reduces the number of ventral α-MNs that execute proprioceptive locomotor responses from the CNS to the PNS (Figure 2.8-2.9, Supplemental Figure 2.1, Figure 3.5, Figure 4.1). Notably, cell populations affected by the loss of *Gbx1* make up two major functional units of the MSR circuit (Figure 1.3, Figure 4.1B).

Injuries to the human SC, regardless of which anatomical segment is impacted, results in weakening of the lower limbs and often, paralysis (Patten et al., 2014). This type of injury immediately eliminates walking ability, which severely affects an individual's quality of life thereafter. The research herein provides data to support that *Gbx1* is critical for development of a fundamental neural circuit that is required for locomotion. Further, the knowledge gained through studying *Gbx1*$^{-/-}$ mice will help to shed light on key mechanisms impacted by injury that underlie SC dysfunction. The data presented in this dissertation has allowed us to generate a model that demonstrates functional roles of *Gbx1* in spinal locomotor circuit formation suggested by cytoarchitectural phenotypes that result due to a loss of *Gbx1* function (Figure 4.2). Importantly, since we did not exhaustively address additional roles for *Gbx* genes in SC development or the establishment of MSR circuitry by *Gbx1*, future research should aim

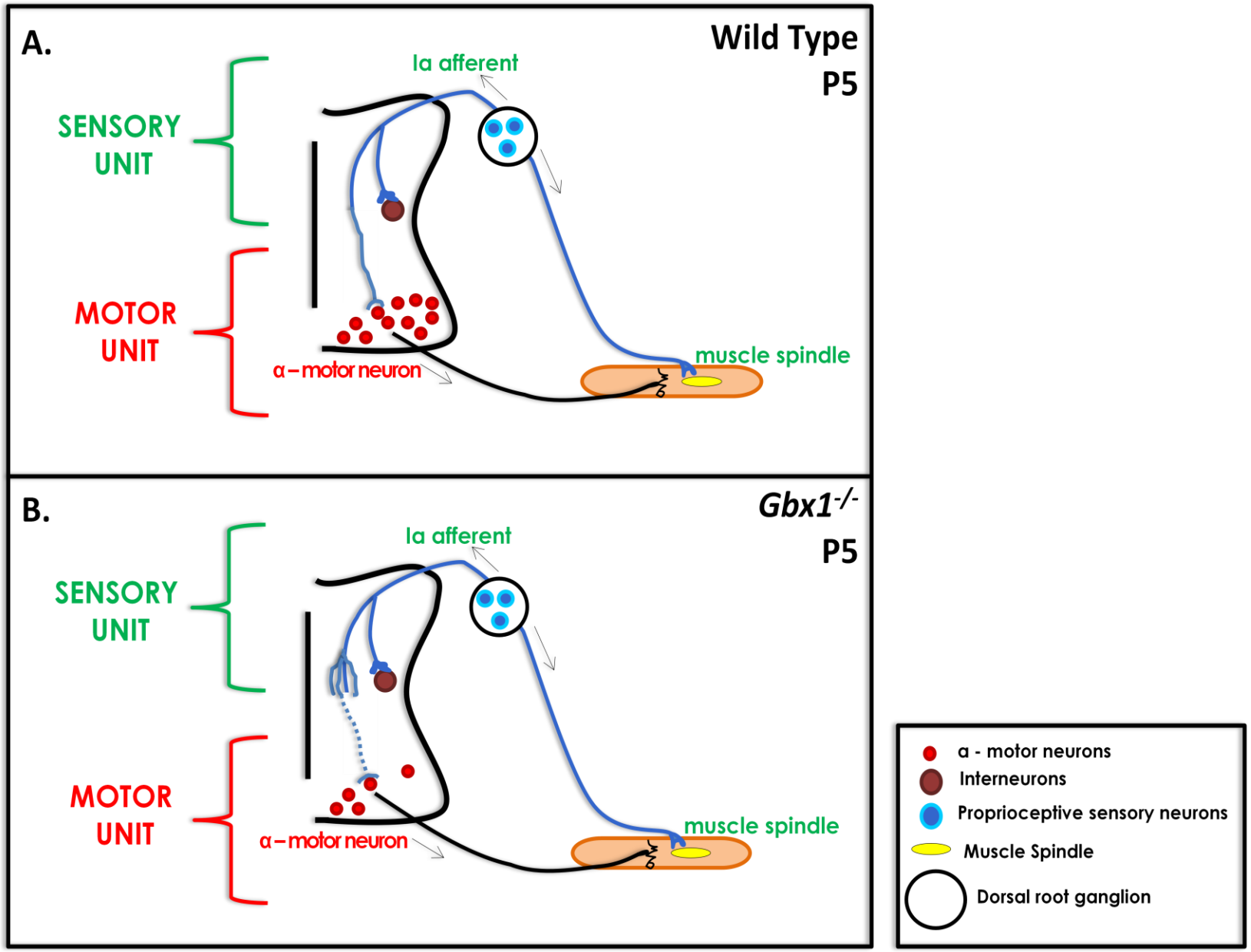
A.
Wild Type
P5
Ia afferent
SENSORY UNIT
MOTOR UNIT
α – motor neuron
muscle spindle
B.
Gbx1-/-
P5
Ia afferent
SENSORY UNIT
MOTOR UNIT
α – motor neuron
muscle spindle
α - motor neurons
Interneurons
Proprioceptive sensory neurons
Muscle Spindle
Dorsal root ganglion

Figure 4.1

Figure 4.1 - Loss of *Gbx1* Perturbs Both Functional Units of MSR Circuitry. (A) Schematic depicting a MSR circuit established at postnatal (P) day 5. The sensory unit is comprised of muscle spindles in the periphery and 1a afferents. Whereas, the motor unit is composed of α-MNs in the ventral SC. (B) Schematic depicting the defects to MSR circuitry in *Gbx1*$^{-/-}$ mutants at P5. A loss of *Gbx1* results in premature termination of 1a afferents and death of α-MNs, affecting both functional unit of the MSR.

Progressional timeline of mouse MSR development
E13.5
E14.5
P0
A.
Wildtype
B.
Gbx1-/-
C.
D.
E.
F.
Ia afferent
Muscle Spindle
?

Figure 4.2

Figure 4.2 - **A model for the involvement of *Gbx1* in development of the monosynaptic stretch reflex circuit**. (A) At E13.5 in the wild-type embryonic SC, post-mitotic ventral motor neurons are clustering into stereotypic motor columns. Motor neurons resident of distinct motor pools protrude axons towards peripheral muscle targets to begin establishing functional synaptic connections for the control of motor output. Axons of proprioceptive sensory neurons have began to innervate muscle targets as well to establish a peripheral sensor that provides information about limb position. Once perceived, information is relayed to the SC through 1a and 1b proprioceptive sensory afferents which are just beginning to penetrate the dorsal root entry zone. (B) At E13.5, a subset of motor neurons are marked for apoptosis in *Gbx1*$^{-/-}$ mutants. (C) In wild-types at E14.5, axons of sensory neurons have penetrated the dorsal SC where synapses are made with 1a interneurons in the intermediate zone, other branches of the axon continue a ventral trajectory towards their motor neuron targets. (D) At E14.5 in the *Gbx1*$^{-/-}$ mutant, motor neurons marked for apoptosis the day before have now been eliminated within the lateral motor column. Notably, these apoptotic motor neurons had already extended axons toward peripheral muscle targets prior to this stage, therefore due to their loss we are uncertain whether this affects the innervation of muscle targets. Also, 1a afferents are defasiculated and terminate prematurely in the intermediate zone. (E) By postnatal day (P) 0, formation of MSR circuit, which is defined by the single synaptic connection between a 1a sensory afferent and an α-motor neuron, is complete in wild-type embryos. (F) The reduction in monosynpatic connections in *Gbx1*$^{-/-}$ mutants due to premature stopping of the 1a afferent affects the proper development of the MSR. The extent of reduction in monosynaptic connectivity remains to be determined.

to expound this understanding. This can be achieved by investigating the functional role of *Gbx1* in other components of MSR circuitry, which might reveal a deeper understanding of mechanisms underlying the cytoarchitectural and locomotor defects that exist in *Gbx1* mutants.

We have shown that a loss of *Gbx1* gene function affects both functional units of the MSR: the sensory unit and the motor unit. However, there are other important embryonic mechanisms influencing development of circuits for locomotion that may be impacted by *Gbx1* that have yet to be explored. These include: (i) regulation of MN survival and targeting of peripheral targets/NMJ formation, (ii) regulation of laminar termination and central targeting of proprioceptive 1a sensory afferents to spinal MNs, and (iii) regulation of synaptic connectivity between 1a proprioceptive afferents and spinal MNs. For conceptual purposes (i) and (ii) are discussed in terms of how *Gbx1* is involved in development of the motor unit, whereas (iii) discusses its involvement in developing the sensory unit. Elucidating the involvement of *Gbx1* in these important regulatory processes will improve the understanding of SC and locomotor circuit

4.1 ROLE OF *Gbx1* IN MOTOR NEURON SURVIVAL IN THE LUMBAR SPINAL CORD

Spinal MNs elicit locomotor output for the MSR in the mammalian SC. They are controlled upstream by a network of spinal neurons that coordinate the rhythmic movements of locomotion. To manage the large number of locomotor responses capable of being produced by an organism, MNs differentiate into several subpopulations and receive a variety of modulating synaptic inputs depending on the motor behavior to be expressed (Goulding, 2009). Therefore the correct specification,

positioning, and innervation of postmitotic MNs is crucial to functioning of the MSR motor unit. In *Gbx1*$^{-/-}$ mutants, we observed an unexpected loss of embryonic spinal MNs at E14.5 (Figure 2.8-2.9). We identified the mechanism underlying MN cell death as apoptosis, through coexpression of capsase-3 and ISL1 in the ventral SC (Figure 3.5). While it was important to unveil the mechanism underlying the loss, the cause for MN death in these mutants remains to be explored.

A highly regulated process of cell death occurs during nervous system development known as apoptosis, a form of PCD. This mechanism is indispensible during spinal neurogenesis. It is responsible for regulating the size of progenitor populations, refinement of synaptic connections and serves to correct developmental errors including the removal of ectopic neurons (Sun et al., 2003). PCD occurs within every population of spinal neurons, and proceeds in a ventral-to-dorsal spatio-temporal gradient beginning during embryogenesis (E14.5) and ending during early postnatal development (P5) (Prasad et al., 2008). Regulated death of spinal neurons is developmentally essential for an organism. However, the uncontrolled and unexpected elimination of neurons such as MNs, following injury or disease, severely affect an organism's quality of life. Abnormal death of MNs results in malfunctioning of motor circuits, and is the major underlying cause of many degenerative diseases (Patten et al., 2014). In the event of MN death without injury or disease, defects to the development of synaptic networks involving MNs is a likely contributing factor (Banks and Noakes, 2002). MNs die embryonically in the *Gbx1*$^{-/-}$ mutant SC. Importantly, death occurs within days of their birth, without sustaining an injury and prior to the complete assembly of any locomotor circuits. This suggests that an embryonic process involved in maintaining

a subset of MNs, and their subsequent assembly into motor circuits, is affected by the loss of *Gbx1*.

A key question that remains unresolved is whether *Gbx1* acts cell-autonomously or non cell-autonomously in the survival of locomotor MNs in the lumbar SC (Figure 4.3B). *Gbx1* is expressed in the ventricular zone of the SC in a region consisting of MN progenitor cells at E10.5 (Waters et al., 2003; Rhinn et al., 2004). Due to the dynamic expression of *Gbx1*, which becomes confined to the dorsal SC by E12.5, it seems unlikely that *Gbx1* has a cell-autonomous effect in MN survival once expression has been downregulated in these cells. However there is possibility that *Gbx1* expression in MN progenitors may exert cell-autonomous properties that influence postmitotic survival. This notion has been demonstrated for Notch signlaling. Thus, MNs become susceptible to apoptosis at mid embryonic stages in *Gbx1*$^{-/-}$ mutant. We also show that in *Gbx1*$^{-/-}$ mutants, projection of proprioceptive afferents to their intended MN target zone in the ventral SC terminates prematurely. This raises the notion that loss of MNs could be a secondary consequence to a lack of functional synaptic connections. However, we show that MNs die prior to the establishment of functional synapses between 1a afferent and MNs, suggesting this defect is not likely a contributing factor to MN death in *Gbx1*$^{-/-}$ mutants.

Future work should aim to directly test the requirement for *Gbx1* in generation, survival and integration of MNs into motor networks. *Gbx1* expression can be specifically ablated in MNs using a conventionally targeted allele that drives Cre recombinase expression in spinal MNs (HB9-Cre). HB9 is a HD TF that is selectively

expressed after E9.5, preceding the onset of ISL1, in developing MNs of the ventral SC (Arber et al., 1999). The HB9-Cre line has been used to successfully manipulate expression of other genes previously and has been verified as a specific MN driver through a cross with the ROSA26:lacz reporter line (Arber et al., 1999; Yang et al., 2001; Patel et al., 2003; Luria and Laufer, 2007; Prasad et al., 2008; Wu et al., 2012). These studies have demonstrated that HB9-driven Cre is delimited to spinal MNs, unlike ISL1-Cre which is expressed in multiple spinal neurons populations and peripheral sensory neurons (Liang et al., 2011). Utilizing the conditional *Gbx1*^{flox} allele, crossed with this MN-specific:Cre driver line, will specifically ablate *Gbx1* expression in MN progenitors.

Ultimately, results from this experiment will directly evaluate the consequence of a *Gbx1* null mutation on MN survival and in turn, establishment of motor units for locomotor circuits, like the MSR (Figure 4.3B). This experiment will answer the question of whether *Gbx1* acts cell-autonomously in MN survival. It will also answer whether the locomotor phenotype is a direct result of the MNs lost through apoptosis. Thus, these studies will provide a better understanding of *Gbx1* involvement in MSR circuitry by testing the direct affect of a *Gbx1* null mutation on a vastly important component.

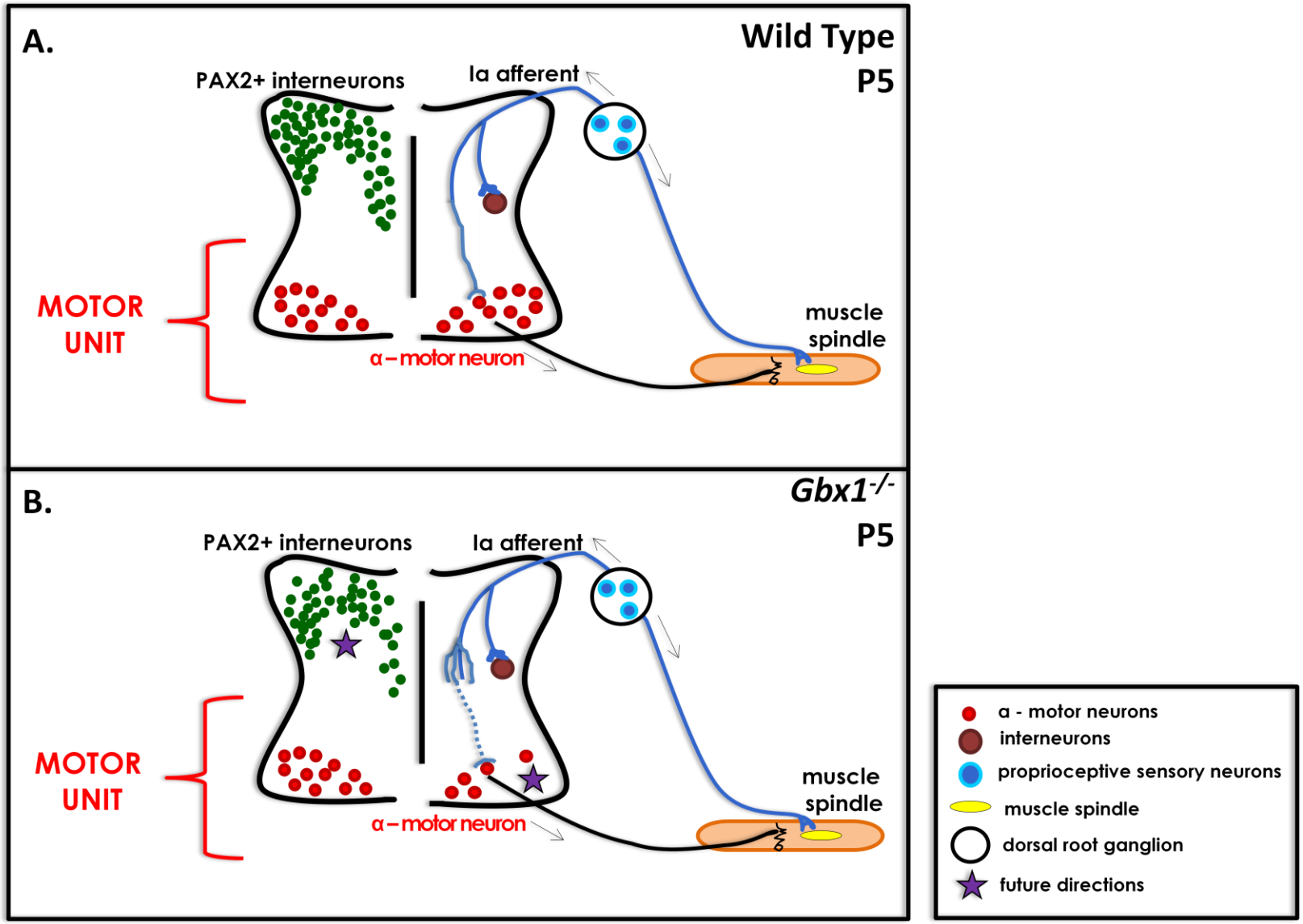
A.
Wild Type
P5
PAX2+ interneurons
Ia afferent
MOTOR UNIT
muscle spindle
α – motor neuron
B.
Gbx1-/-
P5
PAX2+ interneurons
Ia afferent
MOTOR UNIT
muscle spindle
α – motor neuron
α - motor neurons
interneurons
proprioceptive sensory neurons
muscle spindle
dorsal root ganglion
future directions

Figure 4.3

Figure 4.3 - **Loss of *Gbx1* affects spinal neuron populations that influence function of the MSR circuit motor unit.** (A) Schematic representation of MSR circuity at postnatal (P) day 5 in a wild-type SC. Motor unit function is dependent on reflexes generated by MNs. MNs are largely modulated by the balance of inhibitory and excitatory (not featured) neurotransmission within the dorsal SC. GABAergic/glycinergic and glutamatrgic neurons make synapses with sensory afferents monosynaptically connected to ventral motor neurons as a method to accurately control the execution of their motor reflexes. (B) Neuronal populations influencing function of the MSR motor unit in *Gbx1*$^{-/-}$ mutants at P5. Loss of *Gbx1* results in a reduction of PAX2^{+} inhibitory neurons. This possibly affects the balance of neurotransmission modulating motoNr output by α-MNs and remains to be explored. Additionally, MNs die apoptotically in *Gbx1*$^{-/-}$ mutants. It also remains to be resolved whether *Gbx1* acts cell-autonomously in this process.

4.2 ROLE OF *Gbx1* IN PRESERVING THE BALANCE OF INHIBITORY AND EXCITATORY NEURAL CIRCUITS IN THE DEVELOPING SPINAL CORD

In the dorsal horn, the primary relay center for somatosensory processing, most local circuit INs are excitatory using glutamate as their neurotransmitter. Excitation is modulated by local circuit inhibitory neurons, most of which are GABAergic (Sibilla and Ballerini, 2009). Spinal cord analysis for *Gbx1* demonstrates GBX1 protein colocalizes with a set of TFs (LBX1, LHX1/5 and PAX2) distinctive of a dorsal inhibitory IN population (John et al., 2005). These neurons give rise to early-born dI4 (E10.5) and late-born dILA (E12.5) GABAergic dorsal INs (Cheng et al., 2004; Huang et al., 2008).

In our molecular analysis of *Gbx1*;*Gbx2* dKO embryos, we observed a marked reduction of $PAX2^{+}$ cells that populate the superficial most layers of the dorsal horn at E13.5 (Figure 3.2). Analyses of $Gbx1^{-/-}$ and $Gbx2^{-/-}$ single mutants also show the same phenotype (Figure 3.2). These data suggest *Gbx* genes contribute to the maturation or maintenance of dILA INs that normally populate the superficial dorsal horn (Gross et al., 2002). To better understand the observed reduction, we evaluated the level of apoptosis in the SC as a potential mechanism but observed no abnormal apoptosis compared to wild-type (Figure 3.4-3.5). We concluded that *Gbx* genes are not required for cell survival of $PAX2^{+}$ INs. Indeed, results from a recent study analyzing a similar *Gbx1* null mutation, demonstrate a reduced GABAergic neuronal differentiation with no difference in level of apoptosis (Meziane et al., 2013). Recently, it was determined that GABAergic neurons trans-differentiate into glutamatergic neurons and is the cause for the reduction in dorsal PAX2 expression in $Gbx1^{-/-}$ mice (Meziane et al., 2013). The results show a concomitant increase in VGLUT2 expression, a marker for excitatory INs, in the region

of the dorsal horn in which the GABAergic reduction was observed (Meziane et al., 2013). Together these studies demonstrate that *Gbx* genes regulate embryonic differentiation of GABAergic INs in the dorsal horn; it would be interesting to investigate this function further.

The division of late-born excitatory and inhibitory INs requires post-mitotic selector genes *Tlx1* and *Tlx3* that determine glutamatergic versus GABAergic cell fates, respectively (Cheng et al., 2004). Dorsal inhibitory IN populations exclusively express *Ptf1a* (Huang et al., 2008), and are also distinguished by the expression of LHX1/5 and PAX2 (Glasgow et al., 2005). Similar to *Gbx1*$^{-/-}$ mice, genetic elimination of *Ptf1a* results in an increase of excitatory neuron, at the expense of inhibitory neurons. Specifically, dI4 change fate to LMX1B^{+} DI5 INs, and dILA trans-fate to TLX1/3^{+} dILB INs (Huang et al., 2008; Guo et al., 2012). The selective elimination of *Gbx1* in dorsal GABAergic neurons inhibitory INs would allow further investigation of its function in differentiation of this cell type.

Mating of *Gbx1*^{flox} mice with a *Ptf1a*-Cre driver mouse line exclusively eliminates *Gbx1* expression in developing inhibitory dorsal horn neurons (Glasgow et al., 2005; Hori and Hoshino, 2012). This approach directly evaluates the consequence of a *Gbx1* null mutation on GABAergic neuron differentiation. It will determine whether *Gbx1* expression promotes or maintains GABAergic differentiation. Furthermore, it will determine the if the subset of PAX2+ neurons reduced in *Gbx1*$^{-/-}$ mutants contributes to their locomotor phenotype.

Unveiling a role for Gbx in maintenance of a dorsal GABAergic population has provided excellent evidence for a novel role of Gbx transcriptional regulation in the developing SC. Moreover, it has also influenced the notion of another cause for the death of MNs in the *Gbx1*$^{-/-}$ mutant (Figure 4.3B). Many excitatory and inhibitory synapses make contacts with ventral MNs, and a specific balance of these inputs is the basis for normal function. Incorrect development of these modulatory cell populations can lead to over-excitation or over-inhibition, both of which interfere with appropriate synaptic communication (Foran and Trotti, 2009). Excitotoxicity is a pathological process that occurs when the exposure to neurotoxic substances, like excessive glutamate neurotransmission, causes damage and death of neural circuit components (Lau and Tymianski, 2010). This phenomenon has been implicated in the apoptotoic death of MNs in both acute and chronic neurodegenerative diseases (Foran and Trotti, 2009; Ramirez-Jarquin et al., 2013).

Imagine sitting behind the wheel of a race car. In a normal situation, one would engage the ignition, stomp the gas pedal to initiate high speed and press the brake pedal to slow down. This is similar to a motor circuit in which glutamatergic excitatory INs serve as the organism's gas pedals and inhibitory INs mediated by glycine or GABA serve as the brake system. Now using the same example: imagine reaching maximum speed and upon attempting to slow down, the brake system is inoperable. The car keeps accumulating speed, which becomes toxic to the system, causing it to run on overdrive until the engine expires from being over worked. In the case of locomotor circuits, this scenario would equate to an abundance of excitatory neurotransmission at

the expense of inhibitory neurotransmission, which leaves the MNs in a state of over excitation or excitotoxicity, and subsequent death.

A number of studies have addressed this theory by evaluating the abundance of excitatory and inhibitory synaptic connections on MNs (Schutz, 2005; Betley et al., 2009). Future studies using *Gbx1*$^{-/-}$ mutants should approach this analysis by utilizing simple molecular techniques that allow assessment of the relative quantity of glutamatergic and GABAergic synapses on MNs as a measure of balanced or imbalanced neurotransmission. Antibodies raised against two types of vesicular glutamate transporters, VGLUT1 and VGLUT2, identify glutamatergic synapses. GABAergic synapses are identified by α-Gad67, the enzyme that catalyzes the decarboxylation of glutamate to GABA. Localization of these antibodies in synaptic terminals near MNbe representative of the relative density of either type of synapse on MNs, which can be further defined through quantification (Betley et al., 2009). If no differences in the number of glutamatergic or GABAergic axon collaterals in mutant compared to controls are observed, it demonstrates the loss of PAX2 has no overt affect on neuromodulation of MNs.

An imbalance in the level of inhibitory and excitatory neurotransmission in the SC of *Gbx* mutants may also allude to the locomotor phenotype we and others observe in *Gbx1*$^{-/-}$ mutants. This concept has been implicated for other mouse mutants displaying motor dysfunction phenotypes (Kosaka et al., 2012). It is highly noted that there is a dynamic interrelationship between inhibition and excitation in controlling the output of ventral motor networks. During embryonic development, functional spinal networks depend largely on the activity of glycinergic and GABAergic neurons. At this stage,

these neural subtypes mediate excitatory neurotransmission until shortly before birth when their mode of transmission transitions to inhibitory upon the acquisition of alternating motor output between alpha and gamma MNs (Sibilla and Ballerini, 2009). At this late stage of embryonic development, glycine and GABA begin to mediate presynaptic inhibition as GABA receptor subunits become abundantly expressed in ventral MNs between E15-E17 (Laurie et al., 1992). Maturation of the locomotor output pattern corresponds with maturation of synaptic inhibition, where the relationship between left-right alternation is variable at E17.5 but defined after E18.5. This may explain why *Gbx1* mutants do not display a behavioral locomotor phenotype until postnatal maturation of sensorimotor circuits when the mice are becoming accustomed to load-bearing locomotion and sensing proprioceptive changes in muscles. Defining the role of *Gbx1* in development of GABAergic inhibitory systems will improve our overall knowledge on the processes governing abnormal locomotor output in *Gbx1*$^{-/-}$ mutants. Moreover, it will help shed light on the cause of ventral SC MN death, which severely affects the motor unit of the MSR (Figure 4.3B).

4.3 REGULATION OF 1A AFFERENT TARGETING AND SYNAPTIC CONNECTIVITY TO SPINAL MOTOR NEURONS BY *Gbx1*

The establishment of a functional monosynaptic reflex circuit relies on precise termination of 1a afferents near α-MN targets in the ventral SC(Chen et al., 2003). Moreover, synapses made between 1a afferents and MNs contribute to the generation of accurate stretch reflexes (Alvarez et al., 2010). Once 1a afferents innervate the dorsal SC, they extend towards the ventral SC where they encounter a variety of factors that influence their trajectory and help to establish connections with MNs. Studies have

shown the expression of ETS transcription factors by MNs play an important role in this process (Arber et al., 2000; Dalla Torre di Sanguinetto et al., 2008; Usui et al., 2012). In *Gbx1*$^{-/-}$ mutants, 1a afferents terminate prematurely in the intermediate zone, and as a result, likely have reduced numbers of monosynaptic connections with ventral MN targets. The mechanism by which the loss of *Gbx1* causes this defect is currently unknown (Figure 4.4B), and whether this occurs in a cell or non-cell autonomous manner also remains to be explored.

ETS transcription factor, *Er81*, has been implicated in regulating the connection between 1a afferents and MNs (Lin et al., 1998; Arber et al., 2000). *Er81* is not only expressed by the proprioceptive sensory afferent but it is also expressed by MNs in the ventral SC (Arber et al., 2000; Livet et al., 2002). At the time sensorimotor connections are being established in the developing SC (E16-18), individual pools of MNs expressing *Er81* become selectively innervated by afferents expressing the same protein (Lin et al., 1998). This observation suggests that *Er81* expression in both components of the circuit is important in order to form a functional synapse. Our previous *in situ* hybridization analyses show that *Gbx1* expression coincides with a population of MNs in the ventral SC at E10.5 (Waters et al., 2003). Recently, we observed a significant decrease in the total number of MNs in *Gbx1*$^{-/-}$ mutant embryos (Buckley et al., 2013). It is possible that the level of ER81 protein eliminated from the ventral SC by apoptotic death of MNs, could affect the establishment of sensorimotor connections in *Gbx1*$^{-/-}$ mutant embryos.

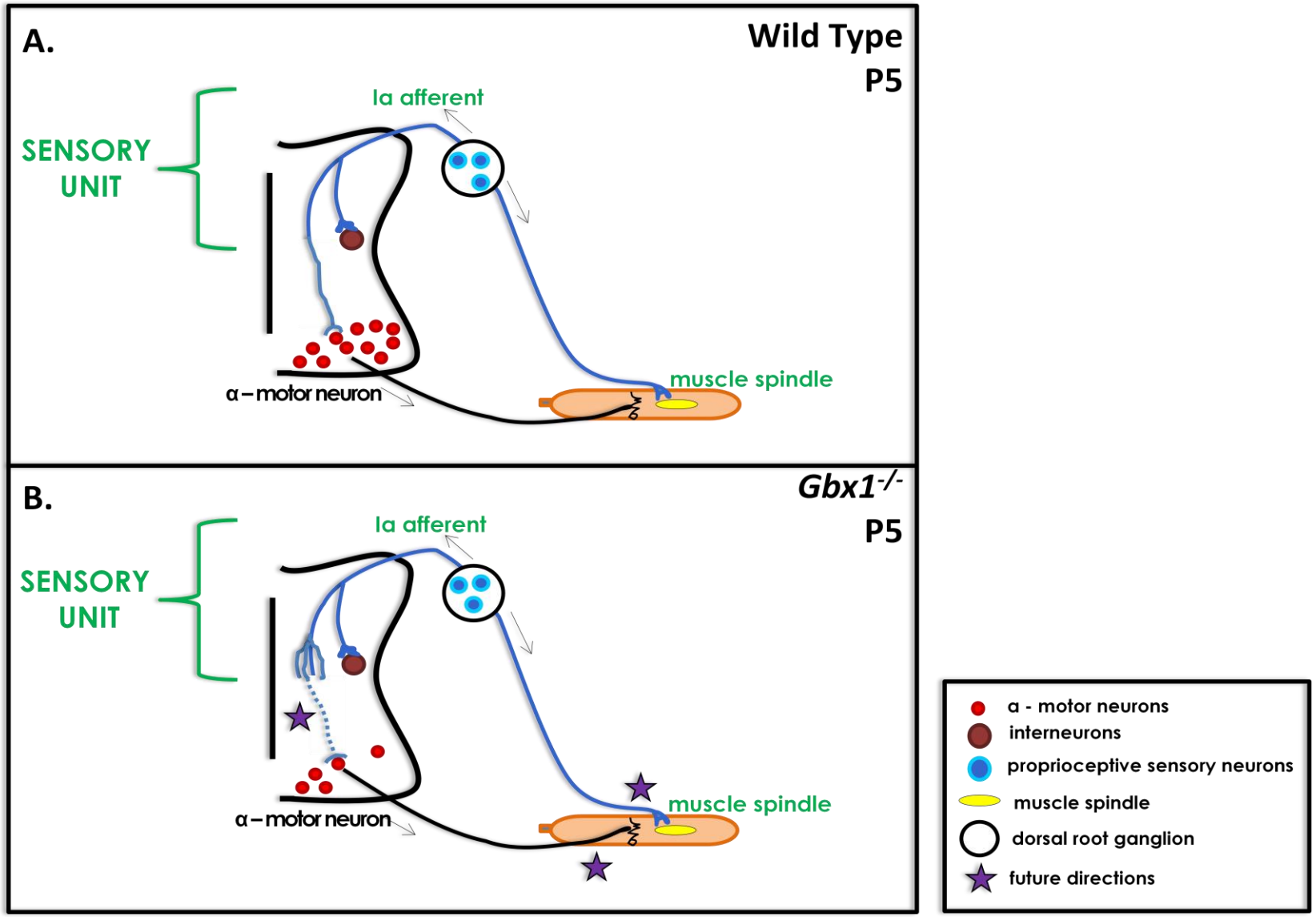
A.
Wild Type
P5
SENSORY
UNIT
Ia afferent
α – motor neuron
muscle spindle
B.
Gbx1-/-
P5
SENSORY
UNIT
Ia afferent
α – motor neuron
muscle spindle
α - motor neurons
interneurons
proprioceptive sensory neurons
muscle spindle
dorsal root ganglion
future directions

Figure 4.4

Figure 4.4 - Loss of *Gbx1* affects the MSR circuit sensory unit. (A) Schematic representation of MSR circuitry at postnatal (P) day 5 in a wild-type SC. Sensory unit function depends on transmission of sensory messages to the motor unit through the 1a afferent. The establishment of synapses between 1a afferents and motor neurons is highly regulated. (B) Representation of the sensory unit defect in *Gbx1*$^{-/-}$ mutants at P5. Loss of *Gbx1* results in premature termination and defasiculation of 1a afferents. This likely reduces the number of functional synapses established between them and their ventral motor neuron targets. This notion remains to be explored.

4.4 GENETIC INDUCIBLE *Gbx1*-CreERT2: AN ALTERNATIVE APPROACH FOR *Gbx1* ANALYSIS

Genetically inducible alleles are the most sophisticated genetic tool used to manipulate the mouse genome (Joyner and Zervas, 2006). They are most often designed to inactivate genes of interest. However, they are also used to activate reporter genes to mark cells expressing a gene of interest; referred to as genetic fate mapping. Genetic fate mapping allows relationships to be established between embryonic gene expression domains and cell fates that arise from within (Joyner and Zervas, 2006). Due to its non-invasiveness, fate mapping has bypassed barriers that previously impeded studies in utero during development, such as the inability to inject embryos with cell lineage markers directly (Branda and Dymecki, 2004).

Genetic inducible fate mapping is, in part, accomplished by use of a transgenic mouse, which contains genetic material that was inserted into the genome by modification of the endogenous genome(Jensen and Dymecki, 2014). The most common transgenes are reporter alleles that are capable of constitutively expressing a fluorescent protein within a specific cell of interest (Jensen and Dymecki, 2014). For example, the ROSA26 reporter mouse line, constitutively expresses *LacZ* when activated (Soriano, 1999). The cell type that expresses the transgene, and reporter, is determined by mating the transgenic mouse with a mouse containing a conditional or "floxed" allele for a specific gene of interest. The advantage of this technology is by using promoter and enhancer elements from an exclusively expressed gene of choice, activation of site-specific recombinase enzymes (Cre or FLP) are restricted only to cells

desired by the investigator. Additionally, the inducible element of this system allows for temporal control by which the recombinase is active (Feil et al., 2009).

In particular, transcription factors are attractive candidates to genetically modify with inducible-elements because they are dynamically expressed during embryonic development (Bertrand et al., 2002). Differential expression patterns correlate with their indispensible role in specifying distinct cell types. *Gbx1* is expressed in neural progenitor cells of the SC ventricular zone at E10.5, and then becomes spatially restricted to the dorsal mantle zone by E12.5 (Waters et al., 2003; John et al., 2005). Due to the dynamic nature of *Gbx1* expression it serves as an excellent candidate for this method of genetic manipulation. Importantly, the creation of an inducible Cre allele for *Gbx1* allows for the direct identification of roles for *Gbx1* in the development of locomotor circuits. For example, it can determine whether *Gbx1* acts cell-autonomously in vMN survival.

The lineage of spinal IN populations expressing *Gbx1* can be determined through inducible-fate mapping. *Gbx1*-CreERT2 female mice mated with *R26R* male mice (Soriano, 1999) allow visualization and the tracing of individual cells derived from *Gbx1*$^{+}$ progenitors over time. Temporal control of cell marking with LacZ is obtained by delivering artificial oestrogen, tamoxifen, to pregnant CreERT2;R26R mice at multiple gestational stages. Embryos carrying a CreERT2;R26R allele, results in the transient activation of CreERT2, upon induction by tamoxifen. CreERT2 then causes recombination between *loxP* sites in the R26R allele, excision of a stop sequence and subsequent expression of *lacZ*. Cells permanently marked by β-galactosidase activity, indicate *Gbx1*$^{+}$ cell -lineage. Currently, the ability to identify roles for *Gbx1* based on the

expression of its protein is largely impeded by the lack of commercially available antibodies. The fate mapping of *Gbx1* will define the cells that depend on *Gbx1* expression for their development, and circumvent the lack of resources that are traditionally used for expression analyses.

Another advantage of the novel *Gbx1*-CreERT2 allele, allows the temporally controlled excision of the $Gbx1^{flox}$ allele (Buckley et al., 2013), rendering $Gbx1^{-/-}$ mutants embryos at various embryonic stages. This approach is far more refined than traditional methods in which genes are inactivated from the time of conception. Inactivation of the $Gbx1^{flox}$ allele with *Gbx1*-CreERT2 permits normal expression of *Gbx1* in early embryos then temporal inactivation at discretion of the investigator. What is key about this study is the ability to define with great precision, the indispensible roles of *Gbx1* in normal development of locomotor circuitry. Mice that are heterozygous for the *Gbx1*-CreERT2 allele ($Gbx1^{CreERT2/+}$) mated with mice homozygous for the conditional ($Gbx1^{flox/\ flox}$) allele will generate pregnant females carrying control ($Gbx1^{flox/+}$), and embryos carrying the inducible and conditional alleles for *Gbx1* ($Gbx1^{CreERT2/flox}$). Embryos carrying the *Gbx1*-CreERT2 allele allow for inactivation of *Gbx1* at any stage desired. Tamoxifen is administered to the pregnant female at the embryonic stage desired by the investigator. Embryos may be left to develop *in utero* to assess them postnatally or harvested from dam embryonically to assess development at various gestational stages. Components of the MSR circuit should be analyzed in $Gbx1^{-/-}$ mutants beginning with E12.5 and assessed developmentally backwards. This will determine the precise time point in which *Gbx1* is first required for normal development of locomotor circuit components.

The multi-use inducible *Gbx1* allele serves as an alternative genetic tool by which roles can be identified versus the characterization of traditional *Gbx1*$^{-/-}$ knockout. *Gbx1*-CreERT2 serves as a multi-use genetic tool that allows for the excision of any allele of choice under the influence of *Gbx1* promoter sequence. Additionally, fate-mapping allows a relationship between *Gbx1* and its cell lineages to be formed. From this, neuronal populations that are influenced by *Gbx1* mutation are directly associated.

A targeting construct was engineered for the generation of an inducible *Gbx1* allele, *Gbx1*-CreERT2 (Figure 4.5). The ligand-dependent pCre-ERT2 construct (Feil et al., 1997) is inserted into exon 1 of the *Gbx1* gene. With this design, spatial control of cell marking is determined by endogenous promoter sequence that drives *Gbx1* expression. The purified construct was electroporated into 129/Svev embryonic stem cells by the University of Missouri Transgenic Core. Two DNA probes were designed for the identification of targeted stem cells by Southern analysis. A single BamHI restriction digest results in the detection of long and short-homology arms which produces product sizes of 13.9 kb and 5.8 kb, respectively. DIG-southern analysis of *Gbx1* BAC DNA and wild-type clones produced product bands at the appropriate sizes for a wild-type *Gbx1* allele (Figure 4.6). From our analysis, none of the embryonic stem cells examined contained product sizes that indicated correct integration of the targeting construct. Thus, *Gbx1*-CreERT2 mice have not been conceived. Once generated, it will be a powerful, multi-purpose genetic tool to analyze *Gbx1.*

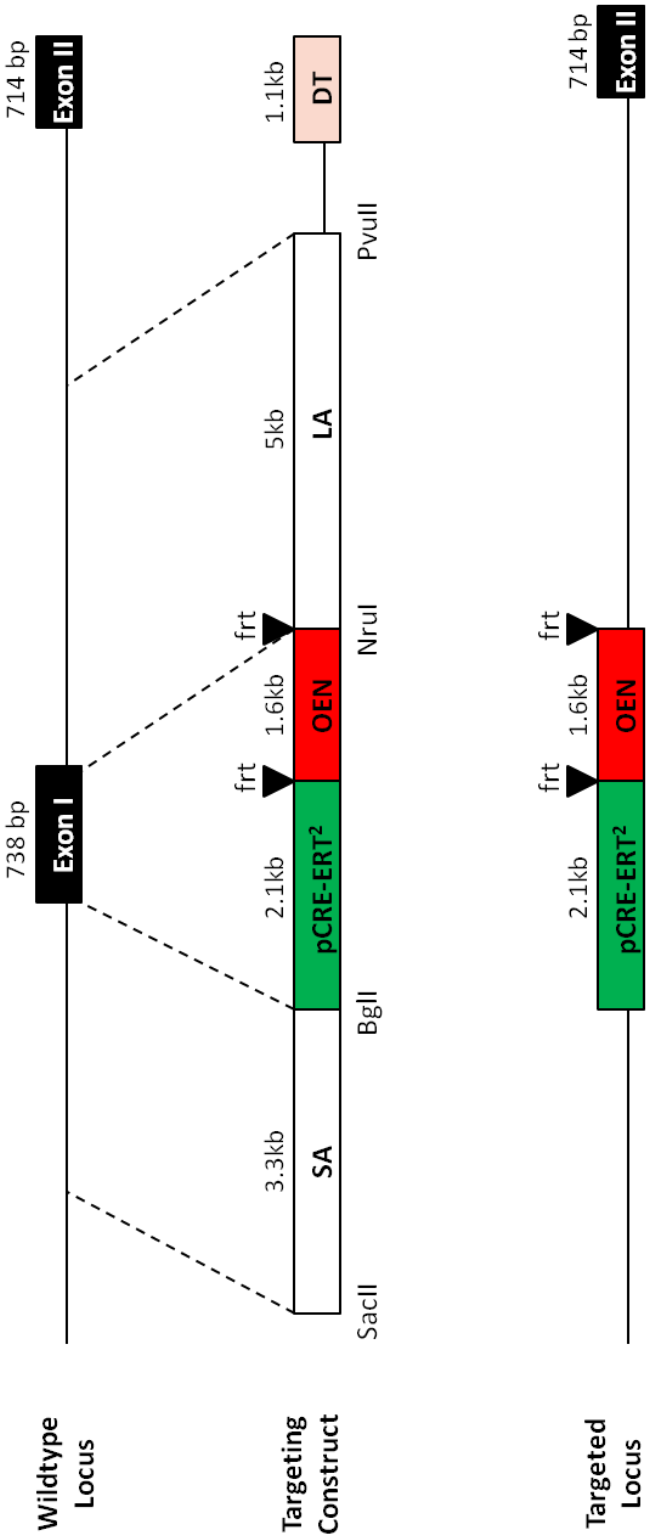
714 bp
Exon II
1.1kb
DT
PvuII
5kb
LA
frt
1.6kb
OEN
NruI
frt
738 bp
Exon I
2.1kb
pCRE-ERT²
BglII
3.3kb
SA
SacII
Wildtype Locus
Targeting Construct
Targeted Locus

Figure 4.5

Figure 4.5 - ***Gbx1*- CreERT2 targeting construct**. General features of the targeting vector design include: a homology arm of 3.3 kb immediately upstream (5') of the first exon of *Gbx1* (SA probe) and a homology arm of 5.1 kb which includes the last 147 bp of exon 1 and the adjoining (3') 4953 bp of intronic sequence (LA probe). The knockin element, pCre-ERT2 has been inserted into exon 1 at the ATG site and is followed (3') by a *frt*-flanked neomycin resistance gene (OEN) in the reverse direction, which serves as a selectable marker. SA, short arm; LA, long arm.

A.

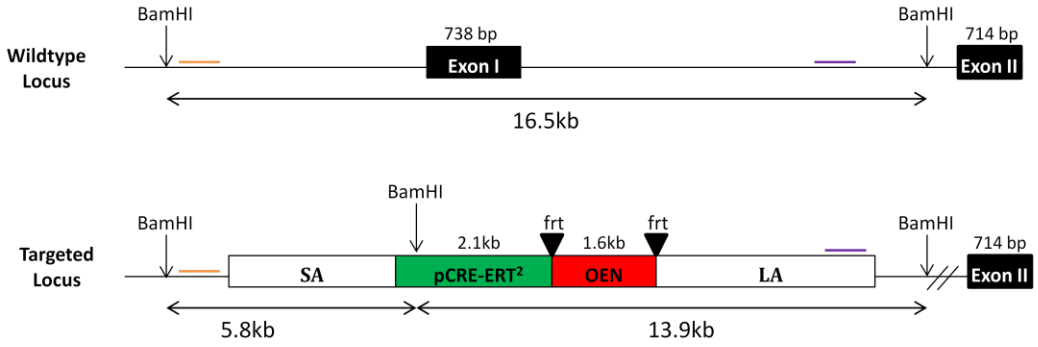

SA Probe
Targeted band size = 5.8kb
WT band size = 16.5 kb

LA Probe
Targeted band size = 13.9kb
WT band size = 16.5 kb

B.

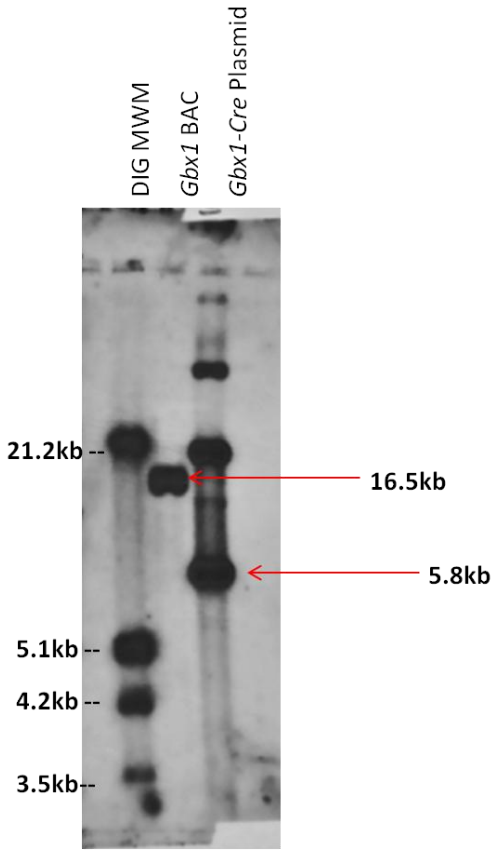

Figure 4.6

Figure 4.6 - Southern Analysis for *Gbx1*-CreERT2 targeting construct. (A) Short arm (SA) and long arm (LA) probes are designed to recognize sequences outside of the homology arm. A single restriction digest of wild-type gDNA with BamHI produces a product size of 16.5 kb. Whereas a single restriction digest of the plasmid containing the targeting vector produces two products: (1) a SA product of 5.8 kb and, (2) a 13.9 kb LA product. (B) Southern blot demonstrating a 16.5 kb product band corresponding to the detection of the wild-type locus for *Gbx1* BAC DNA restriction digested with BamHI and a 5.8 kb SA product corresponding to the detection of the targeted locus within the *Gbx1*-CreERT2 plasmid. DIG MWM, digoxigenin-labeled DNA molecular weight marker; BAC, bacterial artificial chromosome.

CHAPTER 5

MATERIALS, METHODS AND PROTOCOLS

5.1 Ethics Statement: The body of work presented in this document is in compliance with the University of Missouri Office of Animal Care Quality Assurance (ACQA) under the protocol number 6479. No IRB approval is needed. The mice were housed and handled in accordance with the University of Missouri Animal Care and Use Committee (ACUC) guidelines.

5.2 Generation of *Gbx1*$^{-/-}$ mice: Mice carrying the mutant null allele for *Gbx1* were generated through homologous recombination of a targeting construct engineered to allow excision of the functional DNA-binding homeodomain. From a bacterial artificial chromosome containing the full-length *Gbx1* genomic sequence, we isolated 14.4 kb of *Gbx1* DNA. A *frt*-flanked *neomycin* (*neo*) resistance cassette was inserted into the intronic sequence upstream of exon 2 and conferred positive selection by G418. *loxP* sequences inserted 5'- and 3'- to exon 2, which contains the functional DNA-binding motif, facilitated recognition by Cre DNA recombinase and mediated excision of the floxed sequence. Embryonic stem cells electroporated with the targeting construct were screened by Southern blot analysis of XbaI and NdeI/XbaI restriction digested DNA to identify homologous recombination of the short arm and long arm, respectively. We generated a mouse line carrying the *Gbx1*^{flox} allele by the injection of homologous recombinant embryonic stem cells into 129 blastocysts and subsequent mating of the resulting chimeric males to C57BL/6 females to obtain germ-line transmission of the

targeted allele. Mice carrying the *Gbx1*^{flox} allele develop normally, and are reproductively competent. In order to generate the nonfunctional null allele for *Gbx1*, *Gbx1*^{flox} heterozygote mice were mated with transgenic mice that express a DNA recombinase gene in the early embryo under the control of human ß-actin regulatory elements (Lewandoski et al., 1997), resulting in mice lacking exon 2 (*Gbx1*$^{-/-}$). *Gbx1*$^{-/-}$ mice are viable and phenotypically indistinguishable from their littermates at birth. However, by postnatal (P) day 15, *Gbx1*$^{-/-}$ mice display a severe locomotor defect affecting hindlimb locomotion.

5.3 Extraction of Genomic DNA from Embryonic and Postnatal Mouse Tissue:

Genomic DNA from extraembryonic tissue or tail biopsies of embryos was extracted by an overnight incubation of the tissue with 20 µl gentle lysis buffer working solution in a hybridization oven at 55˚C (For working solution, add 1 µl proteinase K to 500 µl gentle lysis buffer stock. Gently invert to mix and aliquot 20 µl of the working solution into tubes needed for number of embryos harvested). Following the overnight incubation, the DNA is ready for subsequent use by PCR or other applications.

Embryonic Gentle Lysis Buffer Stock Solution		
Tris-HCL	**1 M pH 8.3**	**500 µl**
$MgCl_2$	**1 M**	**75 µl**
NP-40	**100%**	**225 µl**
Tween-20	**100%**	**225 µl**
H_20	**-**	**48.75 ml**
Total		**50 ml**

Genomic DNA from postnatal mice was prepared from tail biopsies by an overnight incubation of the tissue with 500 µl tail lysis buffer working solution in a hybridization oven at 55°C (For working solution, add 500 µl tail lysis buffer stock solution to each tube containing a tail biopsy, then add 1µl proteinase K. Invert to mix.) The following day, centrifuge eppendorf tubes containing lysed DNA for 1 minute at 3,000 rpm to pellet hair and other debris. Remove 430 µl of the supernatant and add to a new eppendorf tube. Add 430 µl isopropanol to the supernatant and gently invert to mix until a DNA precipitate forms. Add 30 µl TE buffer to a new eppendorf tube. Transfer DNA precipitate to tube containing TE buffer by swirling the precipitate with the end of a disposable pipette tip until it becomes adhered. Allow DNA precipitate to solubilized in TE buffer for at least 2 hours at 4 °C before subsequent use by PCR or other applications.

Postnatal Tail Lysis Buffer Stock Solution		
Tris-HCL	**1 M pH 8.5**	**50 ml**
NaCl	**5 M**	**20 ml**
EDTA	**500 mM**	**5 ml**
SDS	**10%**	**10 ml**
Autoclaved H_20	**-**	**415 ml**
Total		**500 ml**

5.4 Genotype analysis for *Gbx1* alleles: Genotyping was achieved through PCR using genomic DNA prepared from embryonic stem cells, embryonic tissue or adult tail biopsies. To identify the *Gbx1*^{flox} allele through PCR, a 5' forward primer (6078) located within exon 2 and a 3' reverse primer (E2R1) that anneals immediately downstream of the second *loxP* site, yields a 300 bp product corresponding to the floxed allele. The *Gbx1*$^{-/-}$ allele was detected using a 5' forward primer (1A) contained within the *neo* cassette and the same 3' reverse primer (E2R1) used to detect the floxed allele.

Forward Primer to detect wild-type and/or flox allele (6078)	5'-GTTTGCTGTGCGCAGCCAGCA-3'
Forward Primer to detect null allele (1A)	5'-CGTCAAGAAGGCGATAGAAGG-3'
Reverse Primer (E2R1)	5'-CCTCAGGAATCCACTTCTGCT-3'

PCR analysis was performed with the reaction detailed below:

Reagent	[Stock]	µl/reaction
Nuclease-free H_20	-	9
MasterAmp PreMix HN (Illumina Epicentre)	2X	12.5
Taq DNA polymerase (Invitrogen)	100 units	0.5
Forward Primer	100 µM	0.5
Reverse Primer	100 µM	0.5
Genomic DNA	-	2
TOTAL	-	25

The PCR thermocycler ran the program using the following parameters:

1) 94°C for 3 minutes
2) 94°C for 30 seconds
3) 55°C for 30 seconds
4) 72°C for 3 minutes (steps 2-4 were repeated for 30 cycles)
5) Hold at 4°C

5.5 Generation of *Gbx1*$^{-/-}$;*Gbx2*$^{-/-}$ mice: Mice carrying the mutant null allele for *Gbx1* (*Gbx1*$^{-/-}$) were generated through cre-mediated excision of exon 2, which contains the functional DNA-binding homeodomain (Buckley et al., 2013)(Buckley et al., 2013)(Buckley et al., 2013)[152]. *Gbx1*$^{-/-}$ mice are viable and reproductively competent. Mice carrying the mutant null allele for the *Gbx2* gene (*Gbx2*$^{-/-}$) were also generated through cre-mediated excision of the homeobox contained in exon 2 (Wassarman et al., 1997). However, *Gbx2*$^{-/-}$ mutant embryos die the day of birth due to the inability to nurse. Thus, mutants carrying a homozygous allele for the *Gbx2* gene were obtained by the mating of mice heterozygous for the *Gbx2* null allele which are viable and phenotypically indistinguishable from wild-type littermates. In this study, *Gbx1*$^{-/-}$;*Gbx2*$^{-/-}$ (*Gbx* dKO) embryos were obtained by mating *Gbx1*$^{-/-}$;*Gbx2*$^{-/+}$ or *Gbx1*$^{-/+}$;*Gbx2*$^{-/+}$ mice. The PCR assay used to detect the *Gbx1*$^{-/-}$ allele was performed as described above. The PCR assay used to detect the *Gbx2*$^{-/-}$ allele was performed using a 5' primer that anneals to sequences in the *Gbx2* gene upstream of the genomic segment used in the targeting vector (5'-TGACCTATATAACAATGCCC-3') and a 3' primer that anneals to sequences within the *neo* gene cassette (5'-GTTCTAAGTACTGTGGTTTCC-3') (Wassarman et al., 1997; Waters and Lewandoski, 2006). Timed pregnant mice were

used for all experiments. Noon of the day the vaginal plug was observed was considered E 0.5.

5.6 Euthansia: CO_2 (100%) asphyxiation followed by cervical dislocation was performed to euthanize adult mice. For embryos, immersion in 4% paraformaldehyde was used for embryos E14 or younger. Chilling followed by decapitation was used for embryos older than E14. The invasive procedures used to harvest embryos were only performed following euthanasia.

5.7 *Gbx1*-CreERT2 targeting construct. From a bacterial artificial chromosome (BAC) (RP24, BACPAC resources center) containing the full-length *Gbx1* genomic sequence, we generated the 5'- and 3'- homology arms of the construct. The short homology arm contains 3.3 kb *Gbx1* nucleotide sequence immediately upstream (5') of the ATG in exon 1. Whereas, the long homology arm consists of 5.1 kb *Gbx1* nucleotide sequence beginning with the last 147 bp of exon 1 and the adjoining (3') 4953 bp of intronic sequence. Using conventional cloning, the knockin element pCre-ERT2 (gifted by Dr. Mark Lewandoski, NCI-Frederick) was inserted into *Gbx1* exon 1 at the ATG site, and is followed (3') by a *frt*-flanked *neo* resistance gene that conferred positive selection by G418. Fidelity of the construct was confirmed by sequencing using the University of Missouri DNA Core Facility with the primers listed in Table 2. Embryonic stem cells (W4, 129/SvEv) (Taconic Technologies), were electroporated with the targeting construct and subsequently screened by PCR with primers designed to identify each knock-in component of the construct. Integration of the targeting construct into the wild-type *Gbx1* locus by PCR was strategically detected by having a primer designed to anneal to

sequence outside of the short homology arm that amplified a product with a second primer located within the homology arm. This pre-screening step reduced the overall number of clones to be subsequently examined by Southern blot, which also confirmed recombination occurred accurately through detection of a probe 3' to the LA. Southern analyses were performed using BamHI restriction digested DNA. BAC DNA, plasmid DNA and wild-type genomic DNA served as controls to optimize parameters to observe expected DNA product sizes. Identification of embryonic stem cells that correctly recombined the targeting construct into the endogenous wild-type *Gbx1* locus were further confirmed by southern analysis using Digoxigenin-labeled DNA probes.

Table 2 - Primer and Probe Sequences for *Gbx1*-CreERT2 Construct.

Primers for Sequencing Targeting Construct (PC516)	Sequences
T3-Fwd	5'-AATTAACCCTCACTAAAGGG-3'
SA-Fwd 3	5'-GCTCCTTTAGACTGTGAGG-3'
LA- Fwd	5'-AGCAAAGCTGCTATTGGC-3'
LA-Rev-OEN	5'-AAAGTCTCAGAGAAGTGCGGA-3'
SA-Fwd 5	5'-CAGAGCTTAGAGAACCGAGT-3'
OEN- Fwd	5'-TCTTATCATGTCTGGTCGAC-3'
LA-Rev	5'-AATCTATAAAGGGCGTCA-3'
T7-Rev	5'- GTAATACGACTCACTATAGGGC-3'
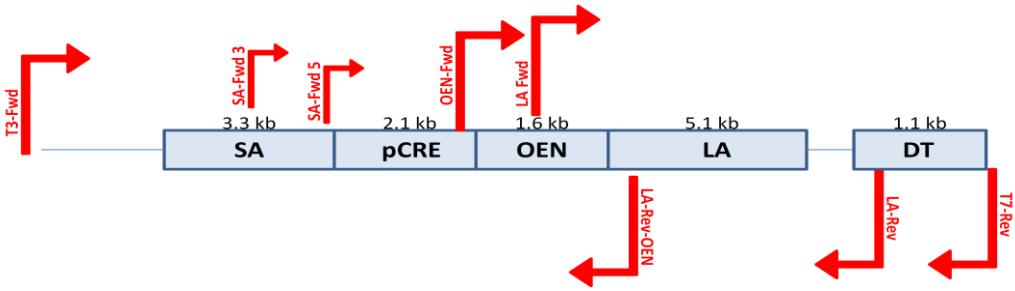	
Primers to Confirm Homologous Recombination of PC516 into ES Cells	
Gbx1-Cre Fwd 2	5'-TGAAGATCTGAGCTCCCTGGCG-3'
Gbx1-Cre Rev 1	5'-CTCGTCAAGAAGGCGATAGAAG-3'
ES 5' UTR-Fwd	5'- TTGCCTGATTCCAGTTCCTCGG-3'
SA Rev 7II	5'- CACTCTATCTCCCTGGCTCC-3'
ES NEO F3	5'-AGAGAATAGGAACTTCGGCCG-3'

ES 3'UTR-R	5'-ACAGCCAGGGCTACACAGAG-3'
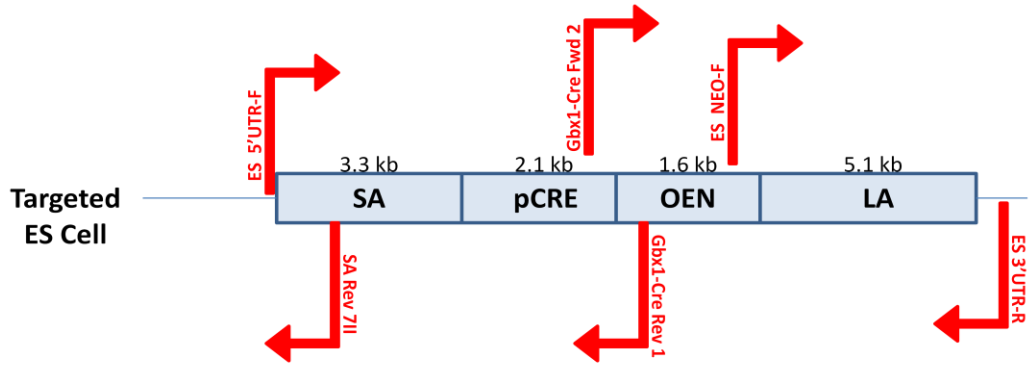	
DNA Probes Used for Detection of Long and Short Homology Arms	
Long Arm Probe	5'-GGGGTACCGTTGGACTGCTTGAAGGCTTAGACGGCAAGTGGGGGTAGGTGCGCCATTAACCAATAGATAGGAGATAAAAACACAAAGAGAGACCGGCATGAGACAGGACACCAGGTTGGATGCTGGACAAGTTAGAATTTCTGTAGCAAGGGCGATGTAAAGGATGTGAGCATGTGAGGGACCAGCCTGAGAGATGCCAGTGTCACGAGCACCATCTTTTAAAAACTGAAAAGGGAAGGATTTGTTAATTTCCGACTGGAGATTGCAGTAATAATGGAAGTCACAGAGGCGACCAGGAAACTTGTCGAC-3'
Short Arm Probe	5'-CGGGGTACCAGCAGCCAGCGGTGGGCTGGGGGGGCGGCAGAGCACCAAGTAAGTGGGTTGGGGGTTGTGATGTCAAGGGTCCCTGGACCCAAGTTTCCAGGATTCAGAGCACTTTTCAGCCAGCTAGAGGCAGCCAGACTATGTGGGGTGGGGTTTCGGGGGGCAGCTAGAAGGCCATAGAGCCAAGTGGACTGGAGGTGGGTAGACTGGCCTCCGAACTTGGCTTTACCATAACTTTGGACAGCTGCGCA-3'

Table 2 - Primer and Probe Sequences for *Gbx1*-CreERT2 Construct. List of primers designed and used to sequence each component of the *Gbx1*-CreERT2 targeting construct before electroporation into ES cells. List of primers used to pre-screen ES cells electroporated with targeting construct to check for accurate incorporation into endogenous *Gbx1* locus. List of sequences for the DNA probes used to detect accurate incorporation of the long and short homology arms in a targeted cell.

5.8 Southern Analysis: To confirm the structural sequence integrity of a properly modified ES cell, Southern analysis was performed using 10 µg wild-type genomic DNA, BAC DNA and genomic DNA from clones electroporated with the construct. DNA was digested with BamHI or BsrGI restriction enzymes overnight at 37˚C, prior to analysis. DNA samples were ran overnight by electrophoresis on a 0.7% TBE agarose gel at 30V. The following day, gel is post-stained with 0.00003% ethidium bromide for 30 minutes, depurinated with.25 M HCl for 10 minutes, rinsed with dH_20, denatured with 0.5 M NaOH, 1.5 M NaCl twice for 15 minutes, rinsed with dH_20 neutralized with 0.5 M Tris HCl pH7.5,1.5 M NaCl twice for 15 minutes, rinsed with dH_20, then equilibrated with 20X SSC for 10 minutes. The gel is then assembled to transfer to a positively charged nylon membrane (Amersham Hybond-XL) by upward capillary motion overnight. The next day, membrane is removed and DNA is immobilized by UV-crosslinking. Membrane is then prehybridized for 3 hours at 71.7˚C to subsequently use the SA probe, or 47˚C for the LA probe. Denatured probes are then added to the membrane to hybridize at the appropriate temperature overnight. Following hybridization, membrane is processed and handled for detection according to the protocol recommended by Roche for the DIG detection of non-radioactive labeled nucleic acids (Catalog # 11585762001). Membrane is washed with low stringency buffer twice for 5 minutes, washed with high stringency buffer twice at 68˚C for 30 minutes, washed with 1X wash buffer for 2 minutes, then incubated for 2 hours in blocking solution at room temperature. Following incubation, anti-digoxigenin antibody (Roche) is added to membrane at 1:10,000 in blocking solution overnight at 4˚C. The next day, membrane is washed twice with 1X wash buffer then equilibrated in 20 ml detection buffer for 20

minutes. Incubate face of membrane with 1 ml of CSPD (Roche) for 10 minutes. Wrap membrane in saran wrap and secure in cassette developer. Expose membrane to film for ≥2 hours.

5.9 Immunohistochemistry: For immunohistochemistry analyses, *Gbx1*$^{-/-}$, *Gbx2*$^{-/-}$, *Gbx* dKO and control embryos were dissected and subsequently fixed with 4% paraformaldehyde (PFA) in 1X phosphate-buffered saline (PBS) for 2 hours at 4°C, washed 3 times in 1X PBS for 1 hour, equilibrated with 25% sucrose overnight at 4°C. Each embryo was transferred to an individual peel-away embedding mold (Electron Microscopy Sciences) and embedded in optimal temperature tissue (OCT) (Tissue-Tec). The mold was subsequently flash frozen using a dry ice/ethanol bath and stored at -80°C until cryosectioning. Transverse, serial 12 µm or 20 µm cryosections were made along the length of the lumbar-sacral SC. Sections were washed with 0.1% Triton X-100 in 1X PBS (PBST), blocked with 1X PBS containing 10% lamb serum, 1% bovine serum albumin, and 0.25% Triton X-100 for 90 minutes and incubated with the appropriate primary antibodies diluted in blocking solution at 4°C overnight. The following day, sections are washed briefly with PBST and incubated with the appropriate fluorescently-conjugated secondary antibodies diluted in blocking solution at 4°C overnight. Stained sections were dehydrated in serial dilutions of ethanol in 1X PBS and mounted using DPX mounting media or glycerol mounting media containing DAPI.

The following primary and secondary antibodies were used:

Antibody	Dilution	Manufacturer
Primary Antibodies		
mouse monoclonal mouse anti-Islet1 (39.45D)	1:100	Developmental Studies Hybridoma Bank (DSHB)
rabbit anti-Pax2	1 mg/ml	Invitrogen
rabbit anti-Caspase-3	1:1,500	Cell Signaling
mouse anti-HB9	1:100	DSHB
rabbit anti-Peripherin	1:200	Millipore
rabbit polyclonal anti-TrkC	1:200	Santa Cruz Biotech
rabbit anti-parvalbumin	1:500	Calbiochem
Secondary Antibodies		
goat anti-rabbit AlexaFluor 488	1:500	Invitrogen
goat anti-mouse AlexaFluor 568	1:500	Invitrogen

5.10 Caspase-3 & H3P Staining: For the labeling of apoptotic cells expressing caspase-3 or mitotically active cells expressing phosphorylated histone H3 (H3P), embryos were dissected and fixed as explained in **5.8**. Sections were post-fixed with 3% formaldehyde in 1X PBS (caspase-3) or 10% neutral buffered formalin (H3P), washed twice with 1X PBS, incubated with 0.3% (w/v) hydrogen peroxidase in methanol to quench endogenous peroxidase activity, washed twice with 1X PBS, blocked with 1X PBS containing 0.3% Triton-X 100 and 5% normal goat serum for 1 hour at RT, followed by an overnight incubation at 4°C with rabbit anti-caspase-3 (Cell Signaling, 1:1500) or

rabbit anti-phospho-H3 (Millipore; 1:500) primary antibody in blocking solution. The next day, sections are washed 3 times with 1X PBS, and incubated overnight at 4˚C with biotinylated anti-rabbit IgG secondary antibody (Vector Laboratories #PK-6101) diluted in blocking solution. To visualize localization of the antigen, sections are washed twice with 1X PBS, incubated with VECTASTAIN Elite ABC (Vector Laboratories #PK-6101) reagent for 30 minutes at RT, incubated with 1X PBS containing 1% DMSO six times for 15 minutes at RT, then incubated with 0.5mg/ml 3,3′-diaminobenzidine tetrahydrochloride (DAB; Sigma #D9015) diluted in 1X PBS containing 1% DMSO for 15 minutes at RT. Peroxidase reaction is initiated by the addition of 200 ul of 0.0003% H_2O_2 to 1X PBS containing 0.5 mg/ml DAB and 1% DMSO. When the desired stain intensity is achieved the reaction is stopped by washing sections several times with ice cold 1X PBS. Slides are mounted with 70% glycerol/1X PBS.

5.11 RNA Probe Synthesis: Sense and antisense digoxigenin (DIG) conjugated RNA probes were prepared from linearized DNA templates using a DIG RNA labeling kit SP6/T7/T3 (Roche) to visualize the localization of endogenous mRNA transcripts. One µg of linearized DNA was added to 50 µl reaction containing: 10X transcription buffer, 10X RNA polymerase, and 25X protector RNase inhibitor. This reaction was incubated for 2 hours in a 37˚C water bath. To precipitate the RNA probe: 1 µl of 20 µg/µl glycogen, 5 µl of 0.2M EDTA, 6.3 µl of 4M LiCl, and 190 µl of 100% ethanol, were added to the sample and incubated at -20˚C for 2 hours. The samples were then centrifuged at 15,000 RPM at 4˚C for 15 minutes. The pellet is washed with 70% ethanol, and centrifuged at 4˚C for 10 minutes. RNA pellets are resuspended in 30 µl

DEPC water and stored at -20˚C until use. To check quality of probe synthesis, 5 µl of the resuspended probe are run on an agarose gel.

5.12 *In situ* Hybridization: Whole-mount RNA *in situ* hybridization assays are most effectively performed in mouse embryos younger than E12.5. The telencephalon is punctured with a fine tip pulled pasture pipette prior to start of assay to facilitate better penetration of reagents and reduces trapping/non-specific staining. Mouse embryos were fixed overnight in freshly thawed 4% PFA-DEPC at 4˚C. The next day, embryos were washed with PBS-DEPC for 5 minutes at 37˚C. Followed by dehydration in serial dilutions of methanol-PBT-DEPC (25%, 50%, 75%, 100%) for 10 minutes each rocking at 37˚C. Embryos were stored at -20˚C in fresh100% methanol until use. To begin an assay, embryos were rehydrated using the same serial dilutions of methanol- PBT-DEPC used for dehydration. Next they were washed twice for 5 minutes in PBT, bleached for 1 hour using 6% H_2O_2 and permeabilized with 10 µg/ml Proteinase K in PBT for various lengths of time depending on the developmental stage examined. Embryos were then incubated in a glycine PBT solution, followed by two 5 minute washes in PBT. After refixing embryos in 4%PFA/0.25% glutaraldehyde for 20 minutes, embryos were washed twice for 5 minutes with PBT. Embryos were then incubated with pre-warmed hybridization solution at 70˚C for 1 hour. To hybridize probes within the embryo, pre-hybridization solution was replaced with fresh, pre-warmed hybridization solution containing 5 µl of a digoxigenin or fluorescein labeled RNA probe overnight at 70˚C.

On day two of the assay, probe solution was removed and embryos were washed twice for 30 minutes each with solution I (10 ml formamide, 4 ml 20X SSC, 2 ml 10% SDS and 4 ml H_2O) at 70˚C with gentle rocking. Next, embryos were washed with a 1:1 mix of solution I and solution II (solution II: 8 ml of 5M NaCl, 0.8 ml of 1M Tris pH 7.5, 80 µl tween-20, and 71 ml H_2O) at 70˚C for 10 minutes. Embryos were then brought to 37˚C with three 5 minute washes in solution II. To remove any non-hybridized free-floating probe, embryos were incubated for 1 hour at 37˚C in 100 µg/ml RNase A/solution II, followed by a final 5 minute wash in solution II. Next, embryos were washed for 5 minutes in solution III (10 ml formamide, 2 ml 20X SSC pH4.5, 8 ml of H_2O), followed by two 30 minute washes in solution III. To block nonspecific binding of the primary antibody, embryos were washed three times for 5 minutes each with 2 ml filtered MABTL (100 ml maleic acid buffer, 100 µl tween-20 and 50 mg levamisol), followed by a three hour incubation with blocking solution (MABTL containing 5% heat-inactivated sheep serum). After the blocking step, blocking solution is replaced with fresh blocking solution containing anti-digoxigenin or anti-fluorescein diluted antibody (1:4000). Embryos were incubated over night at 4˚C.

The next day, unbound antibody is washed from the embryos during eight 1 hour washes with MABTL and one overnight wash at 37˚C. On the last day of the assay, embryos were washed three times for 30 minutes each in freshly prepared and filtered NTMTL (1 ml 5M NaCl, 5 ml Tris pH 9.5, 2.5 ml $MgCl_2$, 50 µl tween-20, 25 mg levamisole) at 37˚C. To initiate color reaction, NTMTL was removed and replaced with 1 ml of BM purple (Roche) or Fast Red TR/Naphthol AS-MX Tablets (Sigma). Vials containing embryos were covered in foil and left to rest undisturbed until desired

staining intensity was achieved. To stop color reaction, embryos were washed twice for 5 minutes in PBT and post-fixed with 4% PFA/1% glutaraldehyde. Embryos were prepared for photography with two washes for 5 minutes in PBT, 10 minutes in 50% glycerol/PBT and 10 minutes in 80% glycerol/PBT. Samples were imaged in a petri dish containing 80% glycerol/PBT and then stored at 4˚C.

To demonstrate that exon 2, which contains the sequence encoding the functional DNA-binding homeodomain (HD) of GBX1, was successfully deleted in the *Gbx1* null mutants, a 588 bp cDNA fragment consisting of the *Gbx1*-HD sequence was amplified from genomic DNA using PCR and cloned in the pBluescript KS(-) vector. Digoxigenin labeled *Sox10* anti-sense RNA probe was provided by A. Chandrasekhar and construct was engineered by P. Trainor's lab. For section RNA *in situ* hybridizations analyses, $Gbx1^{-/-}$, $Gbx2^{-/-}$, $Gbx1^{-/-}$;$Gbx2^{-/-}$ and control ($Gbx1^{+/+}$;$Gbx2^{+/+}$) embryos were dissected and subsequently fixed with 4% paraformaldehyde (PFA) in 1X phosphate-buffered saline (PBS) for 2 hours at 4˚C, washed 3 times in 1X PBS for 1 hour, equilibrated with 25% sucrose overnight at 4˚C and embedded in optimal temperature tissue (OCT) (Tissue-Tec) for cryosectioning. Transverse, serial 20 µm cryosections were made along the length of the lumbar-sacral SC. *In situ* hybridizations were performed on sections using digoxigenin (Roche Molecular Biochemicals) labeled probes specific for mouse *Gbx2* and *Gbx1* as described elsewhere (Waters et al., 2003).

5.13 qRT-PCR Analysis: To quantify the relative number of *Gbx2* RNA transcripts in the SC of $Gbx1^{-/-}$ mutants, quantitative real-time PCR was performed with an ABI Prism

7300 Real-Time PCR system (Applied Biosystems). PCR primers 5′-GGCAACTTCGACAAAGCCGAGG-3′ and 5′-CCAGGCAAATTGTCATCTGAGC-3′, and the TaqMan® probe 5′-CAGGCGTCGCTCGTCGGGGCT-3′ were designed to target the splice junction between *Gbx2* exons 1 and 2. The PCR primers 5′-GCATGGCCTTCCGTGTTCCTA-3′ and 5′-CTGCTTCACCACCTTCTTGA-3′, and the TaqMan® probe 5′-ACGTGCCGCCTGGAGAAACCTG-3′ targeted a 105-bp fragment of glyceraldehyde-3-phosphate dehydrogenase (GAPDH) cDNA. The Taqman® probe was labeled with 6-carboxyfluorescein (FAM) and quencher dye 6-carboxytetramethylrhodamine (TAMARA) on its 5′ and 3′ ends, respectively (Keystone Labs). PCR reactions were performed in a final volume of 50 µl and contained 2X Universal PCR Master Mix (Applied Biosystems). The final concentration of PCR primers and Taqman® probes was 100 nM. Unknown samples were compared with duplicate samples containing 10^7 to 10^1 copies of cDNA reverse transcribed from plasmid DNA containing complete *Gbx2* or GAPDH ORFs. Cycling conditions were: 2 minutes at 50°C; 10 minutes at 95°C; 40 cycles of 95°C for 15 seconds, 60°C for 1 minute. PCR reactions were performed in triplicate.

5.14 Microscopy: Analysis of immunostained SC and DRG sections were examined and photographed using the Zeiss 510 META confocal microscope under 10X, 20X and 40X ocular magnification. *In situ* hybridization images were captured using the Leica DFC290 camera. Identical parameters for gain, focus, exposure and intensity were used consistently for each sample within an experiment during imaging.

5.15 Statistical analysis: PAX2, H3P and caspase-3 cell counting was performed on three lumbar SC sections from three samples of each genotype analyzed (i.e. nine sections each for *Gbx1*$^{+/+}$;*Gbx2*$^{+/+}$ (control), *Gbx1*$^{-/-}$, *Gbx2*$^{-/-}$, *Gbx1*$^{-/-}$;*Gbx2*$^{-/-}$ (dKO)). For PAX2, positive cells within a single quadrant of the superficial dorsal horn were counted for the left and right side of the SC for each section to minimize counting errors. For H3P, positive cells within a single quadrant of the dorsal epedymal layer were counted to assess the level of proliferation within the ventricular zone. Additionally, H3P-positive cells within a single quadrant of the dorsal mantle zone were counted to assess the level of proliferation outside of the ventricular zone. For caspase-3, positive cells within a single ventral quadrant, composed of the left and right side of the SC, were counted to assess the level of apoptosis. Statistical differences in cell numbers were quantified by the comparison of each mutant genotype with the wild-type control group using the unpaired Student's *t*-test algorithm (Graphpad Prism statistical software). Results are represented as mean+SEM, and samples are considered statistically significant by having a value of $*P < 0.05$, $**P < 0.005$, $***P < 0.0005$.

REFERENCES

Adams, J. M. and S. Cory (1998). "The Bcl-2 protein family: arbiters of cell survival." Science **281**(5381): 1322-1326.

Akay, T., W. G. Tourtellotte, et al. (2014). "Degradation of mouse locomotor pattern in the absence of proprioceptive sensory feedback." Proc Natl Acad Sci U S A **111**(47): 16877-16882.

Alaynick, W. A., T. M. Jessell, et al. (2011). "SnapShot: spinal cord development." Cell **146**(1): 178-178 e171.

Alnemri, E. S., D. J. Livingston, et al. (1996). "Human ICE/CED-3 protease nomenclature." Cell **87**(2): 171.

Altmann, C. R. and A. H. Brivanlou (2001). "Neural patterning in the vertebrate embryo." Int Rev Cytol **203**: 447-482.

Alvarez, F. J., K. L. Bullinger, et al. (2010). "Permanent reorganization of Ia afferent synapses on motoneurons after peripheral nerve injuries." Ann N Y Acad Sci **1198**: 231-241.

Anderson, D. J. (1997). "Cellular and molecular biology of neural crest cell lineage determination." Trends Genet **13**(7): 276-280.

Anderson, D. J., A. Groves, et al. (1997). "Cell lineage determination and the control of neuronal identity in the neural crest." Cold Spring Harb Symp Quant Biol **62**: 493-504.

Arber, S. (2012). "Motor circuits in action: specification, connectivity, and function." Neuron **74**(6): 975-989.

Arber, S., B. Han, et al. (1999). "Requirement for the homeobox gene Hb9 in the consolidation of motor neuron identity." Neuron **23**(4): 659-674.

Arber, S., D. R. Ladle, et al. (2000). "ETS gene Er81 controls the formation of functional connections between group Ia sensory afferents and motor neurons." Cell **101**(5): 485-498.

Artus, J. and M. Cohen-Tannoudji (2008). "Cell cycle regulation during early mouse embryogenesis." Mol Cell Endocrinol **282**(1-2): 78-86.

Baehrecke, E. H. (2002). "How death shapes life during development." Nat Rev Mol Cell Biol **3**(10): 779-787.

Banks, G. B. and P. G. Noakes (2002). "Elucidating the molecular mechanisms that underlie the target control of motoneuron death." Int J Dev Biol **46**(4): 551-558.

Bareyre, F. M. (2008). "Neuronal repair and replacement in spinal cord injury." J Neurol Sci **265**(1-2): 63-72.

Ben-Zvi, A., L. Ben-Gigi, et al. (2008). "Semaphorin3A regulates axon growth independently of growth cone repulsion via modulation of TrkA signaling." Cell Signal **20**(3): 467-479.

Ben-Zvi, A., O. Manor, et al. (2008). "The Semaphorin receptor PlexinA3 mediates neuronal apoptosis during dorsal root ganglia development." J Neurosci **28**(47): 12427-12432.

Bertrand, N., D. S. Castro, et al. (2002). "Proneural genes and the specification of neural cell types." Nat Rev Neurosci **3**(7): 517-530.

Betley, J. N., C. V. Wright, et al. (2009). "Stringent specificity in the construction of a GABAergic presynaptic inhibitory circuit." Cell **139**(1): 161-174.

Branda, C. S. and S. M. Dymecki (2004). "Talking about a revolution: The impact of site-specific recombinases on genetic analyses in mice." Dev Cell **6**(1): 7-28.

Briscoe, J., A. Pierani, et al. (2000). "A homeodomain protein code specifies progenitor cell identity and neuronal fate in the ventral neural tube." Cell **101**(4): 435-445.

Briscoe, J., L. Sussel, et al. (1999). "Homeobox gene Nkx2.2 and specification of neuronal identity by graded Sonic hedgehog signalling." Nature **398**(6728): 622-627.

Brody, B. A., C. A. Ley, et al. (1989). "Selective distribution of the 57 kDa neural intermediate filament protein in the rat CNS." J Neurosci **9**(7): 2391-2401.

Brunet, I., C. Weinl, et al. (2005). "The transcription factor Engrailed-2 guides retinal axons." Nature **438**(7064): 94-98.

Buckley, D. M., J. Burroughs-Garcia, et al. (2013). "Characterization of the Gbx1-/- mouse mutant: a requirement for Gbx1 in normal locomotion and sensorimotor circuit development." PLoS One **8**(2): e56214.

Buckley, D. M., J. Burroughs-Garcia, et al. (2013). "Characterization of the gbx1(-/-) mouse mutant: a requirement for gbx1 in normal locomotion and sensorimotor circuit development." PLoS One **8**(2): e56214.

Burek, M. J. and R. W. Oppenheim (1996). "Programmed cell death in the developing nervous system." Brain Pathol **6**(4): 427-446.

Burroughs-Garcia, J., V. Sittaramane, et al. (2011). "Evolutionarily conserved function of Gbx2 in anterior hindbrain development." Dev Dyn **240**(4): 828-838.

Buss, R. R., W. Sun, et al. (2006). "Adaptive roles of programmed cell death during nervous system development." Annu Rev Neurosci **29**: 1-35.

Byrd, N. A. and E. N. Meyers (2005). "Loss of Gbx2 results in neural crest cell patterning and pharyngeal arch artery defects in the mouse embryo." Dev Biol **284**(1): 233-245.

Caspary, T. and K. V. Anderson (2003). "Patterning cell types in the dorsal spinal cord: what the mouse mutants say." Nat Rev Neurosci **4**(4): 289-297.

Chapman, G. and P. D. Rathjen (1995). "Sequence and evolutionary conservation of the murine Gbx-2 homeobox gene." FEBS Lett **364**(3): 289-292.

Chen, A. I., J. C. de Nooij, et al. (2006). "Graded activity of transcription factor Runx3 specifies the laminar termination pattern of sensory axons in the developing spinal cord." Neuron **49**(3): 395-408.

Chen, H. H., S. Hippenmeyer, et al. (2003). "Development of the monosynaptic stretch reflex circuit." Curr Opin Neurobiol **13**(1): 96-102.

Chen, H. H., W. G. Tourtellotte, et al. (2002). "Muscle spindle-derived neurotrophin 3 regulates synaptic connectivity between muscle sensory and motor neurons." J Neurosci **22**(9): 3512-3519.

Cheng, L., A. Arata, et al. (2004). "Tlx3 and Tlx1 are post-mitotic selector genes determining glutamatergic over GABAergic cell fates." Nat Neurosci **7**(5): 510-517.

Cheung, M., M. C. Chaboissier, et al. (2005). "The transcriptional control of trunk neural crest induction, survival, and delamination." Dev Cell **8**(2): 179-192.

Ciruna, B. and J. Rossant (2001). "FGF signaling regulates mesoderm cell fate specification and morphogenetic movement at the primitive streak." Dev Cell **1**(1): 37-49.

Cohen, S., L. Funkelstein, et al. (2005). "A semaphorin code defines subpopulations of spinal motor neurons during mouse development." Eur J Neurosci **21**(7): 1767-1776.

Colas, J. F. and G. C. Schoenwolf (2001). "Towards a cellular and molecular understanding of neurulation." Dev Dyn **221**(2): 117-145.

Copp, A. J., N. D. Greene, et al. (2003). "The genetic basis of mammalian neurulation." Nat Rev Genet **4**(10): 784-793.

Cowan, W. M., J. W. Fawcett, et al. (1984). "Regressive events in neurogenesis." Science **225**(4668): 1258-1265.

Crone, S. A., G. Zhong, et al. (2009). "In mice lacking V2a interneurons, gait depends on speed of locomotion." J Neurosci **29**(21): 7098-7109.

Dalla Torre di Sanguinetto, S. A., J. S. Dasen, et al. (2008). "Transcriptional mechanisms controlling motor neuron diversity and connectivity." Curr Opin Neurobiol **18**(1): 36-43.

Dasen, J. S. (2009). "Transcriptional networks in the early development of sensorimotor circuits." Curr Top Dev Biol **87**: 119-148.

Del Barrio, M. G., S. Bourane, et al. (2013). "A transcription factor code defines nine sensory interneuron subtypes in the mechanosensory area of the spinal cord." PLoS One **8**(11): e77928.

Dietz, V. (2002). "Proprioception and locomotor disorders." Nat Rev Neurosci **3**(10): 781-790.

Dupin, E., S. Creuzet, et al. (2006). "The contribution of the neural crest to the vertebrate body." Adv Exp Med Biol **589**: 96-119.

Ericson, J., P. Rashbass, et al. (1997). "Pax6 controls progenitor cell identity and neuronal fate in response to graded Shh signaling." Cell **90**(1): 169-180.

Ericson, J., S. Thor, et al. (1992). "Early stages of motor neuron differentiation revealed by expression of homeobox gene Islet-1." Science **256**(5063): 1555-1560.

Ernfors, P. (2001). "Local and target-derived actions of neurotrophins during peripheral nervous system development." Cell Mol Life Sci **58**(8): 1036-1044.

Ernfors, P., K. F. Lee, et al. (1994). "Lack of neurotrophin-3 leads to deficiencies in the peripheral nervous system and loss of limb proprioceptive afferents." Cell **77**(4): 503-512.

Escurat, M., K. Djabali, et al. (1990). "Differential expression of two neuronal intermediate-filament proteins, peripherin and the low-molecular-mass neurofilament protein (NF-L), during the development of the rat." J Neurosci **10**(3): 764-784.

Feil, R., J. Wagner, et al. (1997). "Regulation of Cre recombinase activity by mutated estrogen receptor ligand-binding domains." Biochem Biophys Res Commun **237**(3): 752-757.

Feil, S., N. Valtcheva, et al. (2009). "Inducible Cre mice." Methods Mol Biol **530**: 343-363.

Foran, E. and D. Trotti (2009). "Glutamate transporters and the excitotoxic path to motor neuron degeneration in amyotrophic lateral sclerosis." Antioxid Redox Signal **11**(7): 1587-1602.

Francius, C., A. Harris, et al. (2013). "Identification of multiple subsets of ventral interneurons and differential distribution along the rostrocaudal axis of the developing spinal cord." PLoS One **8**(8): e70325.

Gagliardini, V. and C. Fankhauser (1999). "Semaphorin III can induce death in sensory neurons." Mol Cell Neurosci **14**(4-5): 301-316.

Garcia-Campmany, L., F. J. Stam, et al. (2010). "From circuits to behaviour: motor networks in vertebrates." Curr Opin Neurobiol **20**(1): 116-125.

Garcia-Castro, M. I., C. Marcelle, et al. (2002). "Ectodermal Wnt function as a neural crest inducer." Science **297**(5582): 848-851.

Gheldof, A. and G. Berx (2013). "Cadherins and epithelial-to-mesenchymal transition." Prog Mol Biol Transl Sci **116**: 317-336.

Gillespie, P. G. and R. G. Walker (2001). "Molecular basis of mechanosensory transduction." Nature **413**(6852): 194-202.

Glasgow, S. M., R. M. Henke, et al. (2005). "Ptf1a determines GABAergic over glutamatergic neuronal cell fate in the spinal cord dorsal horn." Development **132**(24): 5461-5469.

Golding, J. P. and J. Cohen (1997). "Border controls at the mammalian spinal cord: late-surviving neural crest boundary cap cells at dorsal root entry sites may regulate sensory afferent ingrowth and entry zone morphogenesis." Mol Cell Neurosci **9**(5-6): 381-396.

Gosgnach, S. (2011). "The role of genetically-defined interneurons in generating the mammalian locomotor rhythm." Integr Comp Biol **51**(6): 903-912.

Gosgnach, S., G. M. Lanuza, et al. (2006). "V1 spinal neurons regulate the speed of vertebrate locomotor outputs." Nature **440**(7081): 215-219.

Goulding, M. (2009). "Circuits controlling vertebrate locomotion: moving in a new direction." Nat Rev Neurosci **10**(7): 507-518.

Goulding, M., G. Lanuza, et al. (2002). "The formation of sensorimotor circuits." Curr Opin Neurobiol **12**(5): 508-515.

Goulding, M. and S. L. Pfaff (2005). "Development of circuits that generate simple rhythmic behaviors in vertebrates." Curr Opin Neurobiol **15**(1): 14-20.

Greene, N. D. and A. J. Copp (2009). "Development of the vertebrate central nervous system: formation of the neural tube." Prenat Diagn **29**(4): 303-311.

Griffith, C. M., M. J. Wiley, et al. (1992). "The vertebrate tail bud: three germ layers from one tissue." Anat Embryol (Berl) **185**(2): 101-113.

Grillner, S. and T. M. Jessell (2009). "Measured motion: searching for simplicity in spinal locomotor networks." Curr Opin Neurobiol **19**(6): 572-586.

Gross, M. K., M. Dottori, et al. (2002). "Lbx1 specifies somatosensory association interneurons in the dorsal spinal cord." Neuron **34**(4): 535-549.

Guo, Z., C. Zhao, et al. (2012). "Tlx1/3 and Ptf1a control the expression of distinct sets of transmitter and peptide receptor genes in the developing dorsal spinal cord." J Neurosci **32**(25): 8509-8520.

Gutekunst, C. A., E. N. Stewart, et al. (2012). "PlexinA4 distribution in the adult rat spinal cord and dorsal root ganglia." J Chem Neuroanat **44**(1): 1-13.

Hall, B. K. and S. Ekanayake (1991). "Effects of growth factors on the differentiation of neural crest cells and neural crest cell-derivatives." Int J Dev Biol **35**(4): 367-387.

Han, D. Y., M. Kobayashi, et al. (2009). "Differential Islet-1 expression among lumbosacral spinal motor neurons in prenatal mouse." Brain Res **1265**: 30-36.

Hanks, M., W. Wurst, et al. (1995). "Rescue of the En-1 mutant phenotype by replacement of En-1 with En-2." Science **269**(5224): 679-682.

Hantman, A. W. and T. M. Jessell (2010). "Clarke's column neurons as the focus of a corticospinal corollary circuit." Nat Neurosci **13**(10): 1233-1239.

Helms, A. W. and J. E. Johnson (2003). "Specification of dorsal spinal cord interneurons." Curr Opin Neurobiol **13**(1): 42-49.

Hengartner, M. O. (2000). "The biochemistry of apoptosis." Nature **407**(6805): 770-776.

Hollyday, M. (1980). "Motoneuron histogenesis and the development of limb innervation." Curr Top Dev Biol **15 Pt 1**: 181-215.

Hollyday, M. and V. Hamburger (1977). "An autoradiographic study of the formation of the lateral motor column in the chick embryo." Brain Res **132**(2): 197-208.

Hori, K. and M. Hoshino (2012). "GABAergic neuron specification in the spinal cord, the cerebellum, and the cochlear nucleus." Neural Plast **2012**: 921732.

Huang, M., T. Huang, et al. (2008). "Ptf1a, Lbx1 and Pax2 coordinate glycinergic and peptidergic transmitter phenotypes in dorsal spinal inhibitory neurons." Dev Biol **322**(2): 394-405.

Hutchinson, S. A. and J. S. Eisen (2006). "Islet1 and Islet2 have equivalent abilities to promote motoneuron formation and to specify motoneuron subtype identity." Development **133**(11): 2137-2147.

Hyman, B. T. and J. Yuan (2012). "Apoptotic and non-apoptotic roles of caspases in neuronal physiology and pathophysiology." Nat Rev Neurosci **13**(6): 395-406.

Inoue, K., S. Ozaki, et al. (2002). "Runx3 controls the axonal projection of proprioceptive dorsal root ganglion neurons." Nat Neurosci **5**(10): 946-954.

Jacobson, M. D., M. Weil, et al. (1997). "Programmed cell death in animal development." Cell **88**(3): 347-354.

Jensen, P. and S. M. Dymecki (2014). "Essentials of recombinase-based genetic fate mapping in mice." Methods Mol Biol **1092**: 437-454.

Jessell, T. M. (2000). "Neuronal specification in the spinal cord: inductive signals and transcriptional codes." Nat Rev Genet **1**(1): 20-29.

Johansson, C. B., S. Momma, et al. (1999). "Identification of a neural stem cell in the adult mammalian central nervous system." Cell **96**(1): 25-34.

John, A., H. Wildner, et al. (2005). "The homeodomain transcription factor Gbx1 identifies a subpopulation of late-born GABAergic interneurons in the developing dorsal spinal cord." Dev Dyn **234**(3): 767-771.

Joyner, A. L., A. Liu, et al. (2000). "Otx2, Gbx2 and Fgf8 interact to position and maintain a mid-hindbrain organizer." Curr Opin Cell Biol **12**(6): 736-741.

Joyner, A. L. and M. Zervas (2006). "Genetic inducible fate mapping in mouse: establishing genetic lineages and defining genetic neuroanatomy in the nervous system." Dev Dyn **235**(9): 2376-2385.

Julius, D. and A. I. Basbaum (2001). "Molecular mechanisms of nociception." Nature **413**(6852): 203-210.

Jungbluth, S., E. Bell, et al. (1999). "Specification of distinct motor neuron identities by the singular activities of individual Hox genes." Development **126**(12): 2751-2758.

Kablar, B. and M. A. Rudnicki (1999). "Development in the absence of skeletal muscle results in the sequential ablation of motor neurons from the spinal cord to the brain." Dev Biol **208**(1): 93-109.

Kiehn, O. (2006). "Locomotor circuits in the mammalian spinal cord." Annu Rev Neurosci **29**: 279-306
.
Kiehn, O. (2011). "Development and functional organization of spinal locomotor circuits." Curr Opin Neurobiol **21**(1): 100-109.

Kikuta, H., M. Kanai, et al. (2003). "gbx2 Homeobox gene is required for the maintenance of the isthmic region in the zebrafish embryonic brain." Dev Dyn **228**(3): 433-450.

Klein, C. (2005). "Movement disorders: classifications." J Inherit Metab Dis **28**(3): 425-439.

Klein, R., I. Silos-Santiago, et al. (1994). "Disruption of the neurotrophin-3 receptor gene trkC eliminates la muscle afferents and results in abnormal movements." Nature **368**(6468): 249-251.

Knecht, A. K. and M. Bronner-Fraser (2002). "Induction of the neural crest: a multigene process." Nat Rev Genet **3**(6): 453-461.

Koo, S. J. and S. L. Pfaff (2002). "Fine-tuning motor neuron properties: signaling from the periphery." Neuron **35**(5): 823-826.

Kosaka, Y., H. Kin, et al. (2012). "Distinct development of GABA system in the ventral and dorsal horns in the embryonic mouse spinal cord." Brain Res **1486**: 39-52.

Ladle, D. R., E. Pecho-Vrieseling, et al. (2007). "Assembly of motor circuits in the spinal cord: driven to function by genetic and experience-dependent mechanisms." Neuron **56**(2): 270-283.

Lallemend, F. and P. Ernfors (2012). "Molecular interactions underlying the specification of sensory neurons." Trends Neurosci **35**(6): 373-381.

Lanuza, G. M., S. Gosgnach, et al. (2004). "Genetic identification of spinal interneurons that coordinate left-right locomotor activity necessary for walking movements." Neuron **42**(3): 375-386.

Lau, A. and M. Tymianski (2010). "Glutamate receptors, neurotoxicity and neurodegeneration." Pflugers Arch **460**(2): 525-542.

Laurie, D. J., W. Wisden, et al. (1992). "The distribution of thirteen GABAA receptor subunit mRNAs in the rat brain. III. Embryonic and postnatal development." J Neurosci **12**(11): 4151-4172.

Lee, K. J., P. Dietrich, et al. (2000). "Genetic ablation reveals that the roof plate is essential for dorsal interneuron specification." Nature **403**(6771): 734-740.

Lee, S. K., B. Lee, et al. (2005). "Olig2 and Ngn2 function in opposition to modulate gene expression in motor neuron progenitor cells." Genes Dev **19**(2): 282-294.

Lee, S. K. and S. L. Pfaff (2003). "Synchronization of neurogenesis and motor neuron specification by direct coupling of bHLH and homeodomain transcription factors." Neuron **38**(5): 731-745.

Lesaffre, B., A. Joliot, et al. (2007). "Direct non-cell autonomous Pax6 activity regulates eye development in the zebrafish." Neural Dev **2**: 2.

Levanon, D., D. Bettoun, et al. (2002). "The Runx3 transcription factor regulates development and survival of TrkC dorsal root ganglia neurons." EMBO J **21**(13): 3454-3463.

Levine, A. J., K. A. Lewallen, et al. (2012). "Spatial organization of cortical and spinal neurons controlling motor behavior." Curr Opin Neurobiol **22**(5): 812-821.

Lewandoski, M., E. N. Meyers, et al. (1997). "Analysis of Fgf8 gene function in vertebrate development." Cold Spring Harb Symp Quant Biol **62**: 159-168.

Li, B., S. Kuriyama, et al. (2009). "The posteriorizing gene Gbx2 is a direct target of Wnt signalling and the earliest factor in neural crest induction." Development **136**(19): 3267-3278.

Li, J. Y., Z. Lao, et al. (2002). "Changing requirements for Gbx2 in development of the cerebellum and maintenance of the mid/hindbrain organizer." Neuron **36**(1): 31-43.

Liang, X., M. R. Song, et al. (2011). "Isl1 is required for multiple aspects of motor neuron development." Mol Cell Neurosci **47**(3): 215-222.

Liem, K. F., Jr., G. Tremml, et al. (1997). "A role for the roof plate and its resident TGFbeta-related proteins in neuronal patterning in the dorsal spinal cord." Cell **91**(1): 127-138.

Lin, J. H., T. Saito, et al. (1998). "Functionally related motor neuron pool and muscle sensory afferent subtypes defined by coordinate ETS gene expression." Cell **95**(3): 393-407.

Lin, Z., R. Cantos, et al. (2005). "Gbx2 is required for the morphogenesis of the mouse inner ear: a downstream candidate of hindbrain signaling." Development **132**(10): 2309-2318.

Liu, A. and A. L. Joyner (2001). "EN and GBX2 play essential roles downstream of FGF8 in patterning the mouse mid/hindbrain region." Development **128**(2): 181-191.

Liu, F., A. H. Morrison, et al. (2013). "Dynamic interpretation of maternal inputs by the Drosophila segmentation gene network." Proc Natl Acad Sci U S A **110**(17): 6724-6729.

Liu, X. and R. Jaenisch (2000). "Severe peripheral sensory neuron loss and modest motor neuron reduction in mice with combined deficiency of brain-derived neurotrophic factor, neurotrophin 3 and neurotrophin 4/5." Dev Dyn **218**(1): 94-101.

Livet, J., M. Sigrist, et al. (2002). "ETS gene Pea3 controls the central position and terminal arborization of specific motor neuron pools." Neuron **35**(5): 877-892.

Low, L. K. and H. J. Cheng (2006). "Axon pruning: an essential step underlying the developmental plasticity of neuronal connections." Philos Trans R Soc Lond B Biol Sci **361**(1473): 1531-1544.

Lowrie, M. B. and S. J. Lawson (2000). "Cell death of spinal interneurones." Prog Neurobiol **61**(6): 543-555.

Lundfald, L., C. E. Restrepo, et al. (2007). "Phenotype of V2-derived interneurons and their relationship to the axon guidance molecule EphA4 in the developing mouse spinal cord." Eur J Neurosci **26**(11): 2989-3002.

Luo, L. and D. D. O'Leary (2005). "Axon retraction and degeneration in development and disease." Annu Rev Neurosci **28**: 127-156.

Luria, V. and E. Laufer (2007). "Lateral motor column axons execute a ternary trajectory choice between limb and body tissues." Neural Dev **2**: 13.

Luu, B., D. Ellisor, et al. (2011). "The lineage contribution and role of Gbx2 in spinal cord development." PLoS One **6**(6): e20940.

Ma, Q., C. Fode, et al. (1999). "Neurogenin1 and neurogenin2 control two distinct waves of neurogenesis in developing dorsal root ganglia." Genes Dev **13**(13): 1717-1728.

Marmigere, F. and P. Ernfors (2007). "Specification and connectivity of neuronal subtypes in the sensory lineage." Nat Rev Neurosci **8**(2): 114-127.

Maro, G. S., K. Shen, et al. (2009). "Deal breaker: semaphorin and specificity in the spinal stretch reflex circuit." Neuron **63**(1): 8-11.

Matise, M. P. (2013). "Molecular genetic control of cell patterning and fate determination in the developing ventral spinal cord." Wiley Interdiscip Rev Dev Biol **2**(3): 419-425.

Matise, M. P. and A. L. Joyner (1997). "Expression patterns of developmental control genes in normal and Engrailed-1 mutant mouse spinal cord reveal early diversity in developing interneurons." J Neurosci **17**(20): 7805-7816.

Matsui, T., M. Hirai, et al. (1993). "The HOX complex neighbored by the EVX gene, as well as two other homeobox-containing genes, the GBX-class and the EN-class, are located on the same chromosomes 2 and 7 in humans." FEBS Lett **336**(1): 107-110.

Matsui, T., M. Hirai, et al. (1993). "Expression of a novel human homeobox-containing gene that maps to chromosome 7q36.1 in hematopoietic cells." FEBS Lett **322**(2): 181-185.

Meier, P., A. Finch, et al. (2000). "Apoptosis in development." Nature **407**(6805): 796-801.

Mennerick, S. and C. F. Zorumski (2000). "Neural activity and survival in the developing nervous system." Mol Neurobiol **22**(1-3): 41-54.

Meziane, H., V. Fraulob, et al. (2013). "The homeodomain factor Gbx1 is required for locomotion and cell specification in the dorsal spinal cord." PeerJ **1**: e142.

Mizuguchi, R., S. Kriks, et al. (2006). "Ascl1 and Gsh1/2 control inhibitory and excitatory cell fate in spinal sensory interneurons." Nat Neurosci **9**(6): 770-778.

Moran-Rivard, L., T. Kagawa, et al. (2001). "Evx1 is a postmitotic determinant of v0 interneuron identity in the spinal cord." Neuron **29**(2): 385-399.

Muller, T., H. Brohmann, et al. (2002). "The homeodomain factor lbx1 distinguishes two major programs of neuronal differentiation in the dorsal spinal cord." Neuron **34**(4): 551-562.

Murtha, M. T., J. F. Leckman, et al. (1991). "Detection of homeobox genes in development and evolution." Proc Natl Acad Sci U S A **88**(23): 10711-10715.

Narasimha, M. and M. Leptin (2000). "Cell movements during gastrulation: come in and be induced." Trends Cell Biol **10**(5): 169-172.

Neff, W. D. and J. M. Goldberg (1960). "Higher functions of the central nervous system." Annu Rev Physiol **22**: 499-524.

Nornes, H. O. and M. Carry (1978). "Neurogenesis in spinal cord of mouse: an autoradiographic analysis." Brain Res **159**(1): 1-6.

Oakley, R. A., A. S. Garner, et al. (1995). "Muscle sensory neurons require neurotrophin-3 from peripheral tissues during the period of normal cell death." Development **121**(5): 1341-1350.

Oakley, R. A., F. B. Lefcort, et al. (1997). "Neurotrophin-3 promotes the differentiation of muscle spindle afferents in the absence of peripheral targets." J Neurosci **17**(11): 4262-4274.

Oppenheim, R. W. (1991). "Cell death during development of the nervous system." Annu Rev Neurosci **14**: 453-501.

Ordahl, C. P. and N. M. Le Douarin (1992). "Two myogenic lineages within the developing somite." Development **114**(2): 339-353.

Ozaki, S. and W. D. Snider (1997). "Initial trajectories of sensory axons toward laminar targets in the developing mouse spinal cord." J Comp Neurol **380**(2): 215-229.

Patel, T. D., I. Kramer, et al. (2003). "Peripheral NT3 signaling is required for ETS protein expression and central patterning of proprioceptive sensory afferents." Neuron **38**(3): 403-416.

Patten, S. A., G. A. Armstrong, et al. (2014). "Fishing for causes and cures of motor neuron disorders." Dis Model Mech **7**(7): 799-809.

Pecho-Vrieseling, E., M. Sigrist, et al. (2009). "Specificity of sensorimotor connections encoded by Sema3e-Plxnd1 recognition." Nature **459**(7248): 842-846.

Peng, C. Y., H. Yajima, et al. (2007). "Notch and MAML signaling drives Scl-dependent interneuron diversity in the spinal cord." Neuron **53**(6): 813-827.

Pfaff, S. L., M. Mendelsohn, et al. (1996). "Requirement for LIM homeobox gene Isl1 in motor neuron generation reveals a motor neuron-dependent step in interneuron differentiation." Cell **84**(2): 309-320.

Pierani, A., L. Moran-Rivard, et al. (2001). "Control of interneuron fate in the developing spinal cord by the progenitor homeodomain protein Dbx1." Neuron **29**(2): 367-384.

Portier, M. M., M. Escurat, et al. (1993). "Peripherin and neurofilaments: expression and role during neural development." C R Acad Sci III **316**(9): 1124-1140.

Posada, A. and P. G. Clarke (1999). "The role of neuronal death during the development of topographically ordered projections: a computational approach." Biol Cybern **81**(3): 239-247
.

Prasad, T., X. Wang, et al. (2008). "A differential developmental pattern of spinal interneuron apoptosis during synaptogenesis: insights from genetic analyses of the protocadherin-gamma gene cluster." Development **135**(24): 4153-4164.

Price, S. R. and J. Briscoe (2004). "The generation and diversification of spinal motor neurons: signals and responses." Mech Dev **121**(9): 1103-1115.

Purves, D. and J. W. Lichtman (1980). "Elimination of synapses in the developing nervous system." Science **210**(4466): 153-157.

Ramirez-Jarquin, U. N., R. Lazo-Gomez, et al. (2013). "Spinal inhibitory circuits and their role in motor neuron degeneration." Neuropharmacology.

Relaix, F., D. Rocancourt, et al. (2004). "Divergent functions of murine Pax3 and Pax7 in limb muscle development." Genes Dev **18**(9): 1088-1105.

Rhinn, M., K. Lun, et al. (2003). "Cloning, expression and relationship of zebrafish gbx1 and gbx2 genes to Fgf signaling." Mech Dev **120**(8): 919-936.

Rhinn, M., K. Lun, et al. (2004). "Isolation and expression of the homeobox gene Gbx1 during mouse development." Dev Dyn **229**(2): 334-339.

Roeseler, D. A., S. Sachdev, et al. (2012). "Elongation factor 1 alpha1 and genes associated with Usher syndromes are downstream targets of GBX2." PLoS One **7**(11): e47366.

Sander, M., S. Paydar, et al. (2000). "Ventral neural patterning by Nkx homeobox genes: Nkx6.1 controls somatic motor neuron and ventral interneuron fates." Genes Dev **14**(17): 2134-2139.

Schutz, B. (2005). "Imbalanced excitatory to inhibitory synaptic input precedes motor neuron degeneration in an animal model of amyotrophic lateral sclerosis." Neurobiol Dis **20**(1): 131-140.

Shi, Y. (2002). "Mechanisms of caspase activation and inhibition during apoptosis." Mol Cell **9**(3): 459-470.

Shirasaki, R. and S. L. Pfaff (2002). "Transcriptional codes and the control of neuronal identity." Annu Rev Neurosci **25**: 251-281.

Sibilla, S. and L. Ballerini (2009). "GABAergic and glycinergic interneuron expression during spinal cord development: dynamic interplay between inhibition and excitation in the control of ventral network outputs." Prog Neurobiol **89**(1): 46-60.

Sieber-Blum, M. (1989). "Commitment of neural crest cells to the sensory neuron lineage." Science **243**(4898): 1608-1611.

Siembab, V. C., C. A. Smith, et al. (2010). "Target selection of proprioceptive and motor axon synapses on neonatal V1-derived Ia inhibitory interneurons and Renshaw cells." J Comp Neurol **518**(23): 4675-4701.

Smart, I. H. (1972). "Proliferative characteristics of the ependymal layer during the early development of the mouse diencephalon, as revealed by recording the number, location, and plane of cleavage of mitotic figures." J Anat **113**(Pt 1): 109-129.

Smart, I. H. (1972). "Proliferative characteristics of the ependymal layer during the early development of the spinal cord in the mouse." J Anat **111**(Pt 3): 365-380.

Song, M. R., Y. Sun, et al. (2009). "Islet-to-LMO stoichiometries control the function of transcription complexes that specify motor neuron and V2a interneuron identity." Development **136**(17): 2923-2932.

Soriano, P. (1999). "Generalized lacZ expression with the ROSA26 Cre reporter strain." Nat Genet **21**(1): 70-71.

Stepien, A. E. and S. Arber (2008). "Probing the locomotor conundrum: descending the 'V' interneuron ladder." Neuron **60**(1): 1-4.

Su, C. Y., H. A. Kemp, et al. (2014). "Cerebellar development in the absence of Gbx function in zebrafish." Dev Biol **386**(1): 181-190.

Sugiyama, S., A. A. Di Nardo, et al. (2008). "Experience-dependent transfer of Otx2 homeoprotein into the visual cortex activates postnatal plasticity." Cell **134**(3): 508-520.

Sun, W., T. W. Gould, et al. (2003). "Neuromuscular development after the prevention of naturally occurring neuronal death by Bax deletion." J Neurosci **23**(19): 7298-7310.

Tam, P. P. and R. R. Behringer (1997). "Mouse gastrulation: the formation of a mammalian body plan." Mech Dev **68**(1-2): 3-25.

Tam, P. P. and D. A. Loebel (2007). "Gene function in mouse embryogenesis: get set for gastrulation." Nat Rev Genet **8**(5): 368-381.

Tam, P. P., E. A. Williams, et al. (1993). "Gastrulation in the mouse embryo: ultrastructural and molecular aspects of germ layer morphogenesis." Microsc Res Tech **26**(4): 301-328.

Tanabe, Y., C. William, et al. (1998). "Specification of motor neuron identity by the MNR2 homeodomain protein." Cell **95**(1): 67-80.

Thaler, J., K. Harrison, et al. (1999). "Active suppression of interneuron programs within developing motor neurons revealed by analysis of homeodomain factor HB9." Neuron **23**(4): 675-687.

Thaler, J. P., S. J. Koo, et al. (2004). "A postmitotic role for Isl-class LIM homeodomain proteins in the assignment of visceral spinal motor neuron identity." Neuron **41**(3): 337-350.

Todd, A. J. (2010). "Neuronal circuitry for pain processing in the dorsal horn." Nat Rev Neurosci **11**(12): 823-836.

Tourtellotte, W. G., R. Nagarajan, et al. (2000). "Functional compensation by Egr4 in Egr1-dependent luteinizing hormone regulation and Leydig cell steroidogenesis." Mol Cell Biol **20**(14): 5261-5268.

Tripodi, M. and S. Arber (2012). "Regulation of motor circuit assembly by spatial and temporal mechanisms." Curr Opin Neurobiol **22**(4): 615-623.

Tsuchida, T., M. Ensini, et al. (1994). "Topographic organization of embryonic motor neurons defined by expression of LIM homeobox genes." Cell **79**(6): 957-970.

Ulloa, F. and J. Briscoe (2007). "Morphogens and the control of cell proliferation and patterning in the spinal cord." Cell Cycle **6**(21): 2640-2649.

Urbanek, P., I. Fetka, et al. (1997). "Cooperation of Pax2 and Pax5 in midbrain and cerebellum development." Proc Natl Acad Sci U S A **94**(11): 5703-5708.

Usui, N., K. Watanabe, et al. (2012). "Role of motoneuron-derived neurotrophin 3 in survival and axonal projection of sensory neurons during neural circuit formation." Development **139**(6): 1125-1132.

Vidal, P. P., L. Degallaix, et al. (2004). "Postural and locomotor control in normal and vestibularly deficient mice." J Physiol **559**(Pt 2): 625-638.

Villalon, E., D. J. Schulz, et al. (2014). "Real-time PCR quantification of gene expression in embryonic mouse tissue." Methods Mol Biol **1092**: 81-94.

Wassarman, K. M., M. Lewandoski, et al. (1997). "Specification of the anterior hindbrain and establishment of a normal mid/hindbrain organizer is dependent on Gbx2 gene function." Development **124**(15): 2923-2934.

Waters, S. T. and M. Lewandoski (2006). "A threshold requirement for Gbx2 levels in hindbrain development." Development **133**(10): 1991-2000.

Waters, S. T., C. P. Wilson, et al. (2003). "Cloning and embryonic expression analysis of the mouse Gbx1 gene." Gene Expr Patterns **3**(3): 313-317.

Weiss, S., C. Dunne, et al. (1996). "Multipotent CNS stem cells are present in the adult mammalian spinal cord and ventricular neuroaxis." J Neurosci **16**(23): 7599-7609.

Wilson, L. and M. Maden (2005). "The mechanisms of dorsoventral patterning in the vertebrate neural tube." Dev Biol **282**(1): 1-13.

Wolpert, L. (1969). "Positional information and the spatial pattern of cellular differentiation." J Theor Biol **25**(1): 1-47.

Wu, L. S., W. C. Cheng, et al. (2012). "Targeted depletion of TDP-43 expression in the spinal cord motor neurons leads to the development of amyotrophic lateral sclerosis-like phenotypes in mice." J Biol Chem **287**(33): 27335-27344.

Yang, X., S. Arber, et al. (2001). "Patterning of muscle acetylcholine receptor gene expression in the absence of motor innervation." Neuron **30**(2): 399-410.

Ybot-Gonzalez, P. and A. J. Copp (1999). "Bending of the neural plate during mouse spinal neurulation is independent of actin microfilaments." Dev Dyn **215**(3): 273-283.

Ybot-Gonzalez, P., C. Gaston-Massuet, et al. (2007). "Neural plate morphogenesis during mouse neurulation is regulated by antagonism of Bmp signalling." Development **134**(17): 3203-3211.

Ybot-Gonzalez, P., D. Savery, et al. (2007). "Convergent extension, planar-cell-polarity signalling and initiation of mouse neural tube closure." Development **134**(4): 789-799.

Yoshida, Y., B. Han, et al. (2006). "PlexinA1 signaling directs the segregation of proprioceptive sensory axons in the developing spinal cord." Neuron **52**(5): 775-788.

Yuan, J., M. Lipinski, et al. (2003). "Diversity in the mechanisms of neuronal cell death." Neuron **40**(2): 401-413.

Yuan, J. and B. A. Yankner (2000). "Apoptosis in the nervous system." Nature **407**(6805): 802-809.

Zhang, Y., S. Narayan, et al. (2008). "V3 spinal neurons establish a robust and balanced locomotor rhythm during walking." Neuron **60**(1): 84-96.

Zhong, G., S. Droho, et al. (2010). "Electrophysiological characterization of V2a interneurons and their locomotor-related activity in the neonatal mouse spinal cord." J Neurosci **30**(1): 170-182.

Zhuang, B. and S. Sockanathan (2006). "Dorsal-ventral patterning: a view from the top." Curr Opin Neurobiol **16**(1): 20-24.

VITA

Desirè Buckley has resided in Columbia, MO since the age of 6. She began her undergraduate studies at the University of Missouri in 2006 and became engaged in the Exposure to Research for Science Students (EXPRESS) undergraduate research program where she quickly discovered her passion for scientific research. In 2007, she joined the lab of Dr. Christian Lorson as an undergraduate research assistant and continued for the remainder of her undergraduate studies. In spring of 2010, Desirè was accepted into the University of Missouri Biological Sciences Ph.D. program. She was initially funded by the Missouri Life Sciences and Gus T. Ridgel Fellowships, and then transitioned to the National Science Foundation Graduate Research Fellowship (NSF GRF) in 2012. Desirè successfully completed her graduate education in the lab of Dr. Samuel T. Waters, and earned her Ph.D. in January 2015.